THE DYNAMIC RESPONSE OF TRACER CONCENTRATION IN UNIFORM FLOW SYSTEMS, WITH SPECIAL REFERENCE TO AN ANNULUS

A Thesis submitted for the Degree of Doctor of Philosophy in the Faculty of Engineering in the University of London.

by

Robert Stephen Vines, B.Sc. (Eng.), A.C.G.I.

Department of Chemical Engineering and Chemical Technology,
City and Guilds College,
Imperial College,
London, S.W.7.

January, 1969

ABSTRACT

The work presented in this thesis concerns the study, by means of tracer signals, of flow system of uniform cross-section in which flow is fully developed. Theoretical studies in this field have previously been made by Taylor, Aris and Philip (references 4 to 8). In the present work, the solutions which govern the behaviour of dispersed substances in such flow systems are solved by a method developed from the work of Philip. It is shown that the result of tracer studies of uniform flow systems are only meaningful when the 'convergence' condition is satisfied. This condition is related to the transverse distribution of tracer material in the flow system. A general expression is also derived for the dispersion coefficient employed by Taylor and Aris.

Experimental work was carried out using an annular flow system with water as the fluid. Tracer studies were carried out at eight different flow velocities in the turbulent regime. The tracer employed was sodium chloride, the concentration of which was found from conductivity measurements. Two mathematical models of the flow system are proposed. These models differ mainly in the diffusivity values they predict for the flow system. The models are examined in the light of experimental tracer response data, it being shown how the predicted diffusivity pattern in each case might be improved. The experimental data also furnish evidence of the existence of a 'laminar sub-layer', the thickness of which is calculated for each flow velocity.

It is also shown how the degree of conversion in a chemical reactor, and the dynamic response of reactant concentration to disturbances, may be predicted for a first order reaction from tracer studies. These studies are best carried out using tracer signals of the pulse form. The 'convergence' condition must be satisfied for both the tracer signals and the transverse distribution of reactant in the reactor.

ACKNOWLEDGEMENT

The author wishes to acknowledge his dept to his supervisor, Dr. A.P. Shahbenderian Ph.D., for advice and guidance rendered in the execution of research work and in the presentation of this thesis.

The author also wishes to thank Mr. J. Oakley and his workshop staff for help in the design and construction of experimental apparatus; Mr. L. Tyley and the author's brother, J.M. Vines, for help in connection with electronic apparatus; Messrs. Evershed & Vignoles Ltd., for the loan of equipment; Miss D. Spiller for typing the great bulk of this thesis; and Shell U.K. Ltd., for the use of reproduction facilities.

Page	Line of Type	Corrigendum
2	3	for system read systems
5	5	" signal read signals
8	3	" gneeral read general
14	29	" analoyy read analogy
20	5	" indepdenently read independently
24	6	After factor insert which
32	15	for approximate read appropriate
37	8	" τ_t read τ_r
37	12	" quari read quasi
38	3	" significane read significance
43	14	" expression read expansion
44	14	" periphy read periphery
72	9	" figure f.2 read figure f.6
72	10	" ci-cuit read circuit
72	30	" thermoionic read thermionic
75	23	" alternatively read alternately
79	13	" epxeriment read experiment
81	7	" calulcated read calculated
81	13	" experimenta- read experimental
82	11	" appropraite read appropriate
90	5	after exponential insert decay could be assumed, was found by
90	11	for conetimetres read centimetres
90	13	" tracer read trace
100	11	" is read in
100	17	" include read exclude
101	6	after part, insert β_r,
101	12	for K_t read K_r
104	22	" th read the
105	21	" clearly read closely

Page	Line of Type	Corrigendum
119	2	for X_1 read α_1
125	9	" 311 read 300
125	10	" 112 read 109
125	17	" (1968) read (1958)
127	1	" limitc read limits
161	6, 12	" tepol read teepol
161	20	" chlorplatanic read chloroplatinic
162	17	" binominal read binomial

CONTENTS

Page

CHAPTER I

1.1 Tracer Studies in Flow Systems 9
2.1 Present Theoretical Work 12
2.2 Present Experimental Work 14

CHAPTER II

1. The Basic Equations 16
2. Time Integral Transforms 18
2.1 Cyclical Disturbances in Tracer Concentration 18
2.2 Disturbances of Limited Duration 20
2.3 Equations in Dimensionless Form 23
3. Series Solution of Equations 24
3.1 The Convergence Condition 31
3.2 'Zero Frequency' Solutions 33
4. The Dispersion Model 35
4.1 Complex Dispersion Coefficient 38
4.2 Variable Reference Plane Dispersion Coefficient 39
4.3 Taylor/Aris Dispersion Coefficient 42
4.4 The Taylor/Aris Coefficient for various Flow Systems 48
5. Response Data for a Parallel Wall Flow System 53
5.1 Equations in Matrix Form 55
5.2 Solution of Matrix Equations 59

Page

CHAPTER III

	1.1	Geometry of Experimental Flow System	61
	1.2	Dimensions of Flow System	63
	1.3	Construction of Flow System	66
	2.1	Measurement and Recording of Tracer Signal	71
	2.2	Tracer Injection System	75
3.		Ancillary Equipment	79
4.		Experimental Method	80
	4.1	Preliminary Investigations	80
	4.2	Daily Procedure	82
	4.3	Procedure for each Run	84
	4.4	Analysis of Chart Recordings	87

CHAPTER IV

1.		Tracer Signal Frequency in Experiment	92
2.		Mathematical Models	94
	2.1	Unified Mathematical Model	94
	2.2	Compound Mathematical Model	96
	2.3	Numerical Solution of Matrix Equation	104
3.		Experimental Errors	106

CHAPTER V

1.		Interpretation of Experimental Results	108
	1.1	At Low Frequency	108
	1.2	Comparison of Mathematical Models	110

CONTENTS LIST (Contd.)

2. Extension of work

2.1 Possible Improvements to Present Investigations 112

2.2 Tracer Studies and First Order Reactions 113

References 125

List of Symbols 126

APPENDIX I

Diagrams $a_1 - a_8$ Amplitude Ratio Diagrams 129

" $b_1 - b_8$ Phase Lag Diagrams 137

" $c_1 - c_8$ Phase Lag Diagrams 145

Diagram d_1 Laminar Sublayer Thickness 153

APPENDIX II

1.1 L-U Matrix Inversion 154

1.2 Secondary Solutions of Equation (CII; 5;3) 157

2. Tracer concentration from Recorder Chart Readings 159

3. Electrode Platinisation 161

4. Inverse versus Direct Cross-sectional Mean Concentration 162

5. Least Squares Formulae

5.1 Sinusoidal Tracer Signals 168

5.2 Pulse Tracer Signals 172

APPENDIX III

Table 1	Dimensions of Annular Flow System	175
" 2	Convergence of Solutions of Equation (CII; 5;3)	176
" 3	Decay of Secondary Solutions of Equation with respect to Increment Size. (CII; 5;3)	177
" 4	Flow Rates used in Experiment.	178
Photos. 9 - 14	Tracer Signal Recordings	179

APPENDIX IV

Diagrams f_1-f_{12}	Construction of Annular Flow System and circuit diagrams.	184
Diagrams g_1-g_2	Analysis of Recorder Chart	195
Diagram m_1	Friction Factor versus Reynolds Number	197
Diagram m_2	Pressure Drop in Laminar Flow	198
Diagrams m_3-m_7	Measured versus Actual Conductivity Cell Conductance.	199

PHOTOGRAPHS

		Page
1	Gneeral Layout	65
2	Dismantled Annulus with Electrodes	67
3	Connecting Piece with Mounted Electrode	67
4	Upstream End of Flow System	69
5	Downstream End of Flow System	69
6	Electrical Controls	74
7	Tracer Injection System	77
8	Sine Wave Generator	78
9 - 13	Recorder Tracings from Sinusoidal Tracer Signals	179
14	Recorder Tracings from Pulse Tracer Signal	182

CHAPTER I

1. TRACER STUDIES IN FLOW SYSTEMS

Information may be obtained about fluid flow systems by studying the behaviour of tracer signals in such systems. Danckwerts[1] and other workers have derived and used the concept of 'residence time distribution' for these studies. The residence time distribution may be found directly from the way in which tracer concentration changes in the stream leaving the flow system after a sudden change has been made in the tracer concentration in the inflowing stream. Some knowledge is gained concerning the internal flow patterns and mixing characteristics of the system through comparing the residence time distribution found in experiment with those predicted for the extremes of 'plug flow' and 'perfect mixing' in the flow system. The residence time distribution is also used to find the conversion for first order reactions in chemical reactors. Additional information is required for reactions of higher order.

Fully developed fluid flow in ducts of uniform cross-section is of a less complicated nature than that in arbitrary flow systems. For such well defined systems information of a more definite nature can be obtained from the results of tracer studies. Griffiths[2] observed that a slug of dye injected into water flowing in a glass tube tended to travel at the mean velocity of flow and to spread out evenly along the axis of flow. Flow in the tube was thus shown to comply with a plug flow model with a degree of longitudinal mixing superimposed. At an earlier date, Stewart[3] assumed the validity of a plug flow model for the purposes of measuring the flow in small blood vessels.

The first theoretical analysis of the behaviour of tracer signals in uniform ducts was carried out by Taylor. He found approximate solutions of the fundamental transport equations for pulse tracer signals in laminar[4,5] and in turbulent[6] flow inside tubes. He showed that, provided two conditions are satisfied, the pulse behaviour can be described by the 'plug flow with mixing' model. Taylor also showed that the longitudinal mixing is of the Fickian diffusion type, and derived expressions for an effective longitudinal diffusion or 'dispersion' coefficient The first condition is that a quasi-equilibrium radial concentration profile should be established. This condition is termed the 'convergence' condition in this thesis. Taylor's second condition is that the dispersion coefficient should be very much greater than the diffusivity of the tracer material.

In a more rigorous analysis, Aris[7] showed that the general conclusions of Taylor's analysis were sound. He established Taylor's first condition on a firmer basis. Aris modified the expression for the dispersion coefficient derived by Taylor, so removing the necessity for Taylor's second condition. He introduced a 'minimum dispersal time', after which the effect of time derivative terms in the equations which are of second order importance may be neglected. Aris also extended the equations to describe tracer behaviour in uniform ducts of general geometry.

As applied to pulse tracer signals, the plug flow model postulates that the centre of gravity (with respect to the longitudinal axis) of the pulse should move at the mean velocity of flow. The Fickian type mixing also demands that the second moment of the area of the pulse should increase at a constant rate proportional to the dispersion coefficient. For these integral

quantities to be calculated, measurements of mean tracer concentrations should have to be made at fixed intervals of time over the length of flow system in which tracer is present. Because such measurements cannot conveniently be made, the practical value of the Taylor/Aris analysis is not very great. Its value is further diminished by the impossibility of satisfying the 'minimum dispersal time' conditions.

In a fully rigorous analysis developed by Philip[8], the dispersion concept was entended to cover the case in which time differential terms could not be neglected and in which time based tracer concentration measurements at fixed points in the flow system were of interest. The resulting dispersion coefficient is a complex quantity and thus does not impart a physical picture of the process of dispersion. The analysis is in terms of Fourier transforms and is consequently easily related to experimental frequency response data. Philip also proved that the 'dynamic'dispersion model could only hold if the 'convergence' condition were satisfied.

The main purpose sought by Philip in his analysis was to describe the damping of concentration fluctuations in sampling tubes. His equations were thus only written for laminar flow in circular ducts. The method by which he derived numerical solutions to these equations is suitable for hand computation in laminar flow problems only.

2.1 PRESENT THEORETICAL WORK

The analysis developed in this thesis (in Chapter II) describes the behaviour of tracer signals in fully developed flow in uniform ducts of general geometric configuration. The method of analysis is largely an extension of that of Philip[8] with some useful modifications. A simple and rapid computer solution to the equations for a parallel wall flow system is developed. This numerical solution is suitable for all flow systems in which the geometry of the cross-section permits point values of velocity and diffusivity to be described in terms of a single transverse coordinate. A general expression for the Taylor/Aris dispersion coefficient is also derived.

The concept of a 'variable reference plane dispersion coefficient' is developed in this thesis. This coefficient is the apparent dispersion coefficient relative to a reference plane similar to that of the plug flow model, but moving at a speed different from the mean flow velocity. The speed of the reference plane is such that the dispersion coefficient is a real quantity (as opposed to the complex coefficient in the dispersion model due to Philip). As the tracer signal frequency approaches zero, the reference plane speed approaches the mean flow velocity and the dispersion coefficient approaches the value of the Taylor/Aris coefficient. The dispersion coefficient based upon the variable reference plane has the advantage over that based upon the mean flow in that it carries with it a physical picture.

The study of the dynamic response of a flow system to tracer signals produces a much greater quantity of experimental data than similar dispersion or residence time studies. A similarly greater quantity of information concerning the flow system may therefore be derived from the tracer response data. In the case of a flow

system of uniform cross-section in which the convergence condition is satisfied, tracer response is shown to be determined solely by the transverse fluid velocity and diffusivity profiles. These profiles may therefore be derived from the response data in a flow system in which they (the velocity and diffusivity profiles) are described in terms of a single transverse coordinate. If a direct method were found by which this may be done, tracer response studies would become a useful tool in the study of turbulent flow.

In general cases, where the flow system is not uniform or where the convergence condition is not satisifed, the data from dynamic tracer studies are less conclusive. It is shown how useful information concerning flow patterns and mixing characteristics may be derived from such studies. It is also shown how, for a chemical reactor, the conversion for a reaction of first order and also the response of the conversion to changes in the reactant feeds, may be predicted from tracer response experiments.

2.2 PRESENT EXPERIMENTAL WORK

With the object of studying axial dispersion in turbulent flow, a series of tracer experiments were carried out using water as the fluid in an annular flow system. The flow system was formed by the annular gap between two concentric tubes. The response theory developed in this thesis describes the behaviour of the tracer concentration with respect to the cross-section of the flow system. Therefore, the geometrical configuration of the flow system had to be such that this quantity could be measured directly. Because the size of the annular gap was small compared with the tube diameters, the geometry of the flow system approximated closely to that of a parallel wall flow system, and a straight concentration measurement between the walls was a representative cross-sectional mean.

The experiments were carried out over a range of low Reynold's numbers in the turbulent flow regime. Sodium chloride was employed as the tracer, the concentration of which was found from conductivity measurement. Conductivity cells were formed by electrodes set into the walls of the annulus at either end of the experimental section of the flow system. Tracer signals of both the sinusoidal and the pulse type were used. Frequency response data were obtained directly from the sinusoidal signals and by Fourier analysis from the pulse signals.

Theoretical tracer response data were obtained from full solution of the transport equations with eddy diffusivity predicted by two different models. In the first model, the direct analogy between mass and momentum transfer (commonly called Reynolds' analogy) was assumed to hold over the whole cross-section of the flow system. In the second model, the analogy was assumed

to be true in the turbulent core of flow only, mass transfer in the 'laminar sub-layer' being confined to molecular diffusion. Neither model satisfactorily explained all the features of the experimental response data. The laminar sub-layer model was, however, a significant improvement upon the first model.

For practical reasons, the annular gap which formed the flow system had to be small. Consequently, reliable measurements of point velocity in the cross-section were not possible. Velocity profiles were therefore assumed to be predicted by a method due to Pai[9]. Because this method has not been tested for turbulent water flow at low Reynolds' number in a parallel wall flow system, theoretical response data derived from the velocity profiles are subject to some doubt.

The experimental data were analysed in terms of the variable reference plane concept. In this way, the usefulness of the Taylor/Aris dispersion model was tested under the most severe conditions possible, the effect of the laminar sub-layer being greater in flows at low Reynolds' numbers. It was found that assumption of the velocity of the Taylor/Aris model could lead to up to a four per cent error in a flow velocity measurement. A large error was also possible in the measurement of low frequency mixing characteristics.

CHAPTER II

1. THE BASIC EQUATIONS

Solution is sought to the equations which govern the behaviour of dissolved material in a flow system. The flow system consists of a duct of infinite length completely enclosed by impermeable walls, in which flow is fully developed. The cross-section of the duct (i.e. the domain occupied by the duct in the plane to which flow is normal) is uniform throughout the length of the duct and may be of any geometrical configuration. Under these conditions, the behaviour of the dispersed species of concentration, C_A, is described by a partial differential equation in four independent variables.

$$\nabla_x \left(D \nabla_x C_A \right) - U \frac{\partial C_A}{\partial x_1} - \frac{\partial C_A}{\partial t} = 0$$

.....(CII, 1;1)

In this equation, diffusion is described by a 'Fickian' coefficient, D, which in turbulent flow is the sum of molecular and eddy diffusivity. As the cross-section of the duct is uniform and flow fully developed, diffusivity and point velocity are functions of cross-sectional position only.

$$D = D(x_2, x_3)$$
$$U = U(x_2, x_3)$$

The walls of the duct are denoted by the symbol, Γ. As the walls are impermeable, the transfer rate normal to them at their surfaces is zero.

$$\text{On } \Gamma, \qquad D \frac{\partial C_A}{\partial x_n} = 0$$

.....(CII, 1;2)

A further boundary condition is specified in the cross-section of the duct in which the origin of the longitudinal axis lies.

$$x_1 = 0, \quad C_A(0, x_2, x_3, t) = C_{A0}(x_2, x_3, t)$$

.....(CII, 1;3)

Equation (1;1) cannot be solved before a further boundary condition is defined. Such a condition will arise from a restriction in the structure of concentration disturbances for which this equation is solved.

In equation (1;1) diffusivity is assumed to be an isotropic property. This assumption is not made through necessity, but in order to allow equations to be as simple as possible. Every step in the analysis of this equation would equally be justified if diffusivity were treated as an anisotropic property of the flow system.

2. TIME INTEGRAL TRANSFORMS

Equation (1;1) is solved for well defined perturbations in concentration. These disturbances may be placed into two categories. The first category is that in which the disturbances are of a cyclical nature with respect to time.

$$C_A\,(x_1\,,x_2\,,x_3\,,t) = C\;(x_1\,,x_2\,,x_3\,,t+T)$$

.....(CII: 2;1)

where T is the period of the cycle.

The second category of perturbation is one in which the disturbance in concentration, or any derivative of concentration with respect to time, has a limited duration, T'.

$$t \leq o\;,\quad t \geqslant T'\,,$$

$$\frac{\partial^n}{\partial t^n}\,C_A\,(x_1\,,x_2\,,x_3\,,t) = o$$

.....(CII; 2;2,3)

2.1 CYCLICAL DISTURBANCES

Cyclical disturbances may be broken down into sinusoidal components and represented by a 'Fourier' series.

$$C_A(x_1, x_2, x_3, t) = \sum_{r=0}^{\infty} R\left\{ C_r(x_1, x_2, x_3)\, e^{i r \omega t} \right\}$$

.....(CII; 2;4)

where

$$\omega = \frac{2\pi}{T}$$

.....(CII;2;5)

and, i, denotes the square root of minus one. The letter, R, signifies that only the real part of the expression enclosed in the brackets which it preceeds, is equated. The complex spatial function, C_r, is termed the 'transient function' and is defined as follows in equations (2;6) and (2;7)

$$r = 0, \quad C_0(x_1, x_2, x_3) = \frac{1}{T}\int_{t_0}^{t_0+T} C_A(x_1, x_2, x_3, t)\, dt$$

$$r \neq 0, \quad C_r(x_1, x_2, x_3) = \frac{2}{T}\int_{t_0}^{t_0+T} C_A(x_1, x_2, x_3, t)\, e^{-ir\omega t}\, dt \quad .$$

.....(CII; 2;6,7)

The right hand side of equation (2;4) may be used as a substitution for concentration, C_A, in the mass transport equation (1;1) and in the boundary conditions (1;2) and (1;3). If each of the terms of these equations is then subjected to a Fourier transform of the type in equations (2;6) and (2;7), a set of independent equations and boundary conditions is formed.

$$\nabla \left(D \nabla C_r \right) - U \frac{\partial C_r}{\partial x_1} - i r \omega C_r = 0$$

.....(CII; 2;8)

On Γ , $\qquad D \frac{\partial C_r}{\partial x_n} = 0$

$$x_1 = 0 \ , \quad C_r \left(0, x_2, x_3 \right) = C_{r0} \left(x_2, x_3 \right)$$

.....(CII; 2;9, 10)

as there is a separate equation and separate boundary conditions for each 'harmonic', r, it follows that each harmonic behaves indepdenently of all others within the limitations of the original equations.

2.2 DISTURBANCES OF LIMITED DURATION

Perturbations of this type may be treated in a manner similar to cyclical disturbances. As the perturbation is of limited duration, it may be considered as one of a sequence of identical perturbations. A Fourier series may thus be written

$$\frac{\partial^n}{\partial t^n} C_A \left(x_1, x_2, x_3, t \right) = \sum_{r=0}^{\infty} R \left\{ C_r \left(x_1, x_2, x_3 \right) e^{i r \omega t} \right\}$$

.....(CII; 2; 11)

where

$$\omega = \frac{2\pi}{T'}$$

.....(CII; 2 ; 12)

The transient function is also defined in a way similar to that for periodic disturbances.

$$r = 0 , \quad C_0 = \frac{1}{T'} \int_0^{T'} \frac{\partial^n}{\partial t^n} C_A \, dt$$

$$r \neq 0 , \quad C_r = \frac{2}{T'} \int_0^{T'} e^{-ir\omega t} \frac{\partial^n}{\partial t^n} C_A \, dt$$

.....(CII; 2;13,14)

The terms of equation (1;1) and the boundary conditions (1;2) and (1;3) are differentiated with respect to time the number of times, n, determined by the order of the perturbed derivative. Then by arguments identical to those used in the case of cyclical disturbances, equation (2;8) and the boundary conditions (2;9) and (2;10) are shown to be valid for disturbances of limited duration,

Because no limit is set upon the duration, T', it may in principle be infinite. In this case the alternative statement of the Fourier transform and series must be used.

$$\frac{\partial^n}{\partial t^n} C_A = \frac{2}{\pi} \int_0^{\infty} R \left\{ C_{\omega'} e^{i\omega' t} \right\} d\omega'$$

.....(CII; 2;15)

where the modified transient function is defined;-

$$C_{\omega'} = \int_0^\infty e^{-i\omega' t} \frac{\partial^n}{\partial t^n} C_A \, dt$$

.....(CII; 2;16).

The modification of the integral transforms does not effect the validity of equation (2;8).

Perturbations of both the cyclical and limited duration type are shown to be governed by the same basic equations. These types include all useful tracer signal forms. Perturbations of the second type include pulses where n = o, and step changes, where n = 1.

2.3 DIMENSIONLESS FORM OF THE EQUATIONS

It is convenient at this point to introduce dimensionless variables to equation (2;8) and the boundary condition (2;9). Let

$$\xi_1 = \frac{x_1}{a} \qquad \text{etc.}$$
$$\psi = \frac{D}{\bar{D}}$$
$$\chi = \frac{U}{\bar{U}}$$

where a is a characteristic dimension in the cross-section of the duct and $\bar{D}$ and $\bar{U}$ the mean values of diffusivity and velocity with respect to the cross-section. Further, let

$$\Phi = \frac{\bar{U} a}{\bar{D}}$$
$$\Omega = \frac{\omega a^2}{\bar{D}}$$

Equation (2;8) and the boundary conditions (2;9) and (2;10) may now be rewritten

$$\nabla (\psi \nabla C_r) - \Phi \chi \frac{\partial C_r}{\partial \xi_1} - i_r \Omega C_r = 0$$

.....(CII; 2;17)

where the differential operator, ∇, now refers to the dimensionless coordinates.

$$\text{On } \Gamma, \quad \psi \frac{\partial C_r}{\partial \xi_n} = 0$$

$$\xi_1 = 0, \quad C_r(0, \xi_2, \xi_3) = C_{r0}(\xi_2, \xi_3)$$

.....(CII; 2;18,19)

2.4 LIMITATIONS TO THE MASS TRANSPORT EQUATIONS

Equation (1;1) assumes that the flux of dispersed material in turbulent flow is described by a Fickian eddy diffusion coefficient. This assumption cannot be justified where the period of tracer signals is small enough to be of the order of the time scale of turbulence. This factor places a limitation upon the validity of the equations, is discussed in Chapter V.

3. SERIES SOLUTION OF EQUATION (2;17)

At this stage it is necessary to use mathematical induction in order to proceed with the analysis. It is assumed that any solution of equation (2;17) may be represented as the sum of a series of solutions of this equation, each one of which is the product of a function of longitudinal position, $X_{rs}(\xi_1)$, and a function of cross-sectional position, $f_{rs}(\xi_2, \xi_3)$.

$$C_r = \sum_{s=1}^{\infty} X_{rs}(\xi_1) \cdot f_{rs}(\xi_2, \xi_3)$$

.....(CII; 3;1)

The function of cross-sectional position is so defined that its integral with respect to the cross-section is unity.

$$\int_A f_{rs}\, d\xi_2\, d\xi_3 = 1$$

.....(CII; 3;2)

Any functional product may be used as a substitution in equation (2;17) thus:-

$$f_{rs}\,\psi\,\frac{d\,X_{rs}}{d\,\xi_1} + X_{rs}\sum_{i=2}^{i=3}\frac{\partial}{\partial\,\xi_i}\left(\psi\,\frac{\partial\,f_{rs}}{\partial\,\xi_i}\right) \ldots .$$

$$\ldots . - \Phi\,\chi\,f_{rs}\,\frac{d\,X_{rs}}{d\,\xi_1} - i\,r\,\Omega\,X_{rs}\,f_{rs} = 0$$

.....(CII; 3;3)

Boundary conditions (2;18) and (2;19) must also be satisfied.

$$On \quad \Gamma\ , \qquad \psi\,\frac{\partial\,f_{rs}}{\partial\,\xi_\Gamma} = 0$$

$$\xi_1 = 0\ , \qquad X_{rs}\,(0) = X_{rs\,0}$$

.....(CII; 3;4,5)

Each term of equation (3;3) is integrable with respect to the cross-section. The integral of the second term is evaluated by the use of Green's lemma as applied to a surface integral.

$$\int_A \left\{ \sum_{j=2}^{j=3} \frac{\partial}{\partial \xi_j} \left(\psi \frac{\partial f_{rs}}{\partial \xi_j} \right) \right\} d\xi_2 \, d\xi_2 = \int_\tau \psi \frac{\partial f_{rs}}{\partial \xi_\tau} d\xi_\tau$$

.....(CII; 3;6)

where the length, $d\xi_\tau$, is an infinitessimal part of the periphery of the flow system. The integral of the second term of equation (3;3) is thus seen to be zero on account of the boundary condition (3;4).

Equation (3;3), after each term has been integrated, is reduced to an ordinary second order differential equation.

$$\phi_{rs} \frac{d^2 X_{rs}}{d\xi_1^2} - \tau_{rs} \Phi \frac{d X_{rs}}{d \xi_1} - i r \Omega X_{rs} = 0$$

.....(CII; 3;7)

where the coefficients of this equation are defined by cross-sectional integrals.

$$\phi_{rs} = \int_A \psi f_{rs} \, d\xi_2 \, d\xi_3$$

$$\tau_{rs} = \int_A \chi f_{rs} \, d\xi_2 \, d\xi_3$$

.....(CII; 3;8,9)

The values of the coefficients in equation (3;7) are fixed for each particular cross-sectional function. Equation (3;7) is thus a linear equation with constant coefficients and has an exponential solution,

$$X_{rs} = X_{rs\,o}\, e^{\alpha_{rs}\,\xi}$$

.....(CII;3;10)

In equation (3;10), boundary condition (3;5) is taken into account. The complex exponential coefficient, α_{rs}, is the 'logarithmic transfer factor' associated with the particular cross-sectional function. For a sinusoidal tracer signal, the real part of the transfer factor is the logarithm of the amplification of the signal over one dimensionless unit of length in the direction of flow. Likewise the imaginary part of the transfer factor is the phase shift (in radians) of the sinusoidal signal over this length.

Equations (3;7) and (3;10) are combined to form an auxiliary equation, one solution of which is the logarithmic transfer factor.

$$\phi_{rs}\,\alpha_{rs}^{2} - \zeta_{rs}\,\Phi\,\alpha_{rs} - i\,r\,\Omega = 0$$

.....(CII; 3;11)

Tracer signals must 'travel' in the direction of flow. Therefore the phase shift of a sinusoidal tracer signal increases negatively

in the direction of flow and the logarithmic transfer factor has a negative imaginary part.

$$I \{ \alpha_{rs} \} \leq 0$$

.....(CII; 3;12)

The correct solution of equation (3;11) is now deduced from the condition (3;12)

$$\alpha_{rs} = - \frac{\tau_{rs} \Phi}{2 \phi_{rs}} \left[\sqrt{1 + 4 i \frac{r \Omega \phi_{rs}}{\tau_{rs}^2}} - 1 \right]$$

.....(CII; 3;13)

It is seen from equation (3;13) that the harmonic components of tracer signals must also decay in the direction of flow.

$$R \{ \alpha_{rs} \} \leq 0$$

.....(CII; 3;14)

This condition could also have been derived from physical considerations.

The right hand side of equation (3;10) is used as a substitution in equation (3;3) to obtain a second order partial differential equation which governs the cross-sectional function.

$$\sum_{j=2}^{j=3} \frac{\partial}{\partial \bar{F}_j}\left(\psi \frac{\partial f_{rs}}{\partial \bar{F}_j}\right) + \left(\psi \alpha_{rs}^2 - \Phi \nu \alpha_{rs} - i r \Omega\right) f_{rs} = 0$$

.....(CII; 3;15)

Equation (3;15) cannot be derived from equation (2;17) without the previous assumption of the serial solution (3;1). The serial solution is not therefore a general solution for equation (2;17). However, each solution of equation (3;15) individually satisfies equation (2;17). Hence, if the form of a harmonic is such that it is fully described by a single solution of equation (3;15), this solution is the relevant solution of equation (2;17).

The logarithmic transfer factors associated with the different solutions of equation (3;15) will each be of different value. Therefore the components of each solution will decay at different rates in the direction of flow. The solution which decays least rapidly is called here the 'primary' solution and is signified by the subscript, s, being unity. The transfer factor associated with this solution is that with the smallest negative real part. At some cross-section in the flow system, the component of primary solution will be dominant, all other components having decayed to insignificant levels. At this point the primary solution of equation (3;15) is the relevant solution of equation (2;17).

In the exact analysis of equation (2;17) only the first term of the serial solution (3;1) is of significance. If, however, the term in equation (2;17) which describes diffusion in the direction of flow is small, the serial solution represents a useful approximation.

to a full solution of equation (2;17). With this term disregarded, a modified form of equation (3;15) is derived from equation (2;17) by the method of separation of variables

$$\sum_{j=2}^{j=3} \frac{\partial}{\partial \xi_j}\left(\psi \frac{\partial f_{rs}}{\partial \xi_j}\right) - \left(\Phi \chi \alpha_{rs} + i r \Omega\right) f_{rs} = 0$$

.....(CII; 3;16)

Equation (3;16) has a set of solutions which are orthogonal with respect to the cross-section of the flow system.

A condition for the approximation is based upon the difference between equations (3;15) and (3;16). If the transfer factors in these two equations are assumed to be identical, the difference between the equations lies only in the term containing the square of the transfer factor. The condition is that the omission of this term should not significantly effect the value of the real part of the total coefficient.

$$R\{\alpha_{rs}^2\} \ll \Phi R\{\alpha_{rs}\}$$

.....(CII. 3;17)

A similar expression might be derived for the imaginary part of the coefficient.

3.1 THE CONVERGENCE CONDITION

The series solution (3;1) enables a condition to be defined for the case where only the primary solution of equation (3;15) is of significance. This condition, which is called here the 'convergence condition' demands that the contribution of the primary solution to a harmonic component should be much greater than that of any other solution.

$$s \neq 1 , \qquad X_{r1}(\xi_1) >> X_{rs}(\xi_1)$$

.....(CII; 3;18)

The condition is more usefully expressed if it is assumed that at some cross-section, ξ_1', in the flow system all solutions are of approximately equal importance, In this case only the solution which decays second least rapidly in the direction of flow need be compared with the primary solution.

The condition (3;19) is derived from equation (3;18) through the exponential relationship of equation (3;10).

$$\xi_1 - \xi_1' >> \frac{1}{R\{\alpha_{r1} - \alpha_{r2}\}}$$

.....(CII; 3;19)

If the convergence condition is satisfied, the Fourier series (2;4) is rewritten (in dimensionless space coordinates),

$$C_A(\xi_1, \xi_2, \xi_3, t) = \sum_{r=0}^{\infty} R\{X_{r10} e^{\alpha_{r1}\xi_1 + ir\omega t} f_{r1}(\xi_2, \xi_3)\}$$

.....(CII; 3;20)

Mean concentration with respect to the cross-section, $\bar{C}_A$, is found by integrating the right hand side of equation (3;20) taking the relationship (3;2) into account.

$$\bar{C}_A(\xi_1, t) = \sum_{r=0}^{\infty} R\{X_{r10} e^{\alpha_{r1}\xi_1 + ir\omega t}\}$$

.....(CII; 3;21)

A similar equation may be derived from equation (2;11) under the same conditions.

The terms of the harmonic series in equation (3;21) are separable by Fourier analysis. The logarithmic transfer factors associated with primary solutions of equation (3;15) are therefore measurable in tracer experiments in which cross-sectional mean concentration is measured and in which the convergence condition is satisfied. From the behaviour of the mean concentration in any cross-section, ξ_1, a set of complex coefficients, $\bar{\zeta}_r$, is derived using the approximate Fourier transform. These coefficients are the terms of equation (3;21).

$$\bar{C}_r(\xi_1) = X_{r10} e^{\alpha_{r1}\xi_1}$$

.....(CII; 3;22)

The logarithmic transfer factor, α_{r1}, is calculated from the coefficients for the relevant harmonic found at two different cross-sections.

$$\alpha_{r1} = \frac{a}{L} \log_e \left(\frac{\bar{C}_r(\frac{L}{a})}{\bar{C}_r(0)} \right)$$

.....(CII; 3;23)

If the tracer signal is sinusoidal and the response measurement in terms of phase lag, ϕ, in degrees, and the logarithm of the amplitude ratio, φ, the two parts of the logarithmic transfer factor are found separately.

$$R\{\alpha_{r1}\} = \frac{a}{L}\varphi$$

$$I\{\alpha_{r1}\} = -\frac{\pi a}{180 L}\phi$$

.....(CII; 3;24,25)

3.2 'ZERO FREQUENCY' SOLUTIONS OF EQUATION (3;15)

In the general case, equation (3;15) cannot be solved without the geometrical, flow and diffusion characteristics of the flow system being first fully specified. However, for the static, or 'zero frequency' component of a tracer disturbance a solution of equation (3;15) is available. If the frequency term is zero, equation (3;15) is satisfied by a constant.

$$f_{os}(\zeta_2, \zeta_3) = A$$

The logarithmic transfer factor associated with this solution is zero. As a transfer factor with a negative real part smaller than zero will not satisfy condition (3;14) this solution must be primary. Thus,

$$\alpha_{o1} = o$$

$$f_{o1}(\xi_2, \xi_3) = 1$$

.....(CII; 3;26, 27)

Equation (3;2) is taken into account in equation (3;27).

Consideration of equations (3;26) and (3;27) shows that if the convergence condition (3;19) is satisfied, distribution of the time integral of tracer disturbance as defined in equations (2;6) or (2, 13) is uniform in the flow system. Non-primary solutions of equation (3;15) must therefore refer to where distribution of this integral quantity is not uniform. It may also be shown that primary solutions of equation (3;15) in general refer to the most uniform distribution of tracer disturbance in the cross-section of the flow system.

4. THE DISPERSION MODEL

Taylor [4,5,6] and Aris[7] have shown that the behaviour of dissolved material in a tubular flow system conforms to a 'plug flow with mixing' model under certain conditions. They also showed that the mixing is of the Fickian type and derived expressions for an axial diffusion or 'dispersion' coefficient. In this section a simpler and more satisfactory derivation of the dispersion model is presented. The model is also modified so as to remove one of the qualifying conditions of the Taylor/Aris model. The arguments apply to all flow systems of uniform cross-section (see section 1). and are not limited to tubular flow systems.

If the dispersion model holds, the behaviour of the cross-sectional mean concentration of the dissolved material, $\bar{C}_A$, is governed by a second order partial differential equation in longitudinal space and time.

$$k \frac{\partial^2 \bar{C}_A}{\partial x_1^2} - \bar{U} \frac{\partial \bar{C}_A}{\partial x_1} - \frac{\partial \bar{C}_A}{\partial t} = 0$$

..... (CII, 4;1)

where the coefficient of the first term, k, is the 'Taylor/Aris' dispersion coefficient.

Of the two boundary conditions necessary to equation (4;1), the first specifies the behaviour of mean concentration in the plane of the origin of the longitudinal axis.

$$x_1 = o \quad , \qquad \bar{C}_A (o, t) = \bar{C}_{Ao} (t)$$

..... (CII, 4;2)

The second condition arises from the assumption of the unlimited length of the flow system. In this case, all concentration gradients must decay to zero.

$$\lim_{x_1 \to \infty} \frac{\partial \bar{C}_B}{\partial x_1} = o$$

..... (CII, 4;3)

The terms of equation (4;1) and the boundary conditions (4;2) and (4;3) may be subjected to the same transformations as were the terms of equation (1;1). Equation (4;1) is transformed by this means to an ordinary second order linear equation.

$$K \frac{\partial^2 \bar{C}_r}{\partial x_1^2} - \bar{U} \frac{\partial \bar{C}_r}{\partial x_1} - i_r + \omega \bar{C}_r = o$$

The terms of this equation are reduced to a dimensionless form through the introduction of the same groupings as those in equation (2;17).

$$\frac{\kappa}{\bar{D}} \frac{d^2 \bar{C}_r}{d \xi_1^2} - \Phi \frac{d \bar{C}_r}{d \xi_1} - i r \Omega \bar{C}_r = 0$$

.....(CII , 4;4)

The boundary conditions (4;2) and (4;3) may be treated in the same way.

$$\xi_1 = 0 , \qquad \bar{C}_r(0) = \bar{C}_{r0}$$

$$\underset{\xi_1 \to \infty}{\text{Limit}} \quad \frac{d \bar{C}_r}{d \xi_1} = 0$$

.....(CII. 4;5,6)

It is convenient to consider the validity of equation (4;4) to be based upon two separate assumptions. The first of these assumptions is that the behaviour of the cross-sectional mean transient quantity, $\bar{C}_t$, is described by a single exponential function. It has been shown, in the previous section, that this is only true when the convergence condition (3;19) is satisfied. One of the conditions for the dispersion model (stipulated by Taylor and Aris) is that a quari-equilibrium concentration profile should be established in the cross-section of the flow system. This condition is identical to the convergence condition.

The second assumption underlying equation (4;4) is that there exists a real dispersion coefficient which is the same for all harmonic components of concentration signals. The behaviour of the cross-sectional mean transient quantity is, however, described by equation (3;22), (provided the convergence condition is satisfied). The complex transfer factor, α_{r1}, is determined from primary solutions of equation (3;15). Equation (4;4) can only be satisfied by exponential

functions in which the transfer factor is real, and is thus only true for the zero frequency component of a tracer signal. Because the behaviour of the zero frequency component has no dynamic significane the usefulness of the Taylor/Aris coefficient is confined to its being the limiting value of the two general dispersion coefficients developed in the next two sections of this chapter.

4.1 COMPLEX DISPERSION COEFFICIENT

The Taylor/Aris dispersion coefficient in equation (4;4) may be replaced by a complex coefficient the value of which is such that equation (3;22) satisfies equation (4;4).

$$\frac{K_r}{D}\frac{d^2\bar{C}_r}{d\xi_1^2} - \Phi\frac{d\bar{C}_r}{d\xi_1} - i_r\Omega\bar{C}_r = 0$$

.....(CII, 4;7)

The complex dispersion coefficient, K_r is a frequency dependent quantity. An expression for it in terms of the integral quantities of equation (3;7) is derived through comparing the auxiliary equation of this equation with that of equation (4;7).

$$\frac{K_r}{D} = \phi_{r1} - \frac{\Phi}{\alpha_{r1}}(\zeta_{r1} - 1)$$

.....(CII, 4;8)

The complex dispersion coefficient at the limit of zero frequency is equal to the Taylor/Aris dispersion coefficient.

$$\lim_{\Omega \to 0} \quad K_r = K$$

.....(CII, 4;9)

Philip[8] was able to verify equation (4;9) in the case of laminar flow in tubes through computed values of the complex dispersion coefficient. Equation (4;9) is, however, a definition of the Taylor/Aris coefficient. An expression for the Taylor/Aris coefficient is derived from this equation (see section 4.3 of this chapter), which yields results identical to those of the analysis of Taylor and Aris.

4.2 VARIABLE REFERENCE PLANE DISPERSION COEFFICIENT

The variable reference plane dispersion coefficient is derived in a manner similar to that of the complex dispersion coefficient. The coefficients of both the first and the second terms of equation (4;4) may be adjusted such that equation (3;22) becomes a solution of this equation with both coefficients remaining real. The resulting differential equation is written,

$$\frac{K_r}{\bar{D}} \frac{d^2 \bar{C}_r}{d \xi_1^2} - \Phi_r \frac{d \bar{C}_r}{d \xi_1} - i r \Omega \bar{C}_r = 0$$

.....(CII, 4;10)

where k_r is the variable reference plane dispersion coefficient.

The coefficient of the second term of equation (4;10), Φ_r, is related to the velocity, V_t, of a moving plane of reference.

$$\Phi_r = \frac{V_r\, a}{D}$$

The velocity of the reference plane is a function of frequency and is always greater than the mean flow velocity. The reference plane velocity approaches the mean flow velocity as frequency tends to zero.

$$\lim_{\Omega \to 0} \quad V_r = \bar{U}$$

.....(CII, 4;11)

As with the complex dispersion coefficient, the variable reference plane coefficient may be expressed in terms of the integral quantities of equation (3;7).

$$\frac{\kappa_r}{D} = \phi_{r1} - \frac{\Phi}{\alpha_{r1}} \left(\tau_{r1} - \frac{V_r}{U} \right)$$

.....(CII, 4;12)

Because the left hand side of equation (4;12) must, by definition, be completely real, the reference plane velocity is also determined by this equation. The Taylor/Aris dispersion coefficient is, as may be demonstrated through equations (4;11) and (4;12), the limiting value of the variable reference plane coefficient for zero frequency.

$$\lim_{\Omega \to 0} \quad \kappa_r = \kappa$$

.....(CII, 4;13)

The variable reference plane dispersion coefficient has an important advantage over the complex coefficient in that it conveys a physical picture of the dispersion process. The picture conveyed is one of 'plug flow with axial diffusion' in which both the diffusion coefficient and the flow velocity are functions of frequency. Frequency response data may be derived from the reference plane velocity and dispersion coefficient data in a reasonably straight forward fashion. The complex dispersion coefficient neither offers a physical picture nor a simple method by which response data may be obtained.

The reference plane velocity and dispersion coefficient are more conveniently expressed in terms of the logarithmic transfer factor than in the form of equation (4;12).

$$\frac{V_r}{\bar{U}} = \frac{r\,\Omega}{\gamma_r\,\Phi} \cdot \frac{\beta_r^2 - \gamma_r^2}{\beta_r^2 + \gamma_r^2}$$

$$\frac{K_r}{\bar{D}} = r\,\Omega \cdot \frac{\beta_r}{\gamma_r(\beta_r^2 + \gamma_r^2)}$$

.....(CII, 4;14,15)

where $\alpha_{r1} = \beta_r + i\,\gamma_r$

If the real part of the transfer factor is much smaller than the imaginary part, equations (4;14) and (4;15) are usefully simplified.

$$|\beta_r| << |\gamma_r| \,, \qquad \frac{V_r}{\bar{U}} = -\frac{r\,\Omega}{\gamma_r\,\Phi}$$

$$|\beta_r| << |\gamma_r| \;, \qquad \frac{K_r}{\bar{D}} = \frac{r\,\Omega\,\beta_r}{\gamma_r^3}$$

.....(CII, 4;16,17)

4.3 THE TAYLOR/ARIS DISPERSION COEFFICIENT

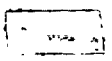
There are two alternative definitions of the Taylor/Aris dispersion coefficient. The first arises from the work of Taylor and Aris where the coefficient describes the rate of spreading out of pulse tracer signals under very restricted conditions. In the second alternative, the coefficient is the limiting value of the complex or the variable reference plane dispersion coefficients which are derived from dynamic response data as in the work of Philip and in this work. The fact that the coefficients arising from these two definitions are identical is demonstrated through comparing expressions for them for particular flow systems. Comparison of general expressions is not possible as one was not developed for the Taylor/Aris analysis. A general expression for the dispersion coefficient as defined by the complex or the variable reference plane coefficients is developed in this section.

Equations (4;8) and (4;9) may be combined to form a limiting expression for the Taylor/Aris dispersion coefficient.

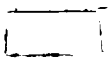
$$\frac{K}{\bar{D}} = \underset{\Omega \to 0}{Limit} \left\{ \phi_{r-1} - \frac{\Phi}{\alpha_{r-1}} \left(\tau_{r-1} - 1 \right) \right\}$$

.....(CII, 4;18)

The solution of equation (3;15) at the limit of 'zero frequency' is expressed in equation (3;27). The values of the integral quantities of equation (4;18) (defined in equations (3;8) and (3;9)) at this limit are therefore unity.



$$\underset{\Omega \to 0}{\text{Limit}} \quad \phi_{r+1} = 1$$



$$\underset{\Omega \to 0}{\text{Limit}} \quad \tau_{r+1} = 1$$

The first term of the right hand side of equation (4;18) is thus evaluated directly and the equation rewritten.

$$\frac{K}{D} = 1 - \underset{\Omega \to 0}{\text{Limit}} \left\{ \frac{\Phi}{\alpha_{r+1}} \left(\tau_{r+1} - 1 \right) \right\}$$

.....(CII, 4;19)

The limiting value of the second term on the right hand side of equation (4;19) cannot be found by direct means. It is necessary to use an alternative expression for the zero frequency solution of equation (3;15) to that of equation (3;27). This expression must contain the logarithmic transfer factor as a multiplying factor for every term. Such an expression is derived from the Maclaurin expression (for two independent variables).

$$f_{r+1}(\zeta_2, \zeta_3) = \sum_{m=0}^{\infty} \sum_{n=0}^{\infty} \frac{\zeta_2^m}{\lfloor m} \cdot \frac{\zeta_3^n}{\lfloor n} D_2^m D_3^n f_{r+1}(0,0)$$

.....(CII, 4;20)

where the differential operator, D_j, is that with respect to space in the axis, ξ_j.

The auxiliary equation related to equation (4;7) may be used to eliminate the frequency term in equation (3;15).

$$\sum_{j=2}^{j=3} \frac{\partial}{\partial \xi_j} \left(\psi \frac{\partial f_{r1}}{\partial \xi_j} \right) = - \alpha_{r1} \left[\left(\psi - \frac{K_r}{D} \right) \alpha_{r1} - (\chi - 1) \Phi \right] f_{r1}$$

.....(CII, 4;21)

with the maclaurin series used as a substitution in the right hand side of equation (4;21), both sides of this equation become integrable with respect to the cross-section of the flow system.

Equation (4;21) is first integrated over a certain part of the area of cross-section, A', the periphery of which is denoted P_T. The left hand side of equation (4;21) is integrated by means of Green's lemma, as expressed in equation (3;6).

$$\int_{P_T} \psi \frac{\partial f_{r1}}{\partial \xi_T} \, d P_T = - \alpha_{r1} \sum_{m=0}^{\infty} \sum_{n=0}^{\infty} D_2^m D_3^n f_{r1}(0,0) \cdots$$

$$\cdots \int_{A'} \left[\left(\psi - \frac{K_r}{D} \right) \alpha_{r1} - (\chi - 1) \Phi \right] \frac{\xi_2^m}{\lfloor m} \cdot \frac{\xi_3^n}{\lfloor n} \, d\xi_2 \, d\xi_3$$

.....(CII, 4;22)

where ξ_T signifies length normal to the periphy of the area over which integration takes place.

The area, A', is determined in such a manner that the differential quantity, $\frac{\partial f_{r1}}{\partial \xi_T}$, normal to its periphery is constant round the periphery.

$$\text{On} \quad P_T \;, \qquad \frac{\partial f_{r1}}{\partial \xi_T} = \text{constant}$$

.....(CII, 4;23)

Since the periphery of the flow system satisfies this definition (see boundary condition (3;4)), and since the cross-sectional function is continuous, all such areas must be completely included within the cross-section of the flow system. The area of integration refers to both the real and the imaginary parts of the complex differential quantity, $\frac{\partial f_{r1}}{\partial \xi_T}$, separately.

For an area as defined in equation (4;23) equation (4;22) may be rewritten to form an expression for the differential quantity.

$$\frac{\partial f_{r1}}{\partial \xi_T} = - \frac{\alpha_{r1}}{\int_{P_T} \psi \, d P_T} \sum_{m=0}^{\infty} \sum_{n=0}^{\infty} D_2^m D_3^n f_{r1}(0,0) \ldots$$

$$\ldots \int_{A'} \left[\left(\psi - \frac{K_r}{D} \right) \alpha_{r1} - (\gamma - 1) \Phi \right] \frac{\xi_2^m}{m} \frac{\xi_3^n}{n} \, d\xi_2 \, d\xi_3$$

.....(CII, 4;24)

This expression may be integrated with respect to the path between the point, (o,o), and any point, (ξ_2', ξ_3'), in the cross-section of the flow system.

$$f_{r+1}(\xi_2', \xi_3') - f_{r+1}(0,0) = \dots$$

$$\dots \alpha_{r+1} \sum_{m=0}^{\infty} \sum_{n=0}^{\infty} D_2^m D_3^n f_{r+1}(0,0) \int_{(0,0)}^{(\xi_2', \xi_3')} \frac{d\xi_T}{\int_{P_T} \psi \, dP_T} \int_{A'} \dots d\xi_2 \, d\xi_3$$

.....(CII, 4;25)

The limiting value of the second term on the right hand side of equation (4;19) is found using equation (4;25) as a substitution for the cross-sectional function.

$$\lim_{\Omega \to 0} \left\{ \frac{\Phi}{\alpha_{r+1}} (\tau_{r+1} - 1) \right\} = \lim_{\Omega \to 0} \left\{ \frac{\Phi}{\alpha_{r+1}} \int_A f_{r+1} (\gamma - 1) \, d\xi_2' \, d\xi_3' \right\}$$

$$= \lim_{\Omega \to 0} \left\{ -\Phi \sum_{m=0}^{\infty} \sum_{n=0}^{\infty} D_2^m D_3^n f_{r+1}(0,0) \int_A (\gamma - 1) \, d\xi_2' \, d\xi_3' \int_{(0,0)}^{(\xi_2', \xi_3')} \dots d\xi_2 \, d\xi_3 \right\}$$

.....(CII, 4;26)

The limiting values of the differential terms of equation (4;26) are found through equations (3;26) and (3;27).

Therefore there is only one non-zero term in equation (4;26). Combining equation (4;19) and the limiting value of equation (4;26), a general expression for the Taylor/Aris dispersion coefficient is derived.

$$\frac{K}{\bar{D}} = 1 - \Phi^2 \int_A (\gamma - 1)\, d\xi_2' d\xi_3' \int_{(0,0)}^{(\xi_2', \xi_3')} \frac{d\xi_T}{\int_{P_T} \psi\, dP_T} \int_{A'} (\gamma - 1)\, d\xi_2 d\xi_3$$

.....(CII, 4;27)

From equation (3;27), it is seen that the definition of the area of integration, A', as expressed in equation (4;23) is not definitive at the limit of zero frequency. The most convenient definition of this area may therefore be used. For the flow systems considered, the most convenient definition of the area of integration is that which states that the diffusivity at the periphery of this area must be constant.

$$\text{On } P_T, \qquad \psi = \text{constant}$$

$$\frac{K}{\bar{D}} = 1 - \Phi^2 \int_A (\gamma - 1)\, d\xi_2' d\xi_3' \int_{(0,0)}^{(\xi_2', \xi_3')} \frac{d\xi_T}{\psi P_T} \int_{A'} (\gamma - 1)\, d\xi_2 d\xi_3$$

.....(CII, 4;28)

4.4 The Taylor/Aris Dispersion Coefficient for various flow systems

Explicit expressions are found for the Taylor/Aris dispersion coefficient of flow systems of parallel walls, tubular and of annular geometry. In all of these flow systems the point properties, fluid velocity and diffusivity, can be expressed as functions of a single co-ordinate.

Parallel Wall Flow System

Because equation (4;28) is written in cartesian co-ordinates, the deviation of the expression of the Taylor/Aris coefficient for a parallel wall flow system is straight forward. The geometrical properties of a parallel wall flow system are described in section five of this chapter. For convenience, the width of the flow system cross-section in the axis parallel to the walls (x_3 axis) is limited to one dimensionless unit. The intermediate area of integration, A', is rectangular in shape, and is symmetrical about the axis of the flow system, its perimeter being represented by the lines:-

$$\xi_2 = -\xi_2' \qquad \& \qquad \xi_2 = +\xi_2'$$

The limit point of the path integral is similarly represented by :-

$$\xi_2' = \xi_2''$$

Equation (4;28) for a parallel wall flow system becomes:-

$$\frac{K}{\bar{D}} = 1 - \frac{\bar{U}^2 a^2}{\bar{D}^2} \int_{-\frac{1}{2}}^{\frac{1}{2}} (\chi - 1)\, d\xi_2'' \int_0^{\xi_2''} \frac{d\xi_2'}{2\psi} \int_{-\xi_2'}^{\xi_2'} (\chi - 1)\, d\xi_2$$

In this expression, it is only necessary to integrate over one half of the flow system because the system is symmetrical. If also the semi-gap width of the flow system, b, and the dimensionless transverse co-ordinate, η , are used as is conventional, this expression becomes:-

$$\frac{K}{\bar{D}} = 1 - \frac{\bar{U}^2 b^2}{\bar{D}^2} \int_0^1 (\chi - 1)\, d\eta'' \int_0^{\eta''} \frac{d\eta'}{\psi} \int_0^{\eta'} (\chi - 1)\, d\eta \qquad \ldots\ldots\ldots \text{(CII,4;29)}$$

A simple expression for the Taylor/Aris dispersion coefficient under laminar flow conditions is derived from equation (4;29). In laminar flow:-

$$\psi = 1$$

$$\chi = 1.5\,(1 - \eta^2)$$

$$\frac{K}{D_A} = 1 + \frac{\bar{U}^2 b^2}{52.5\, D_A^2} \qquad \ldots\ldots\ldots \text{(CII, 4;30)}$$

Equation (4;30) is in complete agreement with the expression found by Wooding [11] for the Taylor/Aris coefficient in laminar flow in a parallel wall flow system, Wooding adapted the method of analysis due to Aris to derive this result.

Tubular Flow Systems

The properties of a tubular flow system are dependent only upon the distance from the axis of flow. Equation (4;28) is therefore converted to a polar co-ordinate system in which the angular co-ordinate is eliminated for such a flow system.

$$\frac{K}{\bar{D}} = 1 - 2\frac{\bar{U}^2 R_t^2}{\bar{D}^2}\int_0^1 (\gamma - 1)\rho^* d\rho^* \int_0^{\rho^*} \frac{d\rho'}{\psi\rho'} \int_0^{\rho'} (\gamma - 1)\rho\, d\rho$$

.....(CII, 4;31)

where the dimensionless radial co-ordinate, ρ, is relative to the radius, R_t, of the flow system.

For laminar flow in a tubular flow system:-

$$\psi = 1$$

$$\gamma = 2(1 - \rho^2)$$

$$\frac{K}{D_A} = 1 + \frac{\bar{U}^2 R_t^2}{48 D_A^2}$$

.....(CII, 4;32)

Equation (4;32) is in agreement with the expression for dispersion coefficient in laminar flow in a tube found by Aris[7].

Annular Flow Systems

Because the central reference point of an annular flow system is outside the area of flow, the first limit of integration in equation (4;28) must be taken at the inner wall of the flow system. For simplicity the converted form of this expression is not written in dimensionless co-ordinates.

$$\frac{K}{\bar{D}} = 1 - \frac{2\bar{U}^2}{\bar{D}^2(R_o^2 - R_i^2)} \int_{R_i}^{R_o} (\chi - 1)\, r''\, dr'' \int_{R_i}^{r''} \frac{dr'}{\psi r'} \int_{R_i}^{r'} (\chi - 1)\, r\, dr$$

.....(CII, 4;33)

where radial position is expressed as the distance, r, from the centre of the flow system, the walls being denoted:-

$$r = R_i$$

$$r = R_o$$

To facilitate comparison between a parallel wall and an annular flow system, a dimensionless radial co-ordinate, η_a, is adopted for the annular flow system.

$$\bar{R} = \frac{1}{2}(R_o + R_i)$$

$$b = \frac{1}{2}(R_o - R_i)$$

$$\eta_a = \frac{r - \bar{R}}{b}$$

The dimension, b, is equivalent to the semi-gap width of the parallel wall system. The aspect ratio of the annular flow system is the ratio of this dimension to the mean wall radius, $\bar{R}$.

The velocity profile and mean velocity for laminar flow in an

annular flow system may be expressed as power series of the aspect ratio.

$$U = -\frac{P'b^2}{2\mu}\left\{1-\eta_a^2-\frac{1}{3}[\eta_a-\eta_a^3]\frac{b}{R}+\frac{1}{12}[1+2\eta_a^2-3\eta_a^4]\frac{b^2}{R^2}\ldots.\right\}$$

$$\bar{U} = -\frac{P'b^2}{2\mu}\left\{1+\frac{1}{15}\cdot\frac{b^2}{R^2}+\frac{11}{315}\cdot\frac{b^4}{R^4}\ldots.\right\}$$

where μ is the viscosity of the fluid and P' is the pressure gradient in the direction of flow. An expression for the Taylor/ Aris dispersion coefficient is therefore derived also in the form of a power series.

$$\frac{K}{D_A} = 1+\frac{\bar{U}^2b^2}{52.5\,D_A^2}\left\{1+1.4\,\frac{b^2}{R^2}\ldots.\right\}$$

.....(CII, 4;34)

Equation (4;34) is expanded to the first four powers of the aspect ratio, the second and fourth terms being zero. As the aspect ratio of an annular flow system tends to zero, the flow system geometry tends to that of a parallel wall flow system, and equation (4;34) tends towards equation (4;30).

5. THEORETICAL RESPONSE DATA FOR A PARALLEL WALL FLOW SYSTEM

In the work described in this thesis, experimental tracer response data for turbulent flow in an annular flow system are compared with theoretical data prepared through the computer solution of equation (3;15). Because the aspect ratio of this flow system was small, it was assumed that its properties differed little from those of a parallel wall flow system. The theoretical response data were therefore computed for a parallel wall flow system. The advantage in solving equation (3;15) for such a flow system arises from the symmetry of the flow system about its centre line. The equation has therefore only to be solved over half the cross-section of the flow system. The amount of computer time required for a solution of given detail is thereby reduced by more than one half.

The closeness of the approach of the annular flow system to a parallel wall flow system for laminar flow is apparent in the expressions for the Taylor/Aris dispersion coefficient. The difference between the right hand side of equation (4;34) and that of equation (4;30) is of no significance in this particular case.

For the system studied:-

$$\frac{b}{\bar{R}} = \frac{1}{17}$$

$$\frac{7}{5}\,\frac{b^2}{\bar{R}^2} \simeq \frac{1}{200}$$

Because turbulent flow in an annular flow system is more uniformly distributed than laminar flow, the effect of the curvature of this flow system must be even smaller under turbulent conditions.

The cartesian coordinate system within which the parallel wall flow system is described, is arranged such that the x_2 axis is normal to the walls of the flow system. The distribution of dissolved material is uniform in the direction of the axis transverse to the flow and parallel to the walls of the flow system (x_3 axis).

$$\frac{\partial f_{rs}}{\partial \zeta_3} = 0$$

Equation (3;15) and the boundary condition (3.4) are rewritten for such a flow system using the dimensionless transverse coordinate, η, which is based upon half the distance between the walls.

$$\frac{d}{d\eta}\left(\psi \frac{d f_{rs}}{d\eta}\right) + \frac{1}{4}\left(\psi \alpha_{rs}^2 - \Phi \chi \alpha_{rs} - i r \Omega\right) f_{rs} = 0$$

$$\eta = \pm 1, \qquad \frac{d f_{rs}}{d\eta} = 0$$

.....(CII; 5; 1,2)

5.1 MATRIX REPRESENTATION OF EQUATION (5;1)

Numerical solutions of equation (5;1) are obtained through 'eigen value' analysis of the finite difference representation of this equation. Point values of the differential terms of the equation are fixed in the manner conventional to finite difference techniques. For a particular point, the values of these terms are determined by parabolic interpolation between the cross-sectional function, f_{rs}, at this point and that at the two points adjacent to it in the cross-section of the flow system. Exceptions to this exist at the centre of the flow system and at the wall where the values of the terms are determined by the boundary condition.

For simplicity, the suffices are dropped from the cross-sectional function. The differential term of equation (5;1) must first be expanded to two terms.

$$\frac{d}{d\eta}\left(\psi \frac{df}{d\eta}\right) = \psi \frac{d^2 f}{d\eta^2} + \frac{d\psi}{d\eta} \cdot \frac{df}{d\eta}$$

Then by parabolic interpolation for the j^{th} point;-

$$\left(\frac{df}{d\eta}\right)_j = -f_{j-1} \frac{\Delta_j}{\Delta_{j-1}(\Delta_{j-1}+\Delta_j)} + f_j \frac{\Delta_j - \Delta_{j-1}}{\Delta_{j-1}\Delta_j} + f_{j+1} \frac{\Delta_{j-1}}{\Delta_j(\Delta_{j-1}+\Delta_j)}$$

$$= f_{j-1} A_j + f_j B_j + f_{j+1} C_j$$

$$\left(\frac{d^2 f}{d\eta^2}\right)_j = f_{j-1} \frac{2}{\Delta_{j-1}(\Delta_{j-1}+\Delta_j)} - f_j \frac{2}{\Delta_{j-1}\Delta_j} + f_{j+1} \frac{2}{\Delta_j(\Delta_{j-1}+\Delta_j)}$$

$$= f_{j-1} A'_j + f_j B'_j + f_{j+1} C'_j$$

where $$\Delta_j = \eta_{j+1} - \eta_j$$

At the point adjacent to the wall, j = J -1, boundary condition (5;2) holds. The value of the differential terms are here determined by the cross-sectional function at this point and at that next in from the wall of the flow system.

$$\left.\frac{df}{d\eta}\right)_{J-1} = \left\{ -f_{J-2} + f_{J-1} \right\} \cdot \frac{2\Delta_{J-1}}{\Delta_{J-2}(\Delta_{J-2} + 2\Delta_{J-1})}$$

$$= f_{J-2} A_{J-1} + f_{J-1} B_{J-1}$$

$$\left.\frac{d^2 f}{d\eta^2}\right) = \left\{ f_{J-2} - f_{J-1} \right\} \cdot \frac{2}{\Delta_{J-2}(\Delta_{J-2} + 2\Delta_{J-1})}$$

$$= f_{J-2} A'_{J-1} + f_{J-1} B'_{J-1}$$

At the central point of the flow system, j = 1, there exist two alternative values of each differential term. These alternatives arise because solutions of equation (5;1) may be either symmetrical or assymmetrical about the centre of the flow system. The type of solution which is sought must therefore be specified. Primary solutions of equation (5;1) are of the symmetrical type. For a symmetrical solution:-

$$\left.\frac{df}{d\eta}\right) = 0$$

$$\left.\frac{d^2 f}{d\eta^2}\right) = \left\{ -f_1 + f_2 \right\} \cdot \frac{2}{\Delta_1^2}$$

$$= f_1 B'_1 + f_2 C'_1$$

and for an assymmetrical solution:-

$$\left.\frac{df}{d\eta}\right)_1 = \{ -f_1 + f_2 \} \cdot \frac{1}{\Delta_1}$$

$$= f_1 B_1 + f_2 C_1$$

$$\left.\frac{d^2 f}{d\eta^2}\right)_1 = 0$$

Equation (5;1) is thus rewritten in finite difference form, for the central point of the flow system:-

$$\frac{4}{\Phi\chi}\left(\psi B_1' + \frac{d\psi}{d\eta} B_1\right) f_1 + \frac{4}{\Phi\chi}\left(\psi C_1' + \frac{d\psi}{d\eta} C_1\right) f_2 \ \ldots\ .$$

$$\ldots\ . + \frac{1}{\Phi\chi}\left(\psi \alpha_{rs}^2 - i r \Omega\right) f_1 = \alpha_{rs} f_1$$

for any point, j:-

$$\frac{4}{\Phi\chi}\left(\psi A_j' + \frac{d\psi}{d\eta} A_j\right) f_{j-1} + \frac{4}{\Phi\chi}\left(\psi B_j' + \frac{d\psi}{d\eta} B_j\right) f_j \ \ldots\ .$$

$$\ldots\ . + \frac{4}{\Phi\chi}\left(\psi C_j' + \frac{d\psi}{d\eta} C_j\right) f_{j+1} + \frac{1}{\Phi\chi}\left(\psi \alpha_{rs}^2 - i r \Omega\right) f_j = \alpha_{rs} f_j$$

and for the point adjacent to the wall:-

$$\frac{4}{\Phi\chi}\left(\psi A_{J-1}' + \frac{d\psi}{d\eta} A_{J-1}\right) f_{J-2} + \frac{4}{\Phi\chi}\left(\psi B_{J-1}' + \frac{d\psi}{d\eta} B_{J-1}\right) f_{J-1} \ \ldots\ .$$

$$\ldots\ . + \frac{1}{\Phi\chi}\left(\psi \alpha_{rs}^2 - i r \Omega\right) f_{J-1} = \alpha_{rs} f_{J-1}$$

These equations may be represented by a single matrix equation:-

$$T\,F = \alpha_{rs}\,F \qquad \text{.....(CII, 5;3)}$$

where F is a vector matrix (single column), the elements of which are point values of the cross-sectional function, and where T is a tridiagonal matrix. The diagonal element in the j^{th} row of the tridiagonal matrix is:-

$$\frac{4}{\Phi\tau}\left(\psi B_j' + \frac{d\psi}{d\eta} B_j\right) + \frac{1}{\Phi\tau}\left(\psi \alpha_{rs}^2 - i r \Omega\right)$$

The element in the lower triangle of the tridiagonal matrix is:-

$$\frac{4}{\Phi\tau}\left(\psi A_j' + \frac{d\psi}{d\eta} A_j\right)$$

and the element in the j^{th} row of the upper triangle:-

$$\frac{4}{\Phi\tau}\left(\psi C_j' + \frac{d\psi}{d\eta} C_j\right)$$

5.2 SOLUTIONS OF THE MATRIX EQUATION (5;3)

Solutions of equation (5;3) are found through analysis of this equation for its two smallest eigen values. This analysis is not straight forward as the coefficient, α_{rs}, on the right hand side of the equation also occurs in the diagonal elements of the tridiagonal matrix on the left hand of the equation. Equation (5;3) is therefore not exactly of the right type for eigen value analysis. For this reason, an iterative form of analysis is used in which the coefficient is first neglected on the left hand side of the equation. In subsequent iterations the value of the coefficient found from the previous iteration is then used in the tridiagonal matrix. In the flow system under investigation, the coefficient after one iteration was insignificantly different from that of the first analysis. It was infered from this that diffusion in the direction of flow, from which the term in the tridiagonal matrix arose, did not significantly effect the process of dispersion.

The primary solution of equation (5;3) is that corresponding to the eigen value with the smallest negative real part (and consequently smallest modulus). In the analysis for this eigen value an arbitrary vector matrix is premultiplied by the inverse of the operating matrix, T, till the vector matrix reaches an 'equilibrium' form. The form of the equilibrium vector is not changed by further premultiplication. Because the operating matrix is tridiagonal, there is a great advantage in the use of the 'LU' inversion method, which is described in Appendix II (section 1). The logarithmic transfer factor, $_{rs}$, may either be found direct from eigen value analysis or by way of the integral quantities defined in equations (3;8) and (3;9). For primary solutions in the flow system under investigation, the latter

method was found to give better convergence with respect to the size of the operating matrix.

As equation (5;3) presents only approximately an eigen value problem, there exists a set of vector matrices which are solutions of this equation and which are only approximately self-orthogonal. The secondary solution of equation (5;3) is the vector matrix associated with the eigen value with the second smallest negative real part. It is found in a manner similar to that of the primary solution. Because the value of the second eigen value is only necessary on account of condition (3;19) the approximate nature of the solution is of little consequence.

The true secondary solution for a parallel wall flow system is assymmetrical. In consequence, it is of no significance if only those solutions which possess non-zero cross-sectional mean quantities are of interest. In this case, the next symmetrical solution must be found. This solution is termed the secondary symmetrical solution.

CHAPTER III

1.1 THE GEOMETRY OF THE EXPERIMENTAL FLOW SYSTEM

An experimental tracer study was carried out in a flow system of uniform cross-section in which flow was turbulent. In the theory developed in Chapter II, it is shown that, for such a flow system in which the 'convergence' condition is satisfied, the cross-sectional mean concentration of tracer is governed by an exponential function of length in the direction of flow. Therefore a definite and reproducible relationship exists between tracer response measurements at different cross-sections of the flow system. Complete tracer response data for the whole flow system is thus obtained from cross-sectional mean concentration measurements at two different cross-sections.

The geometrical configuration of the cross-section of the experimental flow system must be such that direct measurement of the cross-sectional mean tracer concentration is possible. In a tubular flow system, such a measurement must be made over a segment which is representative of the whole cross-section. Tracer concentration in this case may be measured by the photo-extinction technique in which the light beam is focussed on the axis of the tube. This method was not used on account of the insensitivity of the photo-extinction technique.

The simplest and most commonly used method of tracer concentration measurements (in liquids) is through electrical conductivity. Because the path of an electrical current is normally straight, the mean tracer concentration derived from such a measurement will be a cross-sectional mean only in a flow

system enclosed between parallel walls. However, a true parallel wall flow system cannot be realised in practice as the width of the flow system in the direction parallel to the walls should have to be infinite. There are two flow systems whose geometrical configurations may approximate to that of a parallel wall flow system. There are the flow systems of annular and of rectangular cross-section. An annular flow system was chosen for the experimental work because the fluid dynamics of this system is less complicated than that of a rectangular system. It is also easier to obtain uniform tracer distribution in an annular flow system.

It has been implied that a liquid was to be used as the fluid. Because of the quantity needed, water from the main supply was employed. The deviation of the physical properties of this water from those of pure water were neglected. In calculations of tracer concentrations, a residual conductivity was allowed for. Sodium chloride was used as the tracer material.

1.2 Dimensions of the Annular Flow System

The annular flow system was formed in the space between two concentric tubes. In order that the geometry of the flow system should be close to that of a parallel wall system, the relative difference between the sizes of the tubes was as small as was practicable. The limitations lay in the maximum possible gap width between the concentric tubes, and in the length of precision tube available. It was decided, for reasons of continuity, to have the experimental section of the flow system in one length of tube.

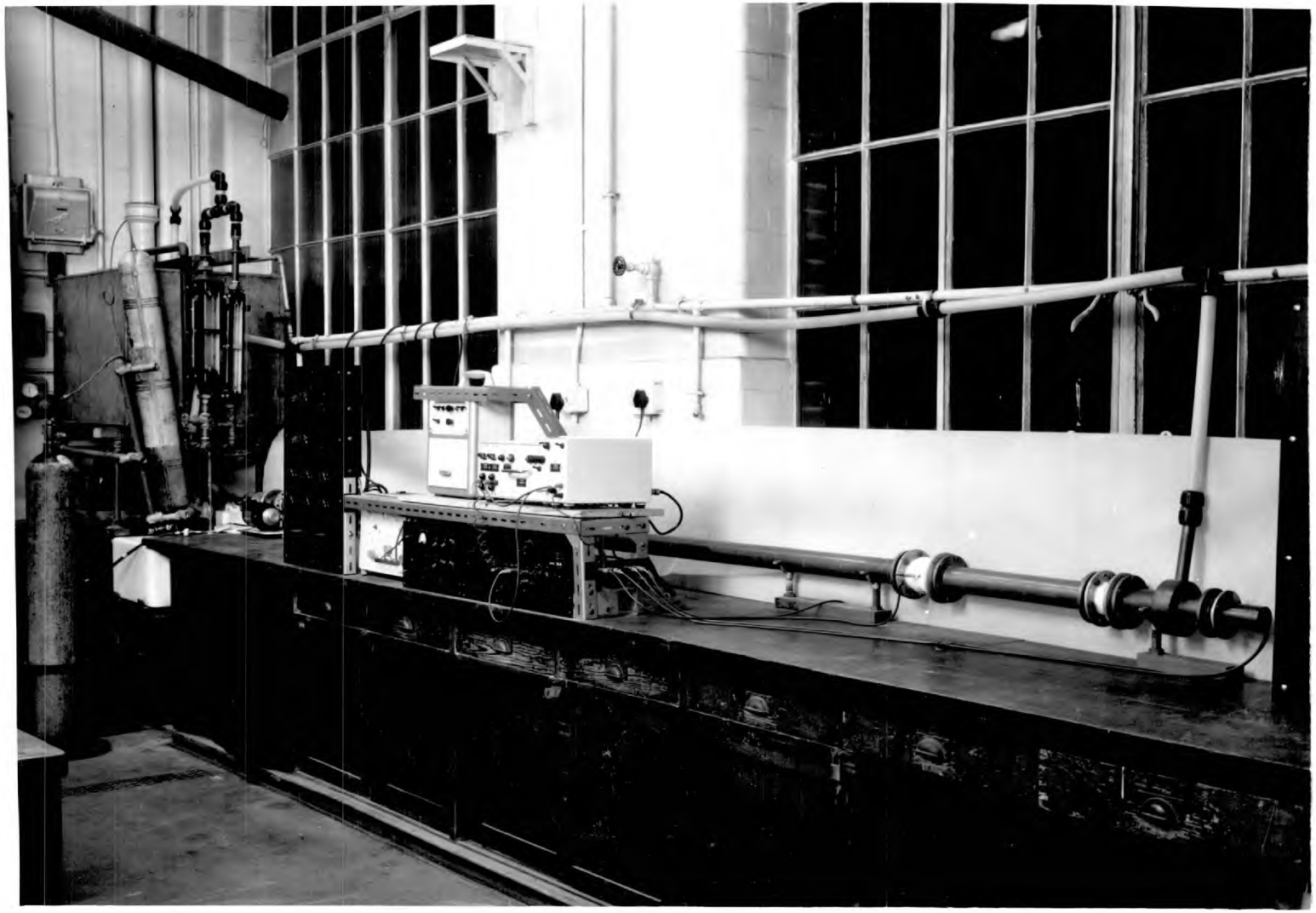
Concerning the gap width, the problem was to maintain uniformity throughout the flow system. Precision drawn brass tube was chosen on account of its availability and the ease with which phosphor bronze could be soldered to it. The two tubes were held apart by means of phosphor bronze ball-bearings which acted as spacers. Taking into account the tolerances of the tubes, and the estimated magnitude of distortion from soldering, it was decided that a gap width of 3/16 inch was the minimum practicable.

Inner and outer tubes of two and two and a half inch nominal diameter respectively, with the same wall thickness of 0.064 inch, were the most convenient available. The tubes were both approximately twelve feet in length, which was sufficient for the purposes of experiment. The ratio of the gap size to tube diameter was also sufficiently small for the flow system geometry to be reasonably close to that of a parallel wall flow system.

A sufficient length of annular flow system upstream of the experimental section must be provided for the velocity profile to become fully developed, and also for the convergence condition (C.II; 3.19) to be satisfied. A flow system length of 130 gap widths

(67 cm) was sufficient to satisfy these conditions. In order to satisfy the convergence conditions for laminar flow, the entry length of the flow system should have been approximately 100 metres

The length of flow system between the downstream end of the experimental section and the outlet is also of importance. It is necessary that this section of annulus should be of sufficient length so that the influence exerted upon experimental results by its actual length should be insignificant. Because an exact boundary condition for the outlet point cannot be defined, a precise length for this section cannot be calculated. A length of 70 centimetres was considered sufficient for the section.



1.3 Construction of the Annular Flow System

The two concentric tubes were held apart by 3/16 inch diameter phosphor-bronze ball bearings, brazed in sets of three evenly spaced round the inner tube, at intervals of one foot (see photograph 2) and figure f.1). To minimise distortion of the inner tube, as little heat as possible was used during brazing. Each ball bearing was filed slightly to enable the inner tube to slide smoothly into the outer tube.

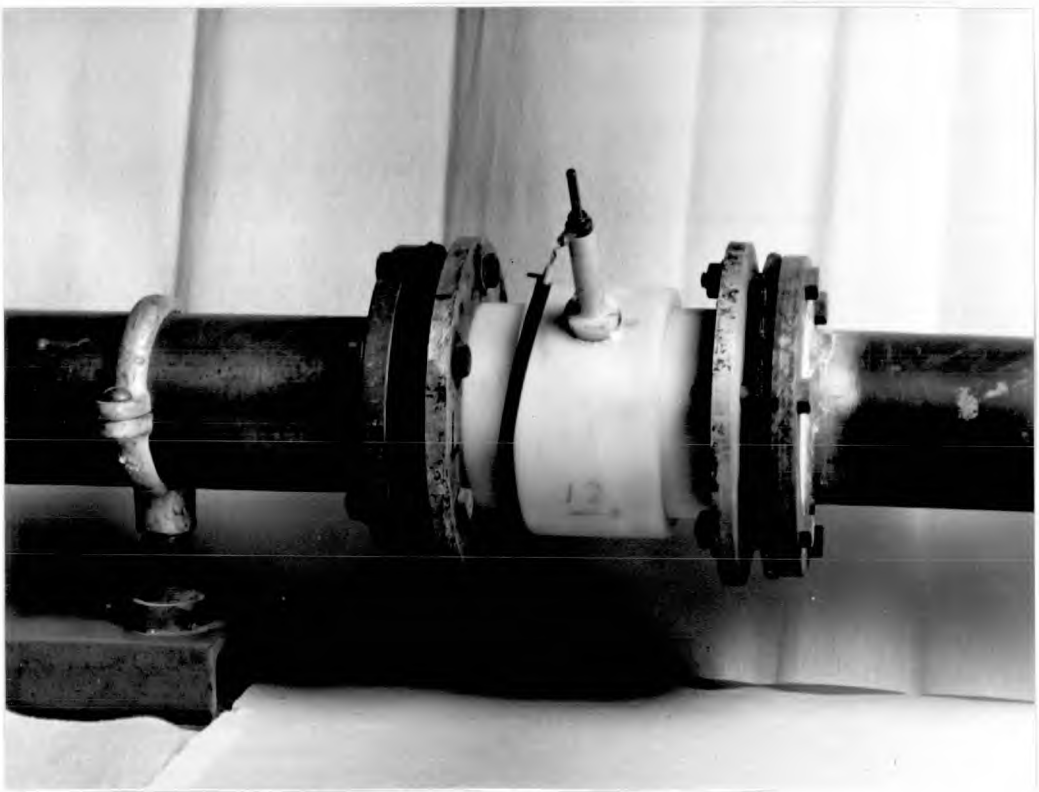
The sections of annulus upstream and downstream of the experimental section were all constructed in a manner identical to that of the experimental section. The inner and outer tube sections were each joined by connection pieces machined from 'delrin', a plastic similar to nylon (see photographs 2 and 3 and figures f.2 and f.3) The use of an electrically insulating material in the connection pieces at either end of the experimental section was necessary since electrodes had to be mounted upon them for conductivity measurements to be made.

The connection pieces for the inner tube (shown in Figure f.3) had a male thread at each end by which they were screwed into threaded discs brazed inside the inner brass tube. The points were made water tight with rubber 'O' rings. A hole 3/8 inch in diameter was drilled through each inner connection piece for electrical leads.

Joints between the outer brass tube sections and the outer connection pieces (see figure f.2) were held by fixed flanges brazed to the former and split backing flanges on the latter. The backing flanges allowed freedom of rotational position. Sealing was effected by rubber gaskets inserted and compressed between the pipe flanges and the flanges of the connection piece. The drawing, F.2 shows an outer connection piece on which an electrode is mounted. For the outer



2. Dismantled annulus with electrodes



3. Connection piece with electrode mounted

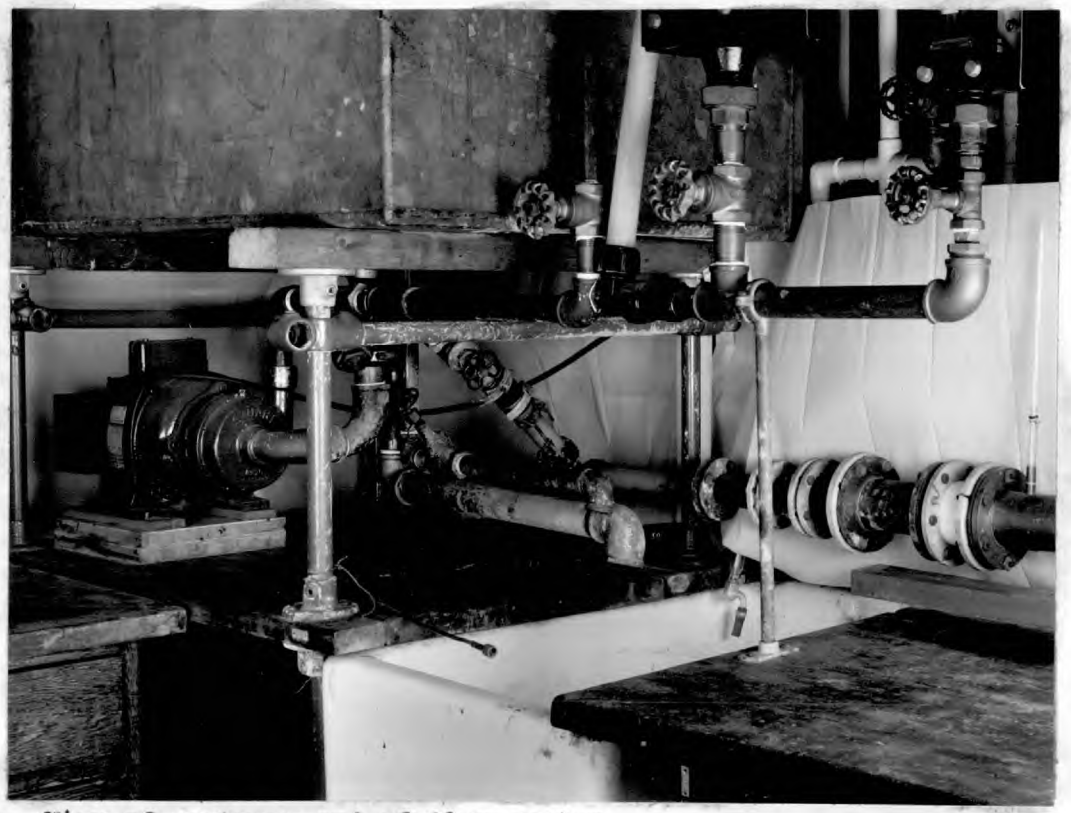
connection pieces without electrodes, the dimensions are identical except that overall length is 2 inches shorter.

The annulus was supported by pipe holders machined to fit the outer tube. These supports were mounted on lengths of mild steel channel, which were themselves screwed to the laboratory bench. The height of each support was adjusted by means of lock nuts on its threaded pillar.

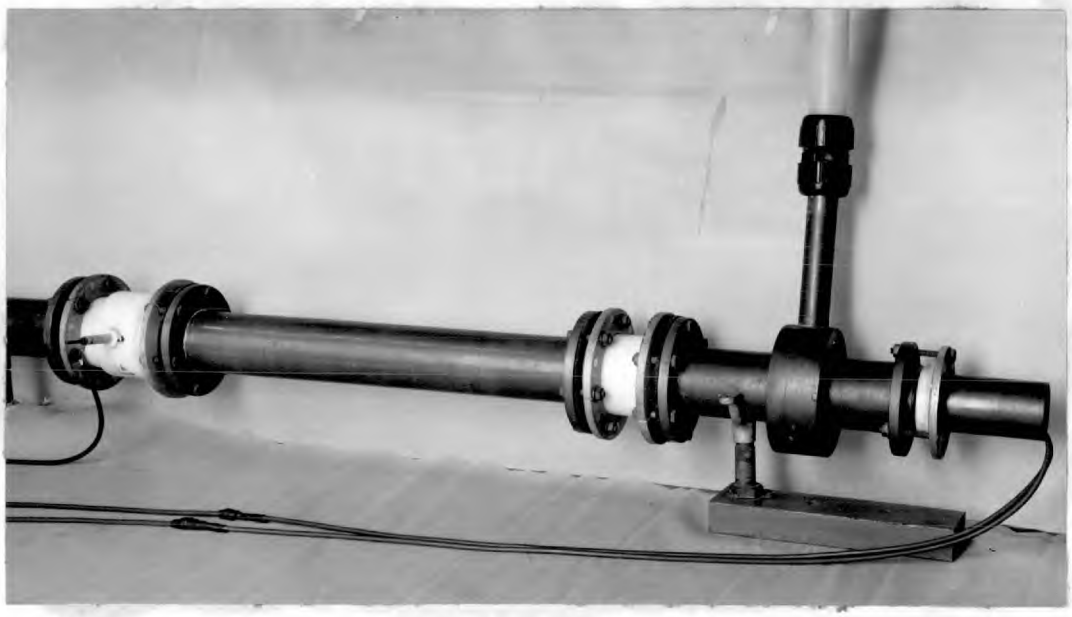
The inlet and outlet points of the annulus were designed so as to encourage circumferential uniformity of flow in the flow system. At the upstream end of the flow system, a cone was fixed to the inner tube and a divergent pipe section fixed to the outer tube to form a smooth entry (see photograph 4 and figure f.4) The cone, which was machined from delrin, was screwed to the inner connection pieces. The divergent pipe section, which was made up from standard divergent pieces in high density polythene, gave an even taper from 1 to $2\frac{1}{2}$ inches diameter.

A similar design was not possible at the downstream end of the annulus. This was on account of the necessity to support the inner tube against drag, and also to allow access for the leads to the electrodes. Water left the annulus through holes evenly spaced around the outer tube in two rows of thirty six each. The holes, which were of 3/16 inch in diameter, were staggered in the two rows relative to each other and led to a space of comparatively large capacity fabricated around the outer tube (see photograph 5 and figure f.5). The end of the annulus gap was sealed by a gland in which a rubber 'O' ring formed the packing.

Facilities for draining, and for temperature and pressure measurement were provided by brazing small brass tubes to the outer tube of the annulus (see figure f.1). To avoid disturbances to flow, none of these were in the experimental section. The temperature of



4. View of upstream end of flow system



5. View of downstream end of flow system

water entering this section was measured with a mercury in glass thermometer at a point close to its upstream end. The thermometer was fixed in a position such that its bulb just did not protude into the annular gap. Because temperature changes along the experimental section never exceeded $0.2^{\circ}C$, the provision of a second thermometer was not necessary.

2.1 Tracer Concentration Measurement and Recording

The cross-sectional mean concentration of the sodium chloride tracer was derived from the water conductivity measured between electrodes set in the inner and outer walls of the annulus. Two difficulties arise from the use of conductivity measurement. The first lies in the fact that an inverse rather than a direct mean conductivity is measured over the volume of liquid enclosed between the electrodes. However, the errors arising from this source are shown (in section 3 of Appendix II) to be very small under the prevailing experimental conditions. The other difficulty is caused by the electrical current paths between the electrodes not being strictly confined to the enclosed volume of liquid. The error due to this is minimised where the electrodes are close together relative to their size.

The two conductivity cells were each formed by a pair of platinum electrodes incorporated in the plastic connection pieces at either end of the experimental section. The inner electrodes were glued into suitable recesses on the surfaces of the inner connection pieces (see photograph 2 and figure f.3). The outer electrodes were mounted on retractable threaded plugs machined from delrin which screwed through the walls of the outer connection pieces (see photographs 2 and 3 and figure f.2). Each electrode was filed down so as to be flush with its surrounding surface. 'Araldite' epoxy resin glue was used for fixing the electrodes.

To avoid corrosion, platinum was used as the electrode material. A special cell was made in which the electrodes could be platinised in the conventional manner with the inner electrode in position. It was found necessary to maintain the platinised

surface on the electrodes in good condition and never allow them to become dry. The electrodes were replatinised twice during experimental work over a period of two months. Deterioration in the platinising introduced a large capacitance effect between the electrodes, and also caused the cell constants to increase.

Conductivity Measuring Circuits

DC electrical signals related to the conductivity of the water in each of the conductivity cells were produced by the bridge/detector circuits (see figure f.2). Each conductivity cell was connected to an arm of an AC wheatstone bridge ci-cuit. Each bridge circuit was supplied with a 5 volt 1000 c/s signal from a source of low impedance. The wheatstone bridge circuits were designed so that the peak potential difference between the electrodes of the cells could not exceed one volt.

The output signal from each bridge was first amplified in a two stage amplification circuit and then converted to DC in a 'phase sensitive detector' circuit. The signals from the detector circuits, which were recorded with a two channel quick response recorder, were thus directly proportional to the out-of-balance AC signals from the bridge circuits. The resistance of each conductivity cell could therefore be calculated from the detector circuit output and from the resistance of the other components in each bridge circuit. The use of the phase sensitive detector circuits largely eliminated the effect of the inductive elements (inter-electrode capacitance etc.) in the bridge circuits.

Each amplification stage was of the 'cathode follower' type to ensure a high degree of stability. The bridge, amplification and detector circuits were all incorporated on the same chassis. The AC supply signal to the bridge circuits and the reference signal to the phase sensitive detector circuits were supplied from an 'Advance' signal generator (type J.1). The thermoionic valves of the amplification

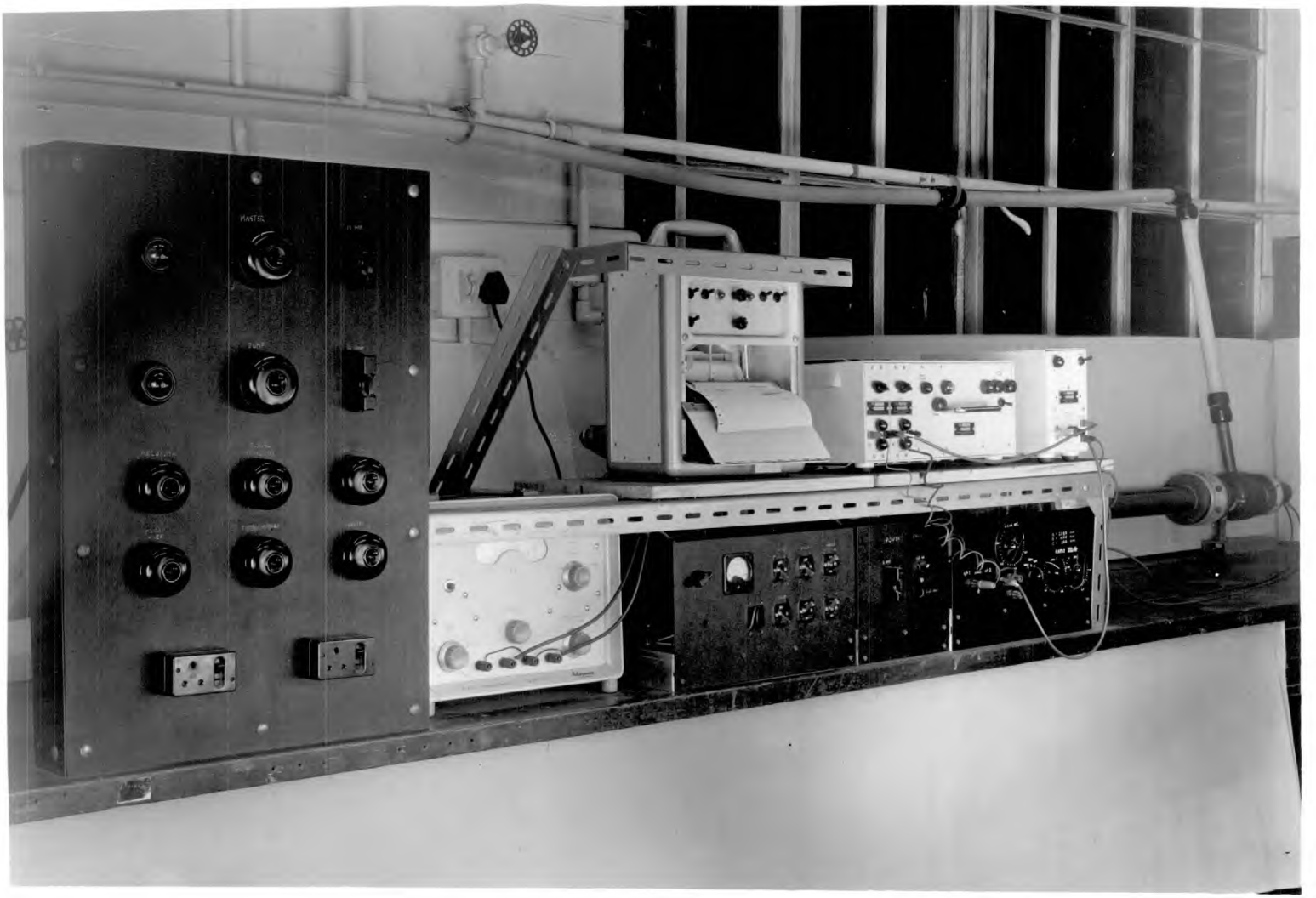
circuits were supplied from a 'power-pack'.

The Recorder

The DC signals from the bridge/detector circuits were recorded on a two channel 'Evershed' quick response recorder (type QU/CRD 21) The pens of this recorder had a full scale (chart width) traverse time of 1/50 second and a linear time constant of 1/60 second. The recorder chart was the 'teledeltos' electrically marked type on which each recorder channel occupied a separate strip three inches wide. With four speed ranges and a choice of two gear boxes, chart speeds of between two inches per minute and six inches per second were available. An event marker pen was also provided.

The recorder had a separate driving amplifier which possessed a range of sensitivities, only the highest of which was used. A pre-amplifier was also included in the downstream cell channel to compensate for the attenuation of tracer signals.

A view of the electrical apparatus is shown in the photograph (6). On the left there is the main switch board. Then on the shelf, from left to right, there are the recorder, recorder driving amplifier and the pre-amplifier. Below on the bench, there are the signal generator the 'time marker', the power pack and the bridge/detector circuits. All connections between these units were by electro-statically screened lead and cable, except where distances were very short. The time marker was a device which generated synchronised electrical pulses (24 per minute) for the measurement of recorder chart speed.


MASTER

2.2. The Tracer Injection System

The tracer injection system (see figure f.8) was designed to impose sinusoidal concentration signals of sodium chloride upon the experimental section by the addition, at a point upstream of the annulus, of a continuously fluctuating stream of the concentrated salt solution. Pulse tracer signals could also be generated by this system. The system operated by inducing sinusoidal variations on top of a steady tracer flow using a 'sine wave generator' consisting of a reciprocating piston and cylinder arrangement. The tracer was then mixed into the water at a suitable point upstream of the annular flow system in a two stage mixing cell.

The concentrated tracer solution was fed from the tracer reservoir (a stainless steel oxygen cylinder) to the control valve at a pressure of 55 p.s.i. The pressure in the reservoir was maintained under nitrogen from a gas cylinder. A photograph (7) shows the cylindrical tracer reservoir above bench level with the control valve connected immediately beneath it.

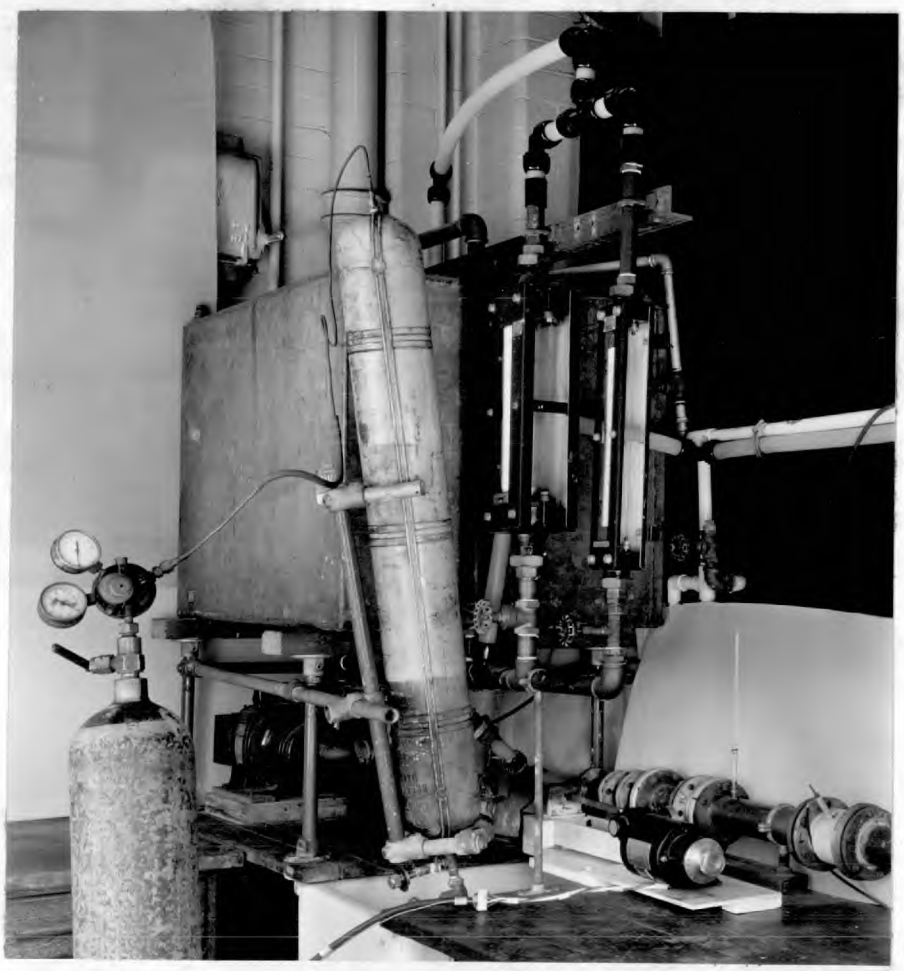
The 'sine wave generator' (see photograph 8 and figure f.10), which was connected between the needle valve and the mixing cell, consisted of a glass syringe, the plunger of which was driven by a crank and connecting rod. The ratio of the connecting rod length to the plunger stroke was large enough to ensure that the plunger never deviated more than one per cent from sinusoidal motion. By alternatively withdrawing and returning tracer solution to the feed line in a sinusoidal fashion, the syringe imposed a sine wave upon the flow from the tracer reservoir. The pressure changes caused by these fluctuations in flow were not large enough to affect significantly the steady nature of the flow through the needle valve.

The use of glass syringes gave rise to advantages of simple

replacement and flexible capacity and the visual detection of trapped gas bubbles. It was considered safe to use glass syringes, as the stresses experienced by them in the sine wave generator could not greatly exceed those for which they were designed. The syringe was clamped between two brass plates in which tapered holes had been drilled to receive the metal ends of the syringe (see figure f. 11). The tapered holes were such that all required sizes of syringe could be accomodated. With this method of mounting, only metallic parts of the syringe were subjected to direct forces. Because of the risk of misalignment, no supporting guide was provided for the plunger rod.

The syringe plunger rod was joined to the connecting rod by a pin coupling. The connecting rod was itself joined to the 3 inch diameter brass crank wheel by a screw. A selection of holes for this screw on the crank wheel provided a choice of plunger strokes. The crank wheel could either be mounted directly to the drive motor, a 'Citenco' ¼ H.P. governor controlled motor (type AB,) or through different arrangements of toothed 'timing belts' and a gear box. In this way sinusoidal tracer signal frequencies of between 0.2 and 187 cycles per minute were possible.

The syringe mounting was bolted directly to the wooden base board of the sine wave generator assembly. The drive mechanism components were mounted on a ¼ inch mild steel plate. This plate was drilled to take all useful arrangements of timing belts and gear box. A length of mild steel channel, firmly bolted to the syringe holder and to the drive mounting plate, prevented the base board from flexing.



7. Tracer Injection System

The Two Stage Mixing Cell

The design of the two stage mixing cell (see figure f.9) was perfected by trial and error. The criterion for satisfactory performance was the ability to inject a reasonably smooth steady tracer signal. The cell was situated (as can be seen in photograph 4) just in front of an elbow in the feed pipe, the elbow being about one foot from the inlet to the annulus. A right angled bend was found to greatly improve mixing.

An 1/8 inch diameter tube, in which the first stage of mixing took place, was fixed in a position along the axis of and inside the one inch diameter feed pipe. The second mixing stage was in the region of baffles downstream of the concentric tube. These baffles were in the form of fixed impellers. The optimum number and positioning of these baffles was also found by trial and error.

All connections in the tracer injection system, except that to the mixing cell, were made with copper tube. To give a degree of flexibility and also to enable gas bubbles in the tracer to be detected, the mixing cell was connected to the rest of the system by a short length of polythene tubing. The tracer reservoir was charged, after evacuation by a laboratory filter pump, by drawing in concentrated brine through a sintered glass filter.



8. Sine Wave Generator

3. Ancillary Equipment

Water was pumped from an 100 gallon tank to the annular flow system and thence returned to the tank by way of a rotameter (see figure f.12). The tank which was of galvanised steel, was further protected from corrosion by a coating of polyvinyl chloride. The pump was of the centrifugal type, the chamber and impeller of which were made of bronze. Driven by a $\frac{1}{4}$ H.P. electric motor, the pump was capable of maintaining a flow rate of 800 gallons per hour through the annular flow system, which was sufficient for the purposes of experiment.

Flow rates could be measured using one of two alternative rotameters. The larger rotameter (140 to 1,300 gallons per hour) completely covered the range of turbulent flow used in epxeriment. A smaller rotameter (10 to 90 gallons per hour) was provided for laminar flow experiments. Flow was controlled by means of a by-pass which returned water to the tank from a point downstream of the pump to the tank, and also by a valve between the by-pass and the annular flow system. This valve and the valve in the by-pass were of the one inch gate valve type. All pipe work was of one inch diameter. Where possible, polythene piping was employed.

4.1 Preliminary Investigations

Because of the small size of the annular flow system, there was no direct method by which the gap width between the two concentric tubes could be measured. Therefore an indirect method had to be employed to establish the mean dimensions and the uniformity of the cross-section of the flow system. The mean diameter of the inner wall of the annulus was calculated from a series of measurements on the brass inner tube of the experimental section. The mean diameter of the outer wall was thencalculated from that of the inner wall and the mean cross-sectional area of the annulus. The cross-sectional area of the annulus was found from the volumetric capacity and the length of the experimental section.

The diameter measurements on the inner tube of the annulus showed there to be a variation of 0.015 inch from the mean diameter. This variation, which was greater than had been hoped for, arose practically entirely from the brazing of the phosphor-bronze spacing ball bearings. The outer brass tube of the experimental section had, as had the inner tube, been manufactured to British Standards Specification 885. Because this tube had had very little treatment after delivery, it was assumed that the specified maximum variation in bore of 0.010 inch was still valid. There was thus a maximum possible variation in annular gap width of 0.0125 inch (half the variation in diameter difference), or ± 3.3 per cent of the mean gap width. The dimensions of the annular flow system are set out in table 1 of appendix III.

ROTAMETER CALIBRATION AND FRICTION FACTOR MEASUREMENT

The rotameters were calibrated using a stop-watch and weigh-tank. Care was taken to ensure that conditions were as close as possible to those prevailing in the experimental runs. At any particular flow rate calibration runs were repeated until the results were reproducible to 0.1 per cent.

Friction factors were calulcated from pressure drop measurements over a length of annular flow system which consisted mostly of the experimental section. For the lower flow rates, including all those in the laminar regime, a water manometer was convenient for this measurement. For the higher flow rates, a mercury manometer was used.

Friction factors (see figure m.2) closely followed the curve equivalent to a pipe 'roughness factor' of 0.006 over the experimenta- range of flow rates. Reynold's numbers for an annulus are based on twice the width of the annular gap, which is equal to the hydraulic diameter of the flow system.

Pressure drop measurements in the laminar regime (see figure m.1) fell very close to the theoretical line in the range of flow rates up to a Reynold's number of 1000. Above this they exceeded the calculated values to an increasing degree. The transition point in an annular flow system is normally lower than that in a tubular flow system. It is also possible that the ball bearing spaces and the variation in annular gap width promoted early turbulence.

CALIBRATION OF THE CONDUCTIVITY MEASURING SYSTEM

The conductivity of the water between the electrodes of each conductivity cell was calculated from the deflection of the appropriate recorder pen and a mathematical model of the conductivity measuring system. This mathematical model (see section 2 of Appendix II and figure f.7) consisted of a non-inductive wheatstone bridge circuit, the detector arm of which had a finite resistance, and an amplifier and recorder. The amplifier was non-linear to a small degree through the inclusion of a third power term.

The parameters for the model of each measuring system channel were found from direct measurement of the appropraite components of the actual system. The reliability of the mathematical model was then tested in a number of calibration runs in which the conductivity cells were replaced by known resistances. The results of these calibration runs, in the form of graphs of measured against actual cell conductance (inverse of resistance) are given in Appendix IV (figures m.3 to m.7)

4.2. DAILY PROCEEDURE

Because all experimental runs were carried out at water temperatures between 19.5°C and 20.5°C, the water in the tank had to be at a temperature of 19.0°C before experiments could commence. Water from the main supply was of too low a temperature (between 7°C and 9°C) and had too great a degree of airation for immediate use, and had to be left standing in the tank for a period of at least twelve hours. A considerable restriction was thus placed upon the operation of the apparatus.

Trapped air was driven from the flow system by the pumping of water

throughout. With the centrifugal pump running, the control valves were opened slowly until bubbles ceased to be observed passing through the rotameters. The valves were then opened fully to ensure that no trapped air remained. The control valves were opened slowly to avoid damage to the electrode platinising through the fast passage of bubbles close to the electrodes.

All electronic apparatus was allowed to warm up for two hours prior to use. The resistance value of the selected resistor, R_8, in the bridge circuit of the downstream electrode channel, was measured every day. This was done to detect any drift resistance which might be expected in a carbon resistor. The particular resistor selected for R_8 was governed by the necessity of maintaining the voltage between the electrodes at less than one volt peak. The variable resistor, R_4, in the bridge circuit of the upstream electrode channel was adjusted so as to be roughly equal to that in the downstream channel (R_8), and then measured accurately.

THE CONDUCTIVITY CELLS

The cell constant of each conductivity cell was measured every day from the output of the conductivity measuring system for when water of known conductivity was pumped through the flow system. Deterioration in the electrode platinising was associated with increasing cell constant (expressed as reciprocal centimeters) and the appearance of an effect similar to that of inter-electrode capacitance. It was desirable to replatinise the electrodes before this effect became significant. It was found to be sufficiently frequent to replatinise after the cell constants had changed by more than one per cent from their values immediately after replatinising. The platinising process is described in section 3 of Appendix II.

4.3. EXPERIMENTAL TECHNIQUE

Experimental runs were carried out at temperatures between the limits of 19.5°C and 20.5°C, but preferably as close to 20°C as was practicable. The temperature rise through the centrifugal pump was of between 0.5°C at the highest flow rates, and 1.5°C at the lowest. It was therefore necessary that the water in the tank should be of a temperature of 19.0°C before experiment commenced. Because water was recycled, the tank water temperature rose slowly while the apparatus was running. This rise in temperature was compensated for by the occasional addition to the tank of fresh cold water from then main supply.

A maximum limit of 0.03 gram-molecules per litre was set upon the concentration of sodium chloride tracer in the tank, above which no experimental work was done. Above this concentration the changes in the physical properties of the water (viz. density and viscosity) were becoming significant. Also the concentration measuring system was less sensitive and less linear above this limit.

Course adjustments to water flow rate were made using the main control valve 'A' (see figure f.12). The by-pass valve 'B' was useful for improving the stability at low flow rates only, and was otherwise kept closed. Fine adjustments to flow were made using the valves in the rotameter arms, which were also used for shutting off flow from either rotameter. It was possible to control all flow rates associated with turbulent flow in the annulus with great accuracy and stability. Trouble was experienced with the laminar regime flow rates when the small rotameter was in use. However, experimental runs in this flow regime were of no consequence.

RUNS WITH SINUSOIDAL TRACER SIGNALS

A suitable combination of syringe size, plunger stroke and needle valve setting in the tracer injection system was found for each experimental run by calculation beforehand. The desired amplitude of the tracer concentration signal was that which would give a recording of sufficient amplitude (approximately one half of the chart width) from the upstream electrode conductivity measuring system channel (channel 1). The sensitivity of this channel was always at its maximum so that tracer signals could be kept as small as possible.

The principle upon which the tracer injection system worked demanded that tracer flow from the reservoir should always be greater than that induced by the action of the syringe. The needle valve was always set so that the flow of the tracer should be about 10 per cent greater than the minimum dictated by this requirement. The effect of insufficient tracer flow was to flatten the peaks of the sinusoidal tracer signal.

With the desired water flow rate and sinusoidal tracer signal frequency, the upstream conductivity measuring system (channel 1) was set into operation. The periodic oscillations of the recorder pen were centralised on the chart by adjustment of the bridge potentiometer (R_2). A few cycles were recorded so that the quality of the concentration signal might be judged. In this, an allowance for the non-linear nature of the measuring system had to be made.

There were two ways in which the amplitude of the recorded signal could be enlarged, if so desired. The first method was to increase the amplitude of the concentration signal through the use of a larger syringe or longer plunger stroke. However, if the mean concentration of tracer was such that the bridge potentiometer setting was less than 0.061 it was possible to change to lower values of the bridge resistors (R_4 and R_8) without applying too great an AC voltage between the conductivity

electrodes. This method was prefered as it permitted tracer accumulation in the tank to be kept as low as possible.

With all equipment functioning satisfactorily, the downstream conductivity measuring system (channel 2) was set into operation. The recorder pen oscillations were centred on the recorder chart as in channel one (using potentiometer R_1), with the pre-amplifier at the minimum sensitivity setting. The sensitivity was then set at a suitable value at which there was no risk of the recorder pen moving off the chart.

A simultaneous recording of the outputs of both channels, and thus the tracer concentration fluctuations in each cell, could now be made. The recorder chart speed was selected so that each cycle occupied a length of about four centimeters of chart. Because the two recorder pens were not exactly coincident in longitudinal position, it was necessary to make a simultaneous mark with each one, to which phase angle measurements were referred.

A recording of about six tracer signal cycles, or more for when the signals were of low quality, was then taken. The recorder traces were terminated by the turning of the bridge/detector unit control switch to the 'zero'setting. Reference marks corresponding to the null setting of the bridge potentiometers were thus made on the chart. The electric current to the recorder pens was then switched off and the chart motor stopped. At this point, all useful data such as bridge potentiometer and recorder settings and chart speed were noted. Then, if so desired, the injection of tracer terminated.

RUNS WITH PULSE TRACER SIGNALS

Pulse signals were introduced by the addition of slugs of concentrated tracer solution from the injection system. The tracer reservoir stop-cock was opened for a short period of time. The length of this period and the setting of the needle valve were found by experiment.

With water flow rate at the desired value, the effect of these two variables (injection period and needle valve setting) was assessed from the tracer signals recorded at the upstream electrodes. When the best combination of the two variables had been found, a pulse was injected with both recorder channels in operation. Recording was continued till both pens had returned to the positions which they occupied before the pulse entered the experimental section of the flow system. The chart speed was selected so that the relevant length of chart was about thirty centimetres. As in the sinusoidal runs, the pen traces were terminated by bridge null reference marks. Readings of flow rate and temperature were taken during actual recording, and the bridge potentiometer and recorder settings noted afterwards.

4.4. ANALYSIS OF THE CHART RECORDINGS

Sinusoidal Tracer Signals

The dynamic response of the annular flow system to tracer signals was described, as is conventional, in terms of frequency response. Thus the employment of sinusoidal tracer signals meant that measurements of pulse shift and amplitude ratio could be made more or less directly from the recorder traces.

Because water was recycled, there was a continuous accumulation of tracer in the tank. The drift in concentration which this gave rise to during runs, was allowed for by assuming it to be steady and that it could be represented by a straight line on the recorder chart. This 'response' line was drawn for each trace so as to be on average parallel to the 'best' lines drawn through each of the two sets of signal peaks (maxima and minima). This line was positioned so that the intervals between each of the intersections with the trace were of approximately equal length. Alternate intersection points were thus in an identical position relative to each cycle. The intervening points were approximately 180° out of phase relative to the first. A recorder trace with the reference line constructed is given in Appendix IV (figure g.1).

Least squares formulae (see Appendix II section 5.1) were applied to measurements of the intersection points of each trace from a common reference point. That for the channel one trace yielded a mean cycle length and a mean phase shift relative to the common reference point. The tracer signal frequency was calculated from the mean cycle length and the chart speed. The formula for the other channel employed the cycle length from the first to find a mean phase shift alone. The frequency measurement was based upon the channel one trace because the signal quality was generally better than that of the other channel.

The phase shift between the two traces was thus calculated, allowing for a small error arising from the longitudinal displacement of the

recorder pens relative to each other. The total angular lag, the sum of the negative phase shift and an unknown number of cycles, was assumed to be less than but not by more than one cycle, the distance velocity lag. Any exception to this rule became obvious in the plotting of the response curves.

The calculation of tracer concentration from the recorder chart readings (see Appendix II section 2) was carried out in three separate stages. First the conductivity in the relevant cell was found from the chart reading and the mathematical model of the measuring system. For this, the bridge potentiometer setting, a number of parameters and in the case of channel two, the preamplifier sensitivity setting had to be known.

From this conductivity, the conductivity of the main supply water, corrected for the run temperarure, was subtracted. This quantity, which did not vary very much, was measured every day. The remaining conductivity, that due to the presence of the tracer, was itself then corrected to 20°C. The temperature corrections were of the exponetial type, that for sodium chloride in water being well known (12), and that for the main supply water found by experiment.

The tracer concentration was then found by the use of the empirical relationship between conductivity and concentration due to Kohlrausch. The parameters for this relationship were found for aqueous solutions of sodium chloride at the prescribed temperature from measurements given in literature (12). A choice of three sets of parameters was employed for different ranges of conductivity, thereby keeping errors very small. The Kohlrausch relationship was solved by iterations of the Newton type.

A formula was then used to find least squares mean values of sinusoidal tracer signal amplitude and mean concentration from the peak values of each trace. This formula also found the mean rate of

drift of each trace as a proportion of the amplitude per cycle. This could then be compared with the slope of the reference lines used in the measurement of phase shift.

The data for all runs were processed by computer. The mean square errors in all results of frequency, phase shift, mean concentration and amplitude, were calculated from these, the presence of mistakes in the original chart measurements could be detected. The regularity of the sinusoidal tracer signals was also assessed from these figures.

RUNS WITH PULSE TRACER SIGNALS

Pulse signals presented a less direct, but possibly more successful means of measuring the dynamic response of tracer signals in the annular flow system. The recorder trace of each channel was subjected to Fourier analysis, as defined in equations (CII; 2;13) and (CII; 2;14) on the same time basis. A set of response data was then derived from the two sets of complex integral transforms.

The longitudinal (time axis) scale on the recorder chart, graduated at quarter inch intervals, was not suitable for the accuracy demanded. The charts for the pulse tracer signal runs were analysed upon a special chart reader, which had also been used for frequency and phase shift measurements in the sinusoidal runs. This chart reader was made up from a drawing board with a built in sliding parallel rule. The position of the parallel rule could be measured accurately on a steel centimetre scale fixed at the side of the board.

The method of quadrature (see fig. g.2) by which the integral transforms of the pulse signals from each channel were found, was fundamentally that of Simpson's rule. Points on each recorder trace were chosen between which the trace was judged to be of parabolic shape. Each of these points was at either a whole or a half millimetre gradation

of the chart recorder scale. Chart readings were taken at these points, and at points halfway between them.

Because of its relative unimportance, the concentration signal at the tail of a pulse was assumed to decay exponentially. The position of a point after which exponential trial and error. This point was generally such that the recorder trace had declined to about one fiftiethof its maximum amplitude. The position of the point at which the trace had decayed a further 1/e relative to the first point was also found, so completing the definition of this region.

Efforts were made to restrict the length of recorder chart occupied by the relevant traces to thirty conetimetres. If this length was exceeded, it was necessary to reset the chart on the chart reader so that the remaining parts of the tracer could be read. To preserve accuracy in the time scale, datum lines were drawn across the chart.

The tracer concentration value for each point was calculated from the chart reading in a manner identical to that used in the sinusoidal tracer runs. By subtracting from this the initial tracer concentration, the concentration value relevant to the pulse was found.

Before Fourier analysis could commence, it was necessary to fix the limits of the period of time over which the analysis was to be conducted. This period, defined in the boundary conditions (CII; 2;2) and (CII; 2;3), was that at the commencement of which no tracer material had entered, and at the termination of which all material had left the experimental length of flow system. The initial limit was fixed at the point on the recorder chart at which the channel one trace first showed a detectable change.

In most runs, especially those at low flow rates, the tails of the recorded pulses could not be completely included within the time limits of the period of analysis on account of their long length. The assumption

of exponential decay implied that this length was infinite, which however, was not the case. The response data for various runs were worked out with different proportions of the channel two pulse excluded, first 1/100 of the total area, then 1/1000 and then 1/10,000. No significant change in the response data was observed.

The integral transforms of the incremental strips and the regions of exponential decay were found from integration formulae (see Appendix II section 5.2). The effect of differences in the sensitivity between the two channels were eliminated by dividing the integral transform of the pulse recorded on each channel by the time integral of that pulse. As in the sinusoidal tracer signal runs, data for pulse tracer signals were processed by computer.

CHAPTER IV

1. TRACER SIGNAL FREQUENCY IN EXPERIMENT

Dynamic tracer studies were carried out on the annular flow system at eight flow rates in the turbulent flow regime. The main object of these tracer studies was to test the validity of two mathematical models that were developed during the course of this research project to describe the flow system. The first of these models was based upon flow velocity profiles proposed for turbulent flow in a parallel wall flow system by Pai[9], and a literal interpretation of Reynold's analogy The second model was developed from a separate consideration of the properties of the laminar sub-layer and of the turbulent core of flow.

Tracer signals of both the sinusoidal and the pulse type were used in compiling response curves for each flow rate. The tracer signal type and frequency was organised such that response information of sufficient detail was obtained as economically as possible. Experimental runs in which pulse tracer signals were employed yielded response information for an harmonic series of tracer signal frequencies. Those in which sinusoidal signals were used yielded data for a single frequency only. However, the use of sinusoidal tracer signals had two advantages. Firstly, the analysis of recorder charts was quick and simple. Secondly, it was possible to choose the tracer signal frequency precisely, and furthermore, use lower frequencies than were possible with pulse tracer signals.

Experimental study of the flow system with respect to the first model demanded that response data should be evenly spaced throughout the available tracer signal frequency range. For this study, the exclusive use of pulse tracer signals would have been suitable. However, in the case of the second mathematical model, a high density of low

tracer signal frequency data were necessary for the study of the laminar sub-layer. Hence, a number of sinusoidal tracer signal runs were necessary.

For each flow rate, the distribution of the tracer signal frequencies of the sinusoidal tracer signal runs was logarithmic. The response data from these runs were supplimented by that from a single, or in some cases two, pulse tracer signal runs. The reproducibility of the response data could therefore be confirmed through comparison of the data from both types of tracer signal. An upper limit on tracer signal frequency with sinusoidal signals existed on account of the deterioration of signal quality with frequency. Response data obtained from pulse signals for frequencies above this limit were subject to uncertainty.

Presentation of Experimental Data

All experimental response data are presented in graphical form. Amplitude ratio (see figures a1 to a8), the proportional decay of the amplitude of a tracer signal over the experimental section of the flow system, is plotted against a logarithmic scale. Phase shift (see figures b1 to b8), as angular phase lag in degrees, is plotted against a linear scale. In order to accentuate the non-linearity of the relationship between phase shift and tracer signal frequency, an angle proportional to the particular frequency is subtracted from each phase shift. A linear tracer signal frequency is used in all response diagrams.

Phase shift diagrams covering the lower end of the tracer signal frequency range for each water flow rate are also included (figures C1 to C8). These diagrams are used to show divergences from the plug flow model at low frequency, and hence enable the thickness of the laminar sub-layer to be measured. No modification of phase shift to accentuate curvature is necessary in these diagrams.

2.1 The Unified Mathematical Model

The 'unified' mathematical model seeks to predict the dynamic behaviour of tracer signals over an unlimited range of signal frequency. Full numerical solutions of the parallel wall flow system equation (CII; 5;1) must be found. Before these solutions can be found, velocity profile and diffusivity data must be available for the flow system. In this case, the data are derived from a theoretical analysis for incompressible turbulent flow due to Pai[9].

Pai solves Reynold's equations using several assumptions, the most important of which being that of anisotropic turbulence. His velocity profile is expressed in the form of a polynominal.

$$U = 1.5\,\bar{U}\left(1 - \frac{n-b'}{n-1}\eta^2 - \frac{b'-1}{n-1}\eta^{2n}\right)$$

.....(CIV; 2;1)

where the constant, n, is the integer most closely satisfying the equation:-

$$n = 0.5\,(0.3168\,f\,R_e - 1)$$

.....(CIV; 2;2)

The constant, b', is chosen such that the laminar flow profile should satisfy equation (2;1).

$$b' = \frac{n}{1.40}$$

.....(CIV; 2;3)

Diffusivity data are derived from a literal interpretation of Reynolds analogy[10]. This analogy assumes that the mechanisms of momentum and mass transfer arising from turbulence are identical. Consequently, ε, the eddy kinematic viscosity must be equal to the eddy mass transfer coefficient, D_ε.

$$\varepsilon = D_\varepsilon$$

The total shear force, R, in any plane is assumed to be the sum of that arising from molecular viscous forces, and that from eddy viscous forces.

$$R = (\nu + \varepsilon) \frac{\partial}{\partial x}(\rho U)$$

Similar assumptions apply in the case of the total mass flux, N_A.

$$N_A = (D_A + D_\varepsilon) \frac{\partial C_A}{\partial x}$$

Hence, total diffusivity may be expressed:-

$$D = D_A + D_\varepsilon = D_A + \frac{R}{\frac{\partial}{\partial x}(\rho U)} - \nu$$

..... (CIV; 2;4)

and in terms of equation (2;1)

$$D = D_A + \nu \frac{n(b'-1)(1-\eta^{2n-2})}{[n-b'+n(b'-1)\eta^{2n-2}]}$$

..... (CIV; 2;5)

Theoretical response data based upon the unified mathematical model and the Pai velocity profile were computed for three water flow rates only; viz. 300, 400 and 700 gallons per hour. The whole range of experimental flow rates in the turbulent regime was thus covered. The data are presented on the amplitude ratio diagrams ('a' diagrams), and the full frequency range phase shift diagrams ('b' diagrams).

2.2 The Compound Mathematical Model

The theoretical analysis due to Pai, by which turbulent flow velocity profiles were deduced, assumes that turbulent conditions exist at the wall of the flow system. Hence the 'unified' mathematical model does not take into account the effect of the 'laminar sub-layer'. An attempt to allow for the effect of this layer is made in the 'compound' mathematical model. In this model the flow system is divided into two regions, that of the laminar sub-layers (at either wall), and that of the turbulent core of flow. Tracer response data for this model were found through consideration of the properties of the sub-layer, and through solution of equation (CII; 5;1) for the turbulent core.

The Laminar Sub-Layer

The laminar sub-layer is defined (in the context of the compound mathematical model), as a layer adjacent to the walls of the flow system over which the liquid velocity gradient is constant and in which diffusion is only of the molecular type. For each flow rate, the thickness of this sub-layer was determined from the experimental phase shift data for low tracer signal frequencies (see figures C1 to C8). It is apparent from these data that phase shift approaches the 'plug flow line'

assymptotically as tracer signal frequency tends to zero, as would be consistent with the dispersion model.

In the compound mathematical model of the flow system, the magnitude of diffusivity in the turbulent core, as predicted in equation (2;5), is many times greater than that in the laminar sub-layer. Hence the response of tracer concentration in the core will be much more rapid than it will be in the sub-layer. There exists, therefore, a minimum tracer signal frequency above which concentration signals, while they are fairly uniformly distributed in the turbulent core, do not penetrate the sub-layer to any significent extent. Such tracer signals will behave as though the interface between core and the sub-layer were an impermeable wall.

Where tracer signals are of sufficiently high frequency, the dispersion model will be applicable to the turbulent core. A plug flow line, or 'core flow line', based upon the turbulent core will exist to which phase shift will approach assymptotically. The slope of this line is determined by the mean flow velocity, $\bar{U}_{Tc}$, in the turbulent core.

$$\phi = 6 \frac{W}{\bar{U}_{Tc}} L$$

.....(CIV; 2;6)

A core flow line for each flow rate in the annular flow system was constructed from the experimental phase shift data. The mean flow velocity in the turbulent core associated with each flow rate was calculated from the slope of the core flow line by way of equation (2;6). The thickness of the laminar sub-layer could then be calculated from the overall mean flow velocity, the mean velocity in the core and the shear force, R, at the walls of the flow system.

The mean flow velocity in the turbulent core is defined,

$$\bar{U}_{Tc} = \frac{1}{\eta_L} \int_0^{\eta_L} U \, d\eta$$

.....(CIV; 2;7)

where the interface between the turbulent core and the laminar sub-layer is denoted,

$$\eta = \eta_L$$

The velocity gradient in the laminar sub-layer is assumed to be constant and is expressed,

$$\left(\frac{dU}{d\eta}\right)_L = \frac{aR}{2\mu}$$

.....(CIV; 2;8)

The volumetric flow rate of liquid flowing in the laminar sub-layer is,

$$-\frac{1}{2}(1-\eta_L)^2 \left(\frac{dU}{d\eta}\right) \frac{a}{2}$$

This must be equal to the difference between the total flow rate and that in the turbulent core. Hence,

$$-\frac{1}{2}(1-\eta_L)^2 \left(\frac{dU}{d\eta}\right)_L = \bar{U} - \bar{U}_{Tc}\,\eta_L$$

which may be rearranged to,

$$1 - \eta_L = - \frac{\bar{U}_{Tc}}{\left(\frac{dU}{d\eta}\right)_L} + \sqrt{\frac{\bar{U}_{Tc}^2}{\left(\frac{dU}{d\eta}\right)_L^2} - \frac{2(\bar{U} - \bar{U}_{Tc})}{\left(\frac{dU}{d\eta}\right)_L}}$$

The right hand side of this equation is then expanded.

$$1 - \eta_L = \theta \left\{ 1 - \frac{\theta}{2\bar{U}_{Tc}} \left(\frac{dU}{d\eta}\right)_L + \left[\frac{\theta}{\bar{U}_{Tc}} \left(\frac{dU}{d\eta}\right)_L \right]^2 \ldots\ldots \right\}$$

.....(CIV; 2;9)

where, $$\theta = \frac{\bar{U}_{Tc} - \bar{U}}{\bar{U}_{Tc}}$$

The calculated values of laminar sub-layer thickness are given in graphical form (see figure d1). There has been no experimental measurement of sub-layer thickness performed in a flow system of similar geometry and in a similar range of Reynolds number by any other worker. Hence the comparison of the present experimental data with those from another source is not possible. However, Nikuradse[13], in his work on a parallel wall flow system of the rectangular type at Reynolds numbers between 60,000 and 120,000, correlated sub-layer thickness with Reynolds number. He found an expression,

$$1 - \eta_L = \frac{120}{R_e \sqrt{f}}$$

.....(CIV; 2;10)

In the range of Reynolds numbers used in this work, 4,000 to 11,000, this expression predicts sub-layer thickness of about ten times those found by experiment.

The effect of the laminar sub-layer upon the rate of decay of tracer signals (for the compound mathematical model) is predicted through the variable reference plane dispersion model. As has previously been shown, the sub-layer only influences the behaviour of tracer signals of low signal frequency. Hence, the effect of the sub-layer will only be apparent in the initial trend of theoretical amplitude ratio data. This trend is predicted using the Taylor/Aris dispersion coefficient in place of the true variable reference plane coefficient is the manner described in Chapter II.

The Taylor/Aris dispersion coefficient for the model of the flow system is derived from equation (CII; 4;29). Because diffusivity is very much greater in the turbulent core than in the laminar sub-layer, the limits of integration in this equation may be modified so as to include the turbulent core.

$$\bar{D} \gg D_A \ ,$$

$$\frac{K}{\bar{D}} = 1 - \frac{\bar{U}^2 a^2}{4 \bar{D} D_A} \int_{\eta_L}^{1} (\gamma - 1)\, d\eta'' \int_{\eta_L}^{\eta''} d\eta' \int_{\eta_L}^{\eta'} (\gamma - 1)\, d\eta$$

.....(CIV; 2;11)

The modification of equation (CII; 4;29) to equation (2;11) suggests that the effect of the sub-layer is paramount at low tracer signal frequencies.

With the assumption of a constant velocity gradient in the laminar sub-layer, equation (2;11) is reduced to a polynomial

$$\frac{K}{\bar{D}} = 1 - \frac{\bar{U}^2 a^2}{12 \bar{D} D_A} (1 - \eta_L)^3 \left\{ 1 - 0.75 \left(\frac{U_L}{\bar{U}} \right) + 0.15 \left(\frac{U_L}{\bar{U}} \right)^2 \cdots \right\}$$

.....(CIV; 2;12)

where the flow velocity, U_L, is that at the boundary between the laminar sub-layer and the turbulent core. The cross-sectional mean diffusivity, $\bar{D}$, in equation (2;12) is taken to be equal to that predicted in the 'unified' mathematical model.

The rate of decay of a tracer signal (with length in the direction of flow), is directly proportional to the real part, of the logarithmic transfer factor. An expression for this quantity is derived through rearrangement of equation (CII; 4;17), using equation (CII; 4;16) to eliminate the imaginary part, γ_r, of the transfer factor.

$$\beta_r = \frac{K_r}{\bar{D}} \cdot \frac{r^2\Omega^2}{\Phi^3} \cdot \frac{\bar{U}^3}{V_r^3}$$

This expression is simplified by assuming that the variable reference plane dispersion coefficient, k_t, may be replaced by the Taylor/Aris coefficient, and that the reference plane velocity, V_t, is equal to the mean flow velocity. The logarithm of the ratio of the amplitudes of tracer signals leaving to those entering the experimental section of flow system, φ, is written,

$$\varphi = \frac{\beta_r L}{a} = \frac{K}{\bar{D}} \cdot \frac{r^2\Omega^2}{\Phi^3} \cdot \frac{L}{a}$$

.....(CII; 2;13)

Therefore the initial trend of amplitude ratio is parabolic.

THE TURBULENT CORE

When tracer signal frequency is greater than a certain minimum, the turbulent core of the flow system is effectively isolated from the laminar sub-layer and becomes a separately identifiable flow system. As such, the core is treated in a manner similar to that in which the whole cross-section of the flow system was treated in the 'unified' mathematical model. Equation (CII; 5;3) is solved for the core, the flow velocity and diffusivity data necessary being derived by the Pai analysis for parallel walled flow systems. Theoretical tracer response data are then found from the logarithmic transfer factors associated with solutions of this equation.

'Slip' occurs at the 'walls' of the turbulent core. This slip is in the direction of flow at velocity, U_L, the flow velocity at the boundary between the sub-layer and the core. Therefore the definition of both Reynolds number and friction factor must be modified for the purposes of the Pai analysis. The Reynolds number for the turbulent core, $Re_{T.C.1}$ is defined in terms of the difference between the mean flow velocity in the core and the'velocity of slip'.

$$Re_{Tc} = \frac{2 a \eta_L}{\nu} (\bar{U}_{Tc} - \bar{U}_L)$$

The shear force at the boundary of the core, $R_{T.C.}$, is lower than that at the walls of the flow system.

$$R_{T.C.} = \eta_L R$$

$$f_{T.C.} = \frac{\eta_L R}{\rho (\bar{U}_{Tc} - \bar{U}_L)^2}$$

The friction factor for the turbulent core, $f_{T.C.}$, and the Reynolds number, $Re_{T.C.}$, are employed in equation (2;2). The flow velocity profile

represented by equation (2;1) now refers to velocity in excess of the velocity of slip, U_L.

Complete theoretical tracer response curves based upon the 'compound' mathematical model are only drawn for water flow rates of 300, 400 and 700 gallons per hour. However, for all flow rates the assymptotic line for phase shift, and the assymptotic parabola for amplitude ratio are given for the range of frequency over which the laminar sub-layer exerted an influence.

2.3 SOLUTION OF EQUATION (CII; 5;3)

The method by which computer solutions of the matrix equation (CII; 5;3) were generated is described in section 5 of chapter II. Two problems arise in the solution of this equation. Firstly there is that concerning the number of increments into which the flow system cross-section must be divided for values of the logarithmic transfer factor of sufficient accuracy to be found. The second problem concerns the validity of these solutions themselves. An important assumption underlying the experimental work was that the convergence condition (CII; 3;9) was satisfied in the flow system. Solutions of equation (CII; 5;3) are tested for this condition.

CONVERGENCE WITH INCREMENT SIZE

The minimum number of increments necessary to produce solutions of equation (CII; 5;3) to the required accuracy was found by trial and error. Both the number of increments into which the flow system cross-section was divided and the distribution of the sizes of these increments could be varied. The most advantageous distribution of increment size was found to be that in which the ratio of the sizes of successive increments was constant, the largest increments being at the centre of the flow system. The length of any increment, Δ_j, is written:-

$$h < 1, \qquad \Delta_j = h\,\Delta_{j-1} = h^{j-1}\,\frac{1-h}{1-h^{d-1}}$$

The optimum value of the ratio, h, was that for which half the increments were concentrated within th eight per cent of the flow system cross-section closest to the walls.

For all flow rates and tracer signal frequencies, forty increments

(over half the flow system cross-section) enabled sufficiently accurate values of the logarithmic transfer factor to be found from solutions of equation (CII; 5;3). The accuracy sought from computed values of amplitude ratio was one per cent, while that for phase shift was one tenth of one per cent. In Appendix III (table 2) samples of amplitude ratio and phase shift are given for various flow rates and tracer signal frequencies, using different numbers of increments in the solution of equation (CII; 5;3). Amplitude ratio is expressed in terms of its natural logarithm, and phase shift is expressed in radians.

THE CONVERGENCE CONDITION

In chapter II (section 3), it is shown that tracer experiments in which the cross-sectional mean concentration of the tracer is measured are only meaningful when the convergence condition (CII; 3;19) is satisfied. If this condition is not satisfied, the experimental data from such an experiment will not be reproducible. Therefore, if cross-sectional mean measurements are perfectly reproducible it may be concluded that the convergence condition is satisfied in the flow system. In actual experiment, however, a degree of irreproducibility arises from the technique by which mean tracer concentration is measured. Hence, it is impossible to determine how clearly the convergence condition is satisfied from the experimental measurements alone.

A theoretical approach to this problem is available through the testing of solutions of equation (CII; 5;3) for the convergence condition. To this end, the real part of the logarithmic transfer factor related to the second most important solution of this equation must be found. Since it is only the order of this quantity which is of significance, it is safe to assume that conclusions drawn by this method will not be subject to large errors.

For the purpose of equation (CII; 5;3), the annular flow system is treated as though it were a parallel wall flow system. Since it is the behaviour of the cross-sectional mean of tracer concentration which is of interest, the assymmetrical solutions of this equation are not relevant. The solution to which the convergence condition refers is the symmetrical non-primary solution with the logarithmic transfer factor which has the smallest negative real part. The method by which this solution is generated is described in Appendix III (section 1).

Some typical values of the right hand side of the convergence condition (CII; 3;19) are given in table 3 of Appendix III. These values, which are in units of dimensionless length (based upon the width of the flow system), are compared with the length of the flow system upstream of the experimental section of 117 dimensionless units. The convergence condition is easily satisfied for all flow rates (where flow is turbulent).

3. EXPERIMENTAL ERRORS

The experimental measurements of the response of the annular flow system to tracer signals are subject to the effects of imperfections both in the flow system and in the tracer concentration measuring system. The annular flow system was formed in the gap between two concentric tubes. Variations in the width of this gap of up to six per cent were found. These variations would most probably have caused channelling in the flow system. The presence of the ball bearing spaces in the gap would also have given rise to channelling. However, there was no evidence of channelling in the experimental results. Low tracer signal frequency phase shift data assymptotically approached the 'plug flow line' within the limits of error (see figures C1 to C8).

The magnitude of experimental errors attributable to the tracer concentration measuring system could have been assessed through consideration of each individual component of this system. However, the system was of too great complexity for this method to be useful. The experimental work was arranged in such a way as to reduce systematic error to a minimum. In this way, the magnitude of error in the concentration measuring system could be found from the scatter of experimental data.

A random method of experimentation was employed. The order in which runs were carried out was chosen so as to avoid any sequences with respect to water flow rate and tracer signal frequency. Hence, the effect of any part of the system which changed with time would be as a purily random factor. The settings of the controls in the tracer concentration measuring system were also frequently changed. This ensured that errors associated with the setting of any particular control would be random with respect to experimental results.

The reliability of the measurements of the response of the flow system to tracer signals is estimated from the scatter of experimental data. It is assumed for this purpose that all systematic errors may be neglected. Phase shift measurements were found to be subject to a 'standard error' of the greater of either 0.2 per cent or one degree (of arc). For amplitude ratio the standard error was found to be five per cent.

CHAPTER V

1. INTERPRETATION OF EXPERIMENTAL RESULTS

Two different aspects of the experimental data are considered. The first aspect concerns the response of the annular flow system to tracer signals of relatively low frequency. From the initial slope of plots of phase shift against tracer signal frequency, the uniformity of the annular flow system is assessed and the thickness of the 'laminar sub-layer' measured. Also, from the low frequency amplitude ratio data, the validity of the Taylor/Aris dispersion model is examined.

The second aspect concerns response at higher tracer signal frequency. Theoretical response data, derived for two mathematical models of the flow system, are compared with that found by experiment. The two models, as 'unified' and a 'compound' model, are described in Chapter IV. Use of these models enables various deductions to be made concerning the flow patterns and diffusional properties of the annular flow system.

1.1 RESPONSE AT LOW FREQUENCY

It is deduced from equations (CII; 4;11) and (CII; 4;16) that, provided tracer signal frequency is sufficiently low, the 'plug flow model' relationship between frequency and phase shift must hold.

$$\phi = -6 \frac{WL}{\bar{U}} \qquad \text{.....(CV; 1;1)}$$

where phase shift, ϕ, is in degrees, frequency, W, in cycles per minute, length, L, in centimetres and mean flow velocity, $\bar{U}$, in centimetres per second. On the low frequency phase shift diagram for

each water flow rate (figures C1, to C8: in Appendix I), a 'plug flow line' is drawn, the slope of which is determined by equation (1;1). Below a certain limiting tracer signal frequency, experimental phase shift measurements lie within their scatter of this line. Hence it is concluded that channelling did not take place to a significant extent in the annular flow system. Channelling in the flow system would cause the measured phase lags of tracer signals to be smaller than expected.

THE LAMINAR SUB-LAYER

Tracer signals of above a certain minimum frequency do not penetrate the laminar sub-layer to any significant extent. Hence, for such tracer signals, the turbulent core of the flow system becomes, in affect, a flow system on its own. From consideration of the 'plug flow model', it is seen that there is a range of tracer signal frequency over which phase shift measurements should follow an assymptote associated with the turbulent core of the flow system. The phase shift diagrams (figures C1 to C8) show that such a trend is discernible. On each diagram the assymptote (referred to as the 'core flow line') is drawn in.

The thickness of the laminar sub-layer is calculated from the slope of the 'core flow line' for each water flow rate by means of equations (CIV; 2;6) and (CIV; 2;9). The thickness of the sub-layer is plotted against Reynolds number in diagram d1 (Appendix I). Measured thickness differed considerably from that predicted by a correlation (equation (CIV; 2;10)) proposed by Nikuradse[13]. Nikuradse's work was, however, confined to flows of high Reynolds number (40,000 to 120,000) in parallel walled flow systems and cannot justifiably be compared to the present work. His expression (equation (CIV; 2;10)) predicts laminar sublayer thickness of up to 50 per cent of the total cross-section of the flow

system for the low flow rates. Measured laminar sub-layer thicknesses are expressed approximately as a function of Reynolds number.

$$1 - \eta_L = 0.2412 - 0.02483 \, Log_e (R_e - 2000)$$

.....(CV; 1;2)

1.2 COMPARISON OF THE MATHEMATICAL MODELS

Two mathematical models are proposed for the annular flow system. These models predict the hydrodynamical properties of the flow system to enable solutions of the matrix equation (CII; 5;3) and hence theoretical response data to be found. The 'unified' model is based upon a theoretical method for predicting velocity profiles in parallel wall flow systems proposed by Pai[9]. The 'compound' model treats the laminar sub-layer as a separate entity from the remainder of the flow system. Velocity profiles in the turbulent core are then found using Pai's method. Both models employ the literal form of Reynold's analogy as in equation (CIV; 2;4). The models are described in detail in Chapter IV, section two. Theoretical response data for them are plotted on the response diagrams for water flow rates of 300, 400 and 700 gallons per hour (see Appendix I).

Experimental phase shift data (see figures b_2, b_5 and b_7) are of significantly lower magnitude than those predicted by either mathematical model of the flow system. From this fact it is deduced that transfer signals did not penetrate as close to the walls of the flow system as is implied by either of the two models. Hence the diffusivity values predicted for the region of the flow system close to the walls must have been too great. The theoretical data derived from the 'compound' mathematical model fit the experimental data better than those from the 'unified'

model. Therefore recognition of the presence of the laminar sub-layer was fully justified.

AMPLITUDE RATIO DATA

Theoretical amplitude ratio data based upon the Taylor/Aris dispersion model are presented in addition to those based upon the 'unified' and the 'compound' mathematical models of the flow system (see figures a2, a5, and a7). Data derived by means of the Taylor/Aris model represent the assymptote to which amplitude ratio measurements are expected to approach as tracer signal frequency approaches zero if the compound model were to hold (see Chapter IV section 2). The parabolic assymptote is generated using equation (CIV; 2;13), the value of the Taylor/Aris dispersion coefficient for which is calculated using the velocity and diffusivity profiles of the 'compound' model. Experimental amplitude ratio data were, however, too inaccurate for the existence of such an assymptotic trend to be observable.

It is necessary to adopt a simplification to enable experimental amplitude ratio data to be interpreted in terms of physical characteristics of the annular flow system. The simplification chosen is that of the Taylor/Aris dispersion model.

Equation (CII; 4;28) shows that, provided the term related to longitudinal diffusion (equal to the cross-sectional mean diffusivity) can be neglected, and provided the cross-sectional profile of diffusivity does not change, the Taylor/Aris dispersion coefficient, k, is inversely proportional to the magnitude of diffusivity as represented by the mean diffusivity, $\bar{D}$. If it is assumed that the rate of decay of tracer signals is proportional to the Taylor/Aris coefficient, this rate will be inversely proportional to the diffusivity in the cross-section of the flow system. This simplification is only completely true in the non-dynamic case (for a tracer signal of 'zero' frequency).

Experimental measurements of amplitude ratio at the lower tracer signal frequencies are smaller than those predicted for the 'unified' model while at the higher frequencies they are greater. Since the regions of the flow system close to the walls are relatively less important at high than at low tracer signal frequency, the 'unified' model must assume too high values of diffusivity close to the walls and too low values in the centre of the flow system. The fact that this model tends to over-estimate diffusivity values in the wall regions of the flow system has already been found from the examination of experimental phase shift data. Using the same arguments, it is seen that the diffusivity values at the centre of the flow system predicted by the 'compound' model are too great.

Since actual measurements of diffusivity are not made in the experimental work described in this thesis, comparison with the results found by other workers can only be on a qualitative basis. Sherwood and Towle (15) and Schwarz and Hoelscher[17] studied radial mass transfer in turbulent gaseous flow in tubes, Sherwood and Woertz[18], Dhanak[16] and Cataneo[14] carried out similar studies in rectangular and annular flow systems. They all found that 'eddy mass diffusivity' tended to be greater than 'eddy momentum diffusivity' (eddy viscosity) in the turbulent core of each flow system, but smaller close to the walls. Since Reynolds analogy assumes eddy diffusivity to be equal to eddy viscosity, it is seen that the conclusions drawn from the present work are in accord with those of previous workers.

2.1. IMPROVEMENTS TO THE PRESENT INVESTIGATION

The usefulness of the experimental work would be increased if it had been possible to find values of diffusivity for the flow system cross-section. To find these values it is necessary to know flow velocity profiles in the

flow system with a considerable degree of accuracy. Then a diffusivity profile could be adjusted till the response curves derived for it fitted the experimental curves within the limits of error in measurement.

The difficulties involved in measuring velocity profiles in the annular flow system have already been described. To overcome them it would be advisable to employ a flow system in which the gap between the concentric tubes was of larger width. Diffusivity profiles could best be adjusted using the rules described in the first part of this chapter. By this means the number of computer solutions of the matrix equation (CII; 5;3) necessary could be kept at a minimum.

The profiles of diffusivity values found for the flow system by this means will be based solely on the response of the flow system to tracer signals of varying frequency. It would be of great interest to compare these profiles with those discovered in experiments in which diffusion in the direction transverse to flow is directly measured (14, 15, 16, 17, 18). These experiments are not subject to any time element as they are carried out in the steady state. In the tracer experiments, the frequency of the tracer signals is a factor, Hence, it could be discovered whether frequency has an effect upon the phenomenon of eddy diffusion.

2.2. TRACER STUDIES AND FIRST ORDER REACTIONS

The conversion for a first order chemical reaction and the dynamic behaviour of the reactant in a reactor of uniform cross-section may be predicted from the results of tracer studies carried out under certain conditions. The response of the reactor to tracer signals of pulse form is analysed by means of suitable integral transforms. The conditions which must be met are the same as those relating to the solution of equation (CII; 2;17), namely that flow in the reactor should be fully developed and that the distribution of the reactant in any cross-section

should be such that the 'convergence' condition (see Chapter II section 3) is satisfied.

STEADY STATE CONVERSION

The behaviour of the reactant (of concentration C_B) in the reactor is governed by a partial differential equation differing from equation (CII; 1;1) in that a reaction term is added and in that the time derivative term is dropped (since steady state conditions prevail).

$$\nabla (\psi \nabla C_B) - \Phi f \frac{\partial C_B}{\partial \xi_1} - \frac{a^2 K_I}{\bar{D}} C_B = 0$$

..... (V; 2;1)

This equation uses the dimensionless quantities of equation (CII; 2;17). The first order reaction constant is denoted, k_I. The boundary condition related to equation (2;1) are basically the same as those related to equation (CII; 1;1).

$$\text{On } \Gamma, \qquad \psi \frac{\partial C_B}{\partial \xi_n} = 0$$

....(CV; 2;2)

$$\xi_1 = 0, \qquad C_B (0, \xi_2, \xi_3) = C_{Bo} (\xi_2, \xi_3)$$

....(CV; 2;3)

Equation (2;1) is solved by the analytical method used in the solution of equation (CII; 2;17) (see section 3 of Chapter II). A series solution for this equation is first proposed. Each term of this series

is the product of a function of longitudinal position, $\bar{C}_{Bs}(\xi_1)$, and a function of cross-sectional position, $g_s(\xi_2, \xi_3)$.

$$C_B = \sum_{s=1}^{\infty} \bar{C}_{Bs}\, g_s$$

.....(CV; 2;4)

The cross-sectional function is chosen such that the integral of it with respect to the cross-section is unity.

$$\int_A g_s \, d\xi_2 \, d\xi_3 = 1$$

It is proposed that each term of the series solution (2;4) itself satisfies equation (2;1) independently. Hence such a term may be substituted into this equation, and into the boundary conditions (2;2) and 2;3)

$$g_s \psi \frac{d^2\bar{C}_{Bs}}{d\xi_1^2} + \bar{C}_{Bs} \sum_{j=2}^{j=3} \frac{\partial}{\partial \xi_j}\left(\psi \frac{\partial g_s}{\partial \xi_j}\right) - g_s \gamma \Phi \frac{d\bar{C}_{Bs}}{d\xi_1} - \frac{a^2 K_I}{\bar{D}} g_s \bar{C}_{Bs} = 0$$

.....(CV; 2;5)

$$\text{On } \Gamma, \qquad \psi \frac{\partial g_s}{\partial \xi_\Gamma} = 0$$

.....(CV; 2;6)

$$\xi_1 = 0, \qquad \bar{C}_{Bs}(0) = \bar{C}_{Bs0}$$

.....(CV; 2;7)

The terms of equation (2;5) are integrated with respect to the cross-section of the reactor. Green's lemma (see equation (CII; 3;6)) and the boundary condition (2;6) enable the second term of equation (2;5) to be eliminated.

$$\phi_s \frac{d^2 \bar{C}_{Bs}}{d\xi_1^2} - \tau_s \Phi \frac{d \bar{C}_{Bs}}{d\xi_1} - \frac{a^2 \kappa_I}{\bar{D}} \bar{C}_{Bs} = 0$$

.....(CV; 2;8)

where, $$\phi_s = \int_A g_s \psi \, d\xi_2 \, d\xi_3$$

$$\tau_s = \int_A g_s \phi \, d\xi_2 \, d\xi_3$$

Equation (2;8) is a linear second order equation with constant coefficients; and therefore has an exponential solution.

$$\bar{C}_{Bs} = \bar{C}_{Bso} e^{\alpha_s \xi_1}$$

.....(CV; 2;9)

Boundary condition (2;7) has been taken into account in equation (2;9).

The conversion, y, in the reactor is defined in terms of the cross-sectional mean concentration, $\bar{C}_B$, of reactant at upstream and downstream boundaries of the reactor.

$$1 - y = \frac{\bar{C}_B (\xi)}{\bar{C}_B (0)}$$

.....(CV; 2;10)

Substituting the series solution (2;4) (integrated with respect to cross-section) combined with the exponential solution (2;9) in the right hand side of equation (2;10).

$$1 - y = \frac{\sum_{s=1}^{\infty} \bar{C}_{Bso}\, e^{\alpha_s \xi_1'}}{\sum_{s=1}^{\infty} \bar{C}_{Bso}}$$

.....(CV; 2;11)

If the distribution of reactant concentration in the upstream boundary cross-section is such that all terms of the series solution (2;4) other than the first may be neglected, the conversion in the reactor will depend solely upon its flow and diffusional characteristics.

$$\bar{C}_{B1o} >> \bar{C}_{B2o}\ , \qquad 1 - y = e^{\alpha_1 \xi_1'}$$

.....(CV; 2;12)

Equation (2;12) is the 'primary' solution of equation (2;1), the qualifying condition being equivalent to the 'convergence' condition (CII; 3;19).

Equation (CII; 1;1) and boundary conditions (CII; 1;2) and (CII; 1;3) govern the behaviour of a non-reactive tracer in a flow system of uniform cross-section. The terms of this equation may be subjected to the 'Laplace' integral transform.

$$c_P = \int_o^{\infty} c_A\ e^{-Pt}\, dt$$

.....(CV; 2;13)

$$\nabla(\psi \nabla C_p) - \gamma \Phi \frac{\partial C_p}{\partial \xi_1} - \frac{a^2 P}{\bar{D}} C_p = 0$$

.....(CV; 2;14)

The transformed equation (2;14) (in dimensionless form) differs from equation (2;1) only that it is written for the transform of tracer concentration, Cp, as opposed to reactant concentration, C_B. Hence a series solution may be derived for equation (2;14) in the same manner as that for equation (2;1)

$$C_p = \sum_{s=1}^{\infty} \bar{C}_{pso} e^{\alpha_s \xi_1} g_s$$

.....(CV; 2;15)

If the distribution of the transform quantity, Cp, in the upstream boundary cross-section of the reactor is such that the 'convergence' condition is satisfied, an expression similar to equation (2;12) may be written for the decay of the cross-sectional mean of the transform through the reactor.

$$\bar{C}_{p1o} >> \bar{C}_{p2o} , \qquad \frac{\bar{C}_p(\xi_1')}{\bar{C}_p(o)} = e^{\alpha_1 \xi_1'}$$

.....(CV; 2;16)

The left hand side of this equation may be quantified experimentally since the cross-sectional mean of the transform of tracer concentration signal is identical to the transform of the cross-sectional mean signal.

$$\bar{C}_p = \int_o^{\infty} \bar{C}_A e^{-pt} dt$$

Provided the Laplace integration constant, P, is chosen so as to be equal to the reaction constant, k_I, the exponential decay factor, x_1, will be the same for both equations (2;12) and 2;16). Therefore a simple relationship exists between the observed decay of the transform quantity and the conversion of the reactant.

$$P = K_I \quad , \qquad y = 1 - e^{\alpha_1 \xi_1'} = 1 - \frac{\bar{C}_P(\xi_1')}{\bar{C}_P(0)}$$

.....(CV; 2;17)

Equation (2;17) demonstrates that in a chemical reactor of uniform cross-section in which flow is fully developed, the conversion of a first order reaction may be predicted from a tracer study, provided the 'convergence' condition is satisfied for both tracer signal and reactant. The question of whether this condition is satisfied in the case of the tracer study may be resolved by examination of the reproducibility of results. With sufficient reproducibility, it may be assumed that the condition holds for tracer signals in the reactor. If this is so it may also be assumed that the 'convergence' condition will hold with respect to the reactant since the secondary terms of the series solutions for both cases behave in the same manner.

Tracer signals of pulse form are recommended for the tracer study since only these are of limited duration. For other signal forms, integration to obtain Laplace transforms (defined in equation (2;13)) must of necessity be lengthier and more complicated. The ratio of the numerical value of the appropriate transform, as found at the downstream boundary of the reactor, to that found at the upstream boundary is equal to the right hand side of equation (2;16).

DYNAMIC RESPONSE IN THE REACTOR

Equation (2;18) governs the behaviour of reactant in the reactor at unsteady state.

$$\nabla(\psi \nabla C_B) - \gamma \Phi \frac{\partial C_B}{\partial \xi_1} - \frac{a^2}{\bar{D}} \frac{\partial C_B}{\partial t} - \frac{a^2 K_I}{\bar{D}} C_B = 0$$

.....(CV; 2;18)

The wall boundary condition (2;2) applies directly to equation (2;18). The upstream boundary condition (2;3) must, however, be modified since reactant concentration is a function of time in this case.

To eliminate the steady state solutions of equation (2;18), the terms of this equation and of its related boundary conditions are differentiated once with respect to time.

$$\nabla(\psi \nabla C'_B) - \gamma \Phi \frac{\partial C'_B}{\partial \xi_1} - \frac{a^2}{\bar{D}} \frac{\partial C'_B}{\partial t} - \frac{a^2 K_I}{\bar{D}} C'_B = 0$$

.....(CV; 2;19)

Or

$$\text{On } \Gamma, \qquad \psi \frac{\partial C'_B}{\partial \xi_\Gamma} = 0$$

.....(CV; 2;20)

$$\xi_1 = 0 \qquad C'_B(0, \xi_2, \xi_3, t) = C'_{Bo}(\xi_2, \xi_3, t)$$

.....(CV; 2;21)

where:-

$$C'_B = \frac{\partial C_B}{\partial t}$$

If the disturbances in reactant concentration are of either limited duration or are repetitive, they may be represented by Fourier series (see Chapter II section 2).

$$C_B' = \sum_{r=0}^{\infty} R \{ C_r' (\xi_1, \xi_2, \xi_3) \, e^{i r \omega t} \}$$

.....(CV; 2;22)

Equation (2;19) and the boundary conditions (2;20) and (2;21) are transformed for the series solution (2;22)

$$\nabla (\psi \nabla C_r') - \gamma \Phi \frac{\partial C_r'}{\partial \xi_1} - \left(\frac{a^2 K_I}{\bar{D}} + i \Omega \right) C_r' = 0$$

.....(CV;2;23)

Or

$$\text{On } \Gamma, \qquad \psi \frac{\partial C_r'}{\partial \xi_n} = 0$$

.....(CV; 2;24)

$$\xi_1 = 0, \qquad C_r' (0, \xi_2, \xi_3) = C_{r0}' (\xi_2, \xi_3)$$

.....(CV; 2;25)

A series solution for equation (2;23) is derived in the same manner as those for equations (CII; 2;17) and (2;1).

$$C_r' = \sum_{s=1}^{\infty} \bar{X}_{rs0}' \, e^{\alpha_{rs}' \xi_1} \, f_{rs}' (\xi_2, \xi_3)$$

.....(CV; 2;26)

If the 'convergence' condition is satisfied, the complex transfer factor, Y, through the reactor is dependent on the flow and diffusional characteristics of the reactor alone.

$$\bar{X}'_{r1o} >> \bar{X}'_{r2o} , \qquad Y = \frac{\bar{C}'_r(\xi'_1)}{\bar{C}'_r(o)} = e^{\alpha'_{r1}\xi'_1}$$

.....(CV; 2;27)

The complex transfer factor is the quantity whose modulus is equal to the decay and whose argument is equal to the phase shift (in radians) as experienced by a sinusoidal tracer signal upon passing through the reactor.

The terms of the non-reactive tracer equations, equation (CII; 1;1) and boundary conditions (CII; 1;2) and (CII; 1;3) are subjected to a special integral transform.

$$C''_r = \int_o^T C_A \, e^{-(p + i_r\omega)t} \, dt$$

.....(CV; 2;28)

$$\nabla(\psi \nabla C''_r) - \gamma \Phi \frac{\partial C''_r}{\partial \xi_1} - \left(\frac{a^2 p}{\bar{D}} + i_r \Omega\right) C''_r = o$$

.....(CV; 2;29)

$$On \ \Gamma , \qquad \psi \frac{\partial C''_r}{\partial \xi_n} = o$$

.....(CV; 2;30)

$$\xi_1 = 0 \,, \qquad C_r''(0, \xi_2, \xi_3) = C_{r0}''(\xi_2, \xi_3)$$

.....(CV; 2;31)

Equation (2;29) has a series solution similar to that of equation (2;23).

$$C_r'' = \sum_{s=1}^{\infty} \bar{X}_{rs0}'' e^{\alpha_{rs}'' \xi_1} f_{rs}''(\xi_2, \xi_3)$$

.....(CV; 2;32)

With the 'convergence' condition satisfied, the response is determined by the reactor alone.

$$\bar{X}_{r10}'' >> \bar{X}_{r20}'' \,, \qquad \frac{\bar{C}_r''(\xi_1')}{\bar{C}_r''(0)} = e^{\alpha_{r1}'' \xi_1'}$$

.....(CV; 2;33)

If the integration constant, P, is chosen so as to be equal to the reaction constant, k_I, the logarithmic transfer factors, α_{r1}' and α_{r1}'', of equations (2;27) and (2;33) respectively are the same. Hence the response of the reactor with respect to the transform of a tracer signal (defined in equation (2;28)) is equal to the response of the reactor to a disturbance in reactant concentration.

$$P = k_I \,, \qquad Y = \frac{\bar{C}_r'(\xi_1')}{\bar{C}_r'(0)} = \frac{\bar{C}_r''(\xi_1')}{\bar{C}_r''(0)}$$

.....(CV; 2;34)

This relationship is subject to the same conditions as that concerning the conversion in the first order reaction (equation (2;17)).

REFERENCES

1 Danckwerts, P.V., C.E.S. 2, 1 (1953)

2 Griffiths, A., Proc. Roy. Soc. (Lond.) 23, 190 (1911)

3 Stewart, G.M., J. of Physiology 15, 1 (1894)

4 Taylor, G.I., Proc. Roy. Soc. (Lond.) A219, 186 (1953)

5 Taylor, G.I., Proc. Roy. Soc. (Lond.) A225, 473 (1954)

6 Taylor, G.I., Proc. Roy. Soc. (Lond.) A223, 446 (1954)

7 Aris, R., Proc. Roy. Soc. (Lond.) A235, 67 (1956)

8 Philip, J.R., Austr. J. of Physics 16, 287, 311 (1963)

9 Pai, Shih I., J. of Appl. Mech. p. 112 (March 1953)

10 Knudsen & Katz, "Fluid Dynamics and Heat Transfer" McGraw-Hill N.Y. (1958)

11 Wooding, R.A., J. of Fluid. Mech. 7 501 (1960)

12 International Critical Tables

13 Nikuradse, J., V.D.I. Forschungsheft 289 (1929)

14 Cataneo, F.C., Ph.D. Thesis Lehigh Univ. 1963

15 Sherwood, T.K., & Towle, W.L., I.E.C. 31 457 (1939)

16 Dhanak, A.M., A.I.Ch.E. J. 4 190, (1968)

17 Schwarz, W.H., & Hoelscher, H.E., A.I.Ch.E. J. 2 101 (1956)

18 Sherwood, T.K., & Woertz, B.B., Trans. A.I.Che.E. 35, 517 (1939)

LIST OF SYMBOLS

a	Characteristic dimension of flow system. (Width of parallel wall flow system).
b	Half the width of parallel wall flow system.
C_A	Concentration of tracer
C_B	Concentration of reactant
Cp, C_r	Integral transforms of concentration
D	Total diffusivity
D_A	Molecular diffusivity
D_E	Eddy diffusivity
D_j	Differential operator
F	Water flow rate (gallons/hour)
F_{rs}	Vector solution of equation (CII; 5;3)
f	Fanning friction factor
f_{rs}	Function of position in flow system cross-section
g_{rs}	As f_{rs}
i	$\sqrt{-1}$
j	Integer
K_r	Complex dispersion coefficient
k	Taylor/Aris dispersion coefficient
k_r	Variable reference plane dispersion coefficient
k_I	First order chemical reaction constant
L	Length of experimental section of flow system
P	Integration constant in Laplace transform
R	Shear stress in flow system
Re	Reynolds number
R_i	Radius of inner wall of annular flow system
R_o	Radius of outer wall of annular flow system
R_t	Radius of turbular flow system
$\bar{R}$	Average of radii, R_i and R_o
t	Integer
s	Integer

T	Limite of time in integral
T_r	Transfer matrix of equation (CII; 5;3)
t	Time
U	Point fluid flow velocity
V_r	Reference plane velocity
W	Tracer signal frequency (cycles/minute)
X_{rs}	Function of longitudinal position in flow system
x_j	Cartesian space coordinate
r	Radius in polar coordinate system
Y	Transfer factor in chemical reactor
y	Conversion in chemical reactor
α_{rs}	Logarithmic transfer factor
Γ	Wall boundary of flow system
∇	Differential operator in three dimensional cartesian coordinate system (dimensionless).
ε	Eddy viscosity
ζ_{rs}	Quantity defined by equation (CII; 3;9)
η	Dimensionless transverse coordinate in parallel wall flow system
φ	Logarithm of attenuation of tracer signal
μ	Viscosity
ν	Kinematic viscosity
ξ_j	Dimensionless cartesian space coordinate
ξ_1'	Longitudinal coordinate of downstream boundary of flow system
ρ	Density
Φ	Dimensionless quantity, $\frac{\bar{U}a}{\bar{D}}$
ϕ	Phase lag of tracer signal
ϕ_{rs}	Quantity defined by equation (CII; 3;8)
ψ	Dimensionless point flow velocity
ψ	Dimensionless diffusivity
Ω	Dimensionless quantity, $\frac{\omega a^2}{\bar{D}}$
ω	Tracer signal frequency (radians/second)

N.B. Line over symbol denotes mean of quantity with respect to cross-section of flow system.

$R\{....\}$	Real part of quantity enclosed between brackets
$I\{....\}$	Imaginary part of above

APPENDIX I

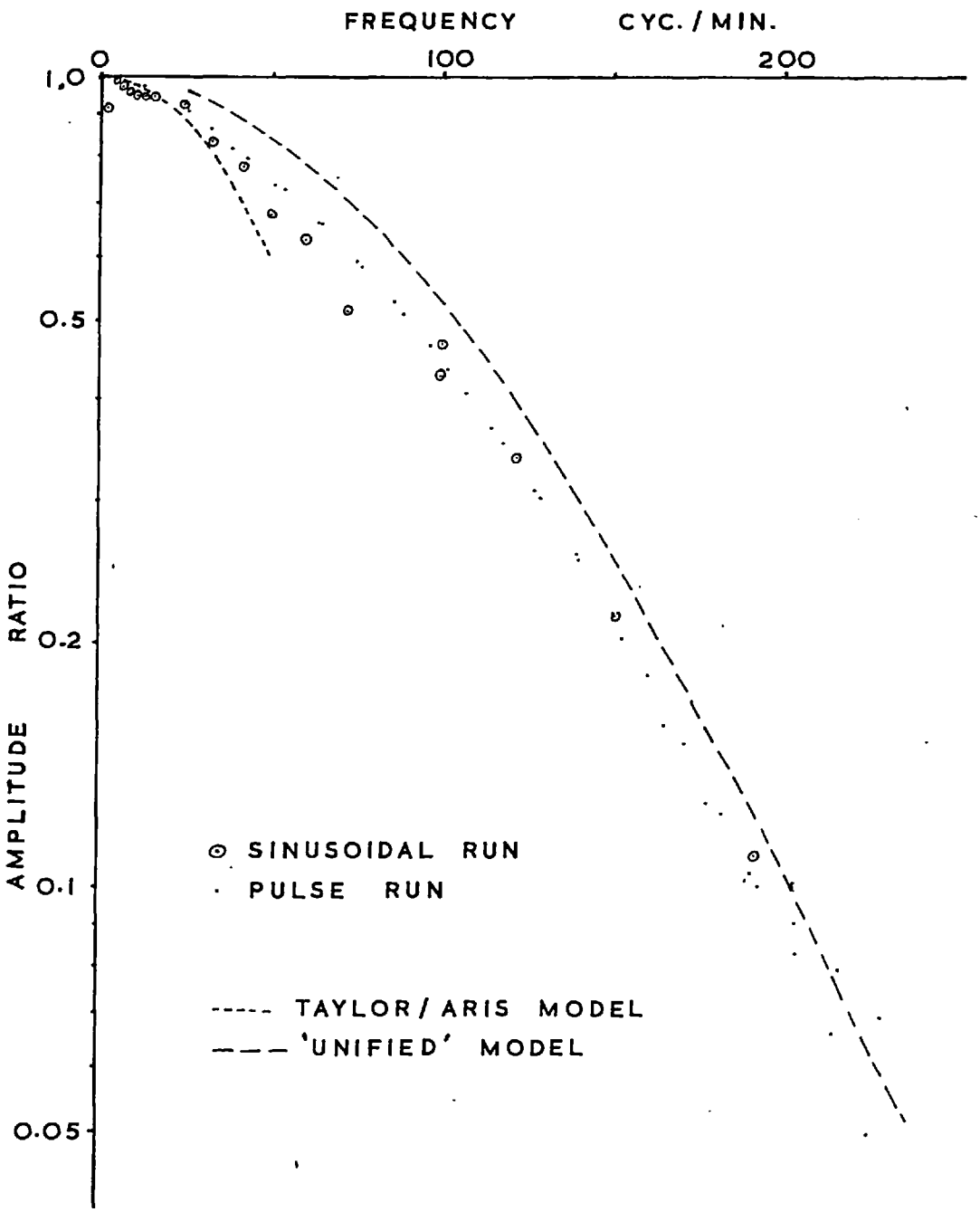


FIG. a1 780 GAL./HR.

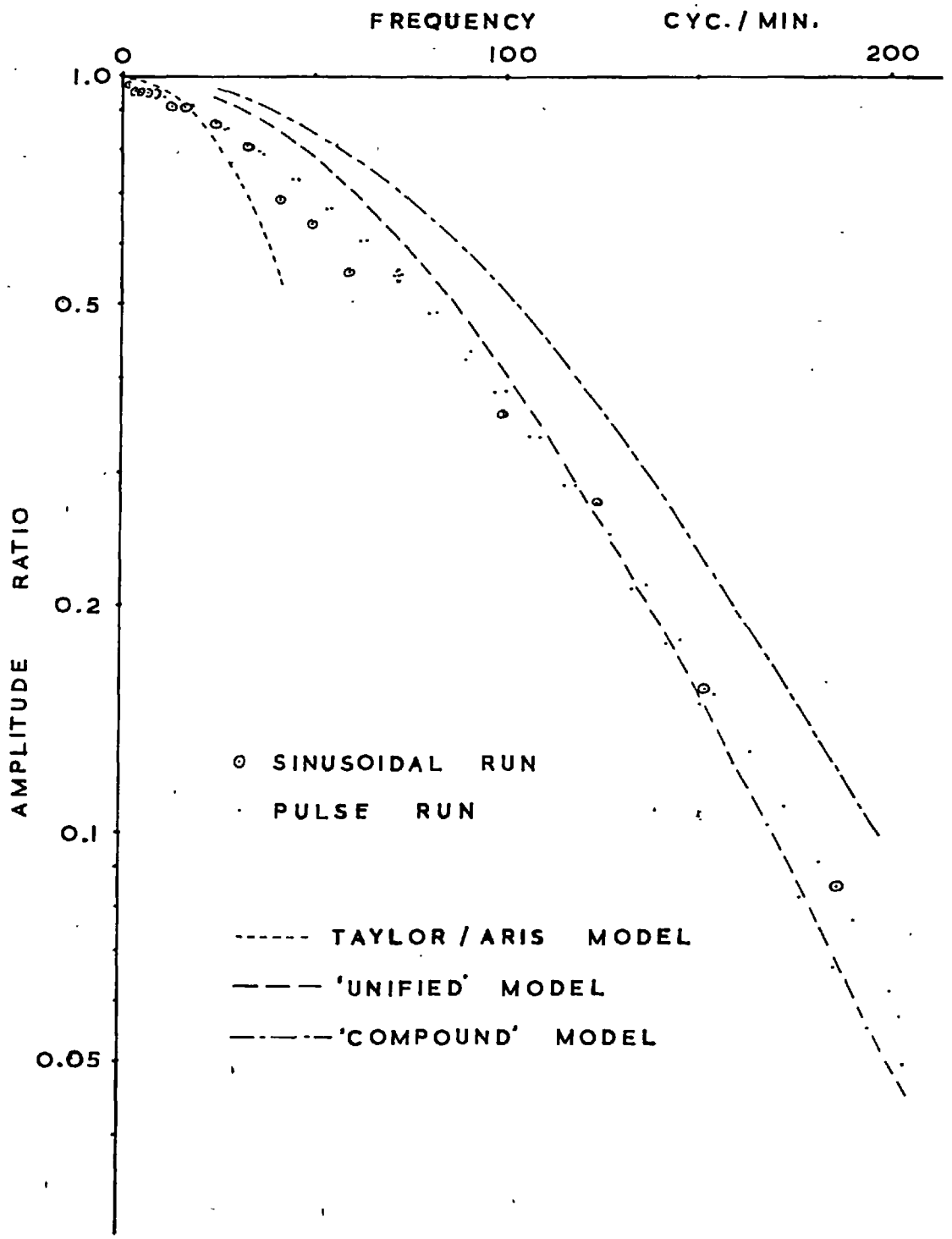


FIG. a2 700 GAL./HR.

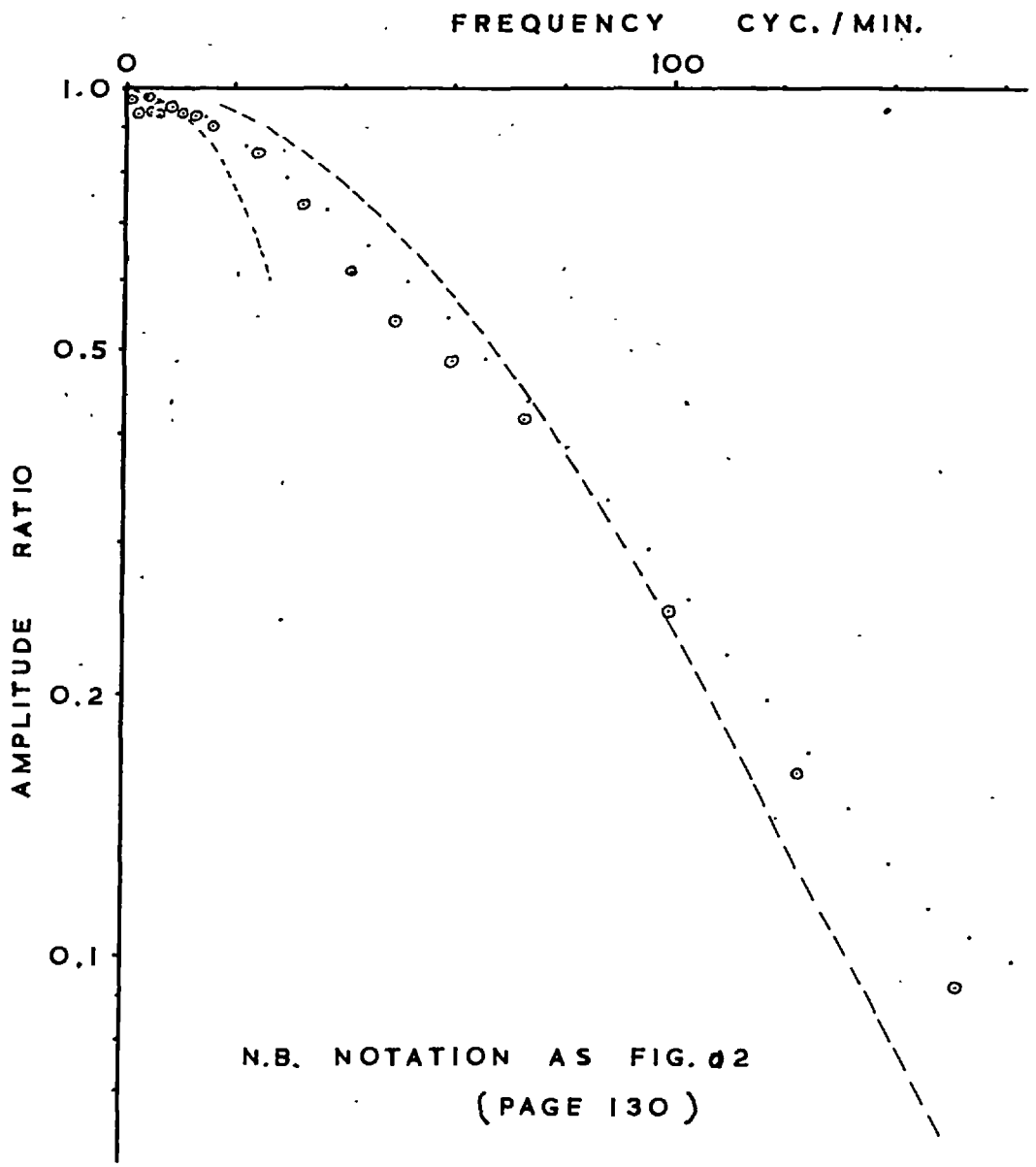


FIG. a3 600 GAL./HR.

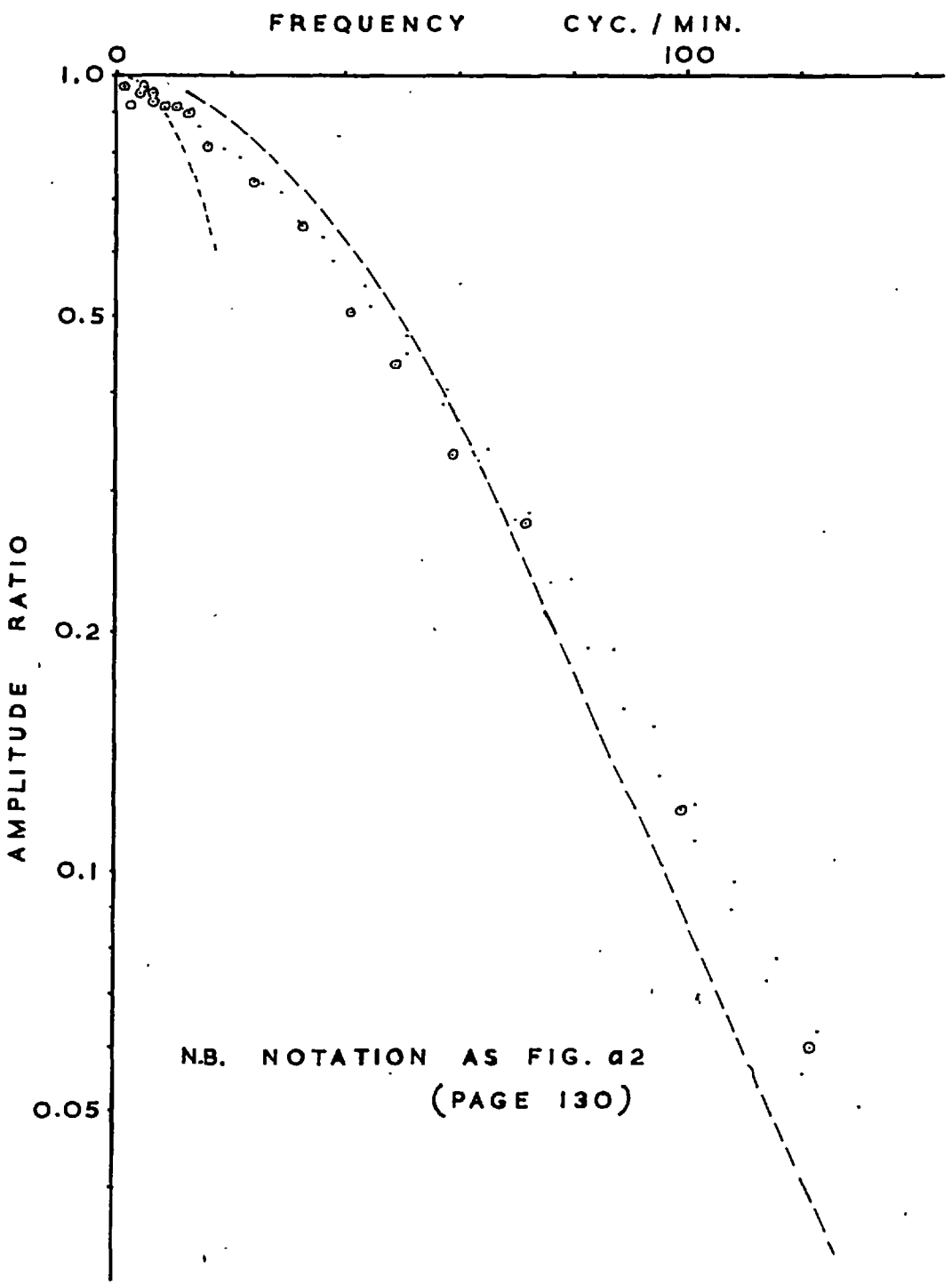


FIG. a4 500 GAL./ HR.

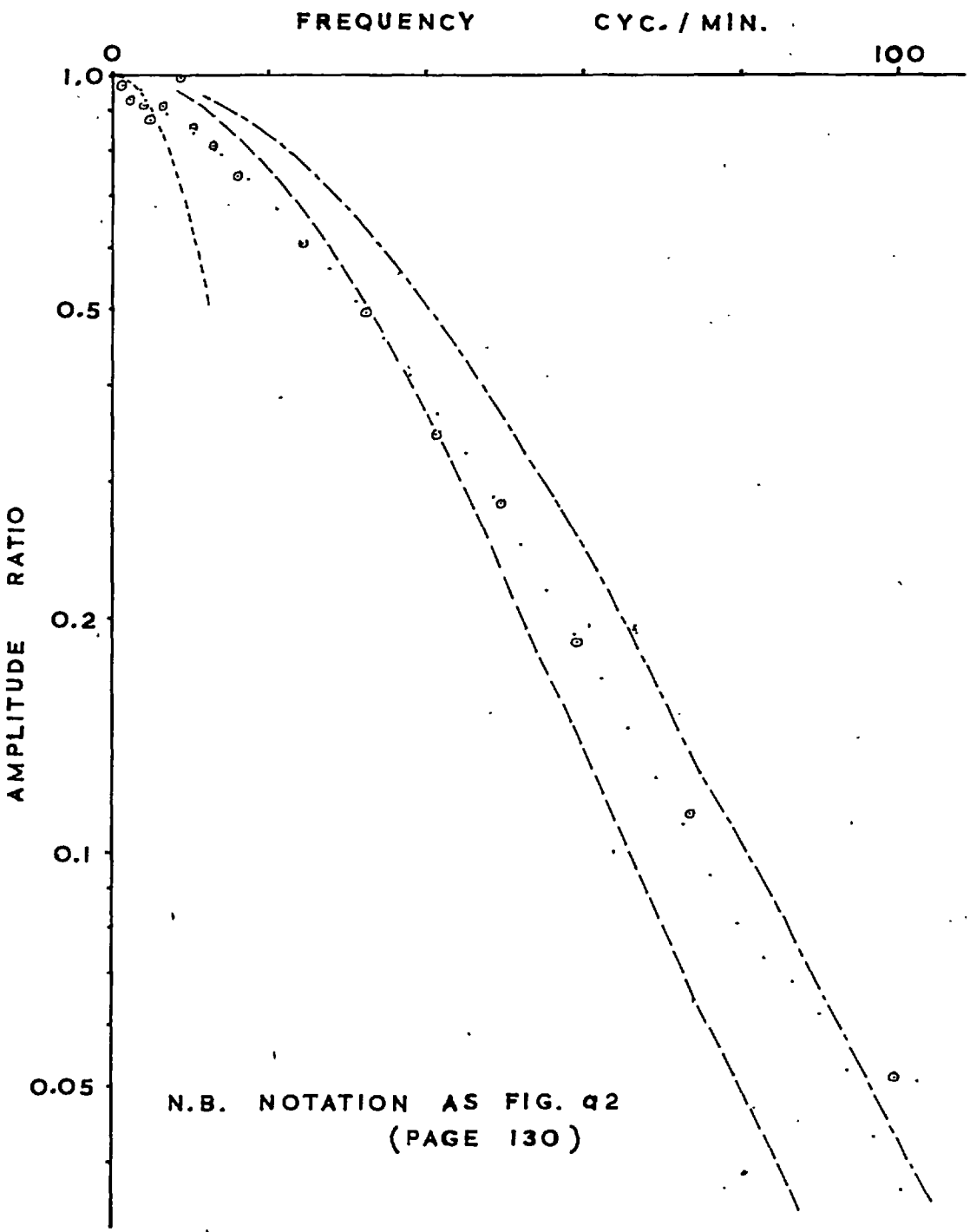


FIG. a5 400 GAL./HR.

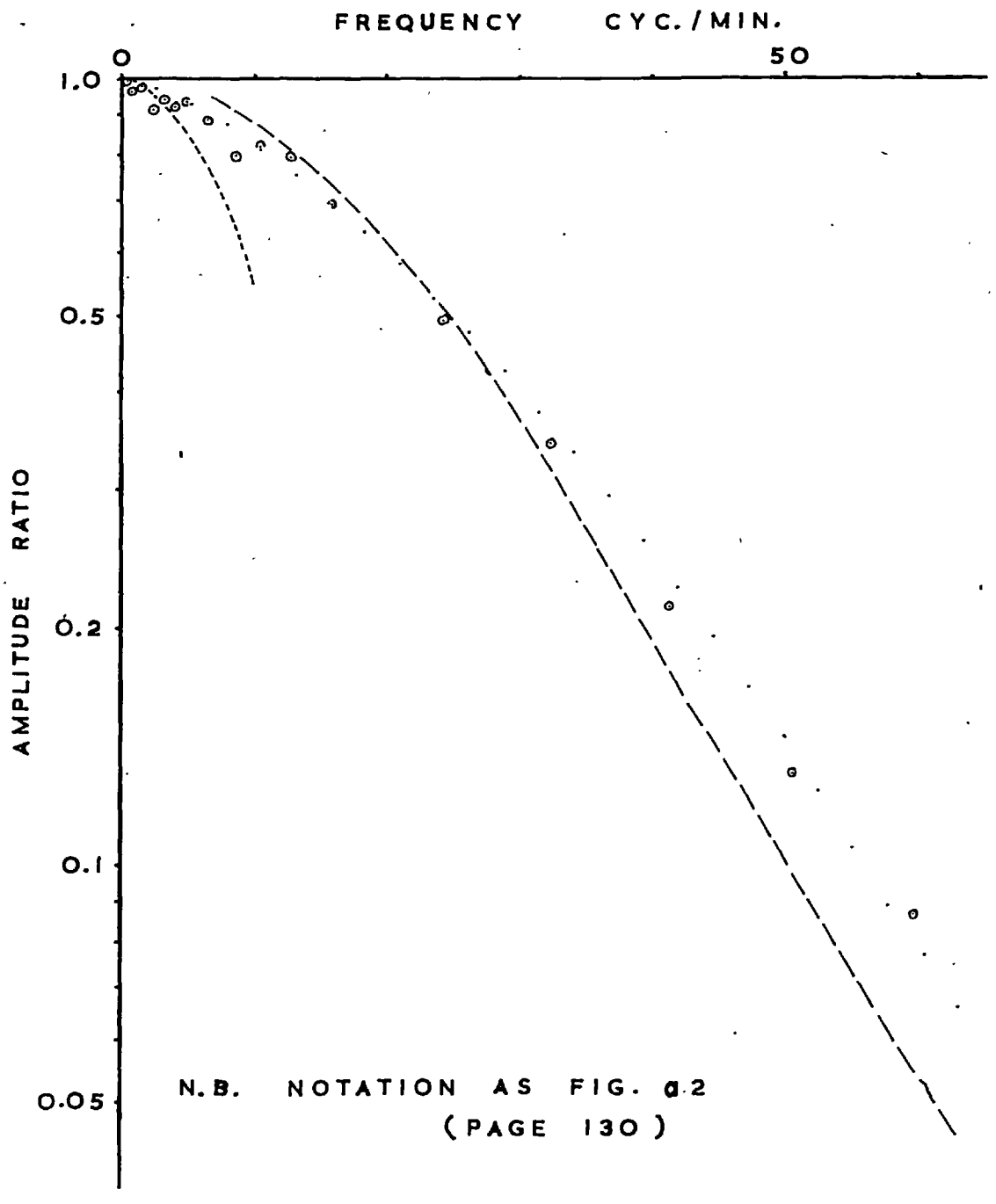


FIG. a 6 340 GAL./HR.

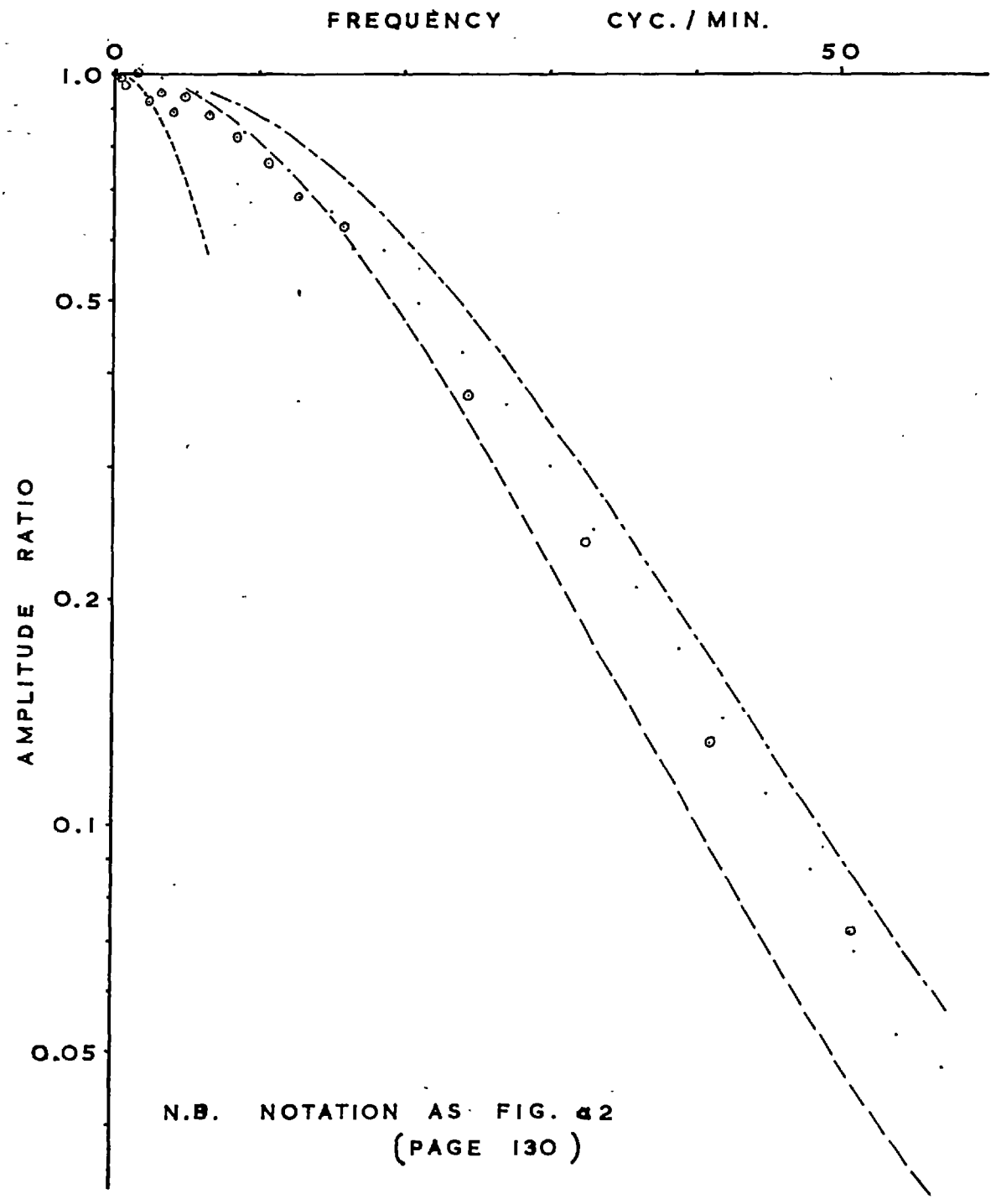


FIG. a 7 300 GAL./HR.

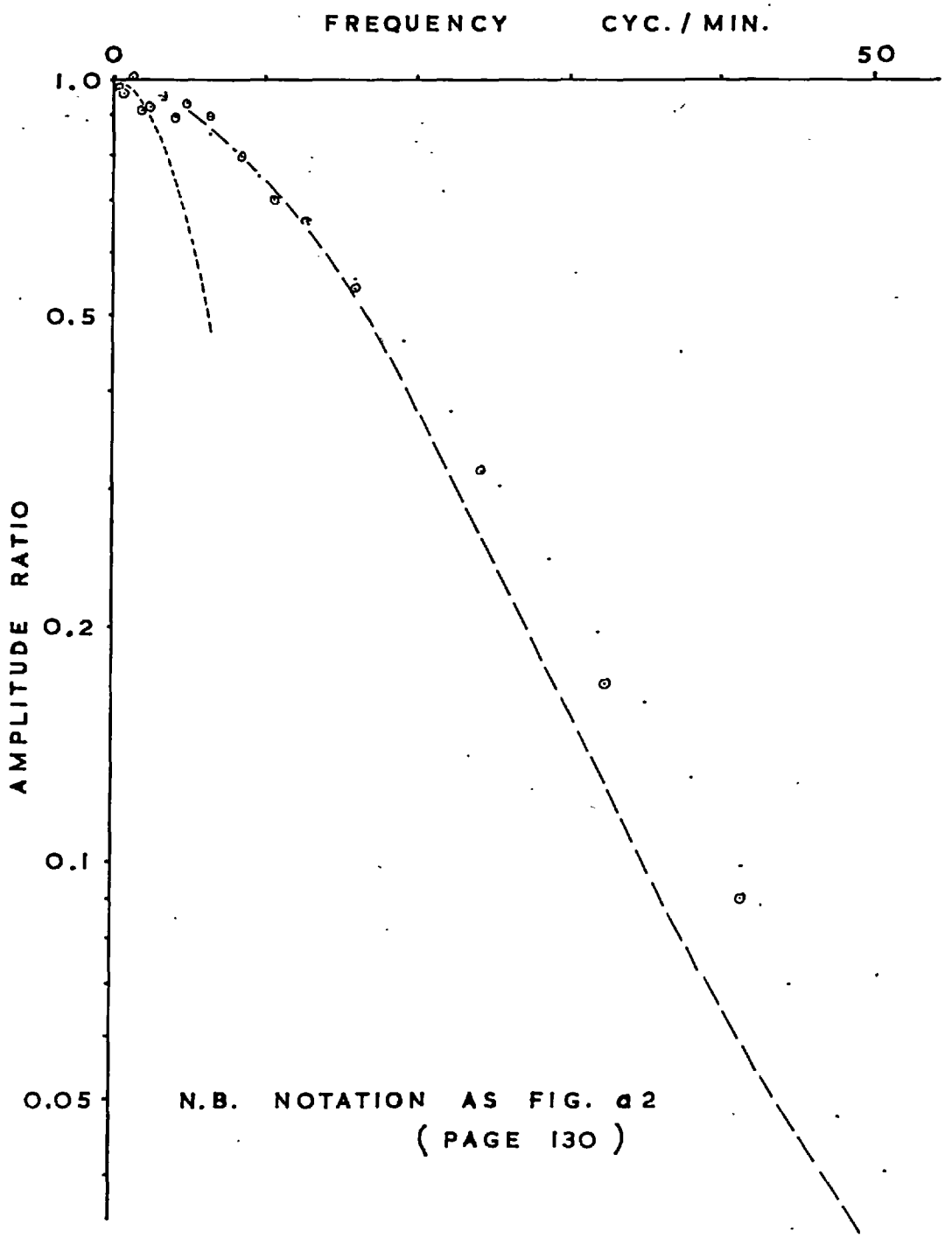


FIG. a 8 280 GAL./HR.

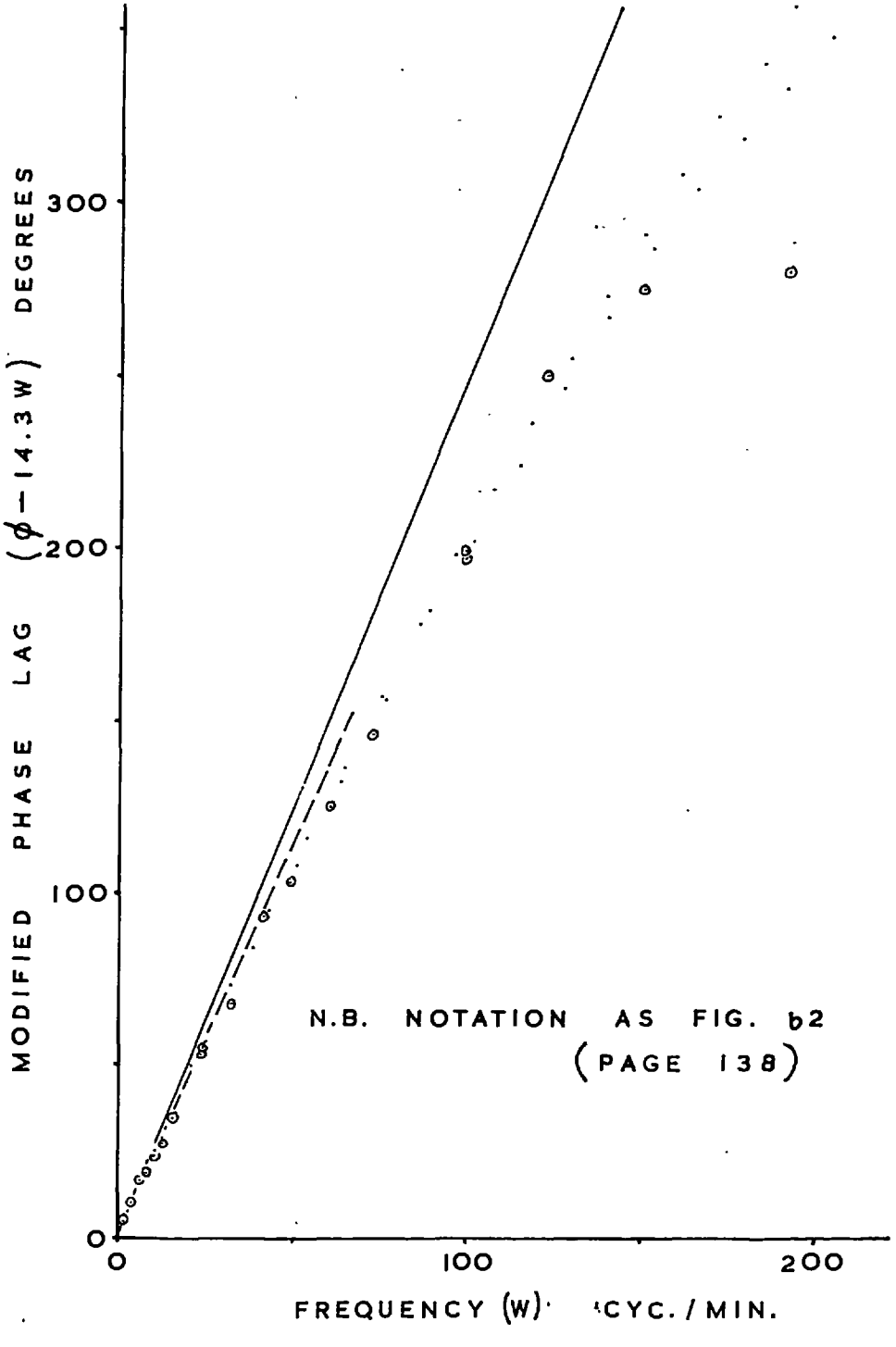


FIG. b1 780 GAL./HR.

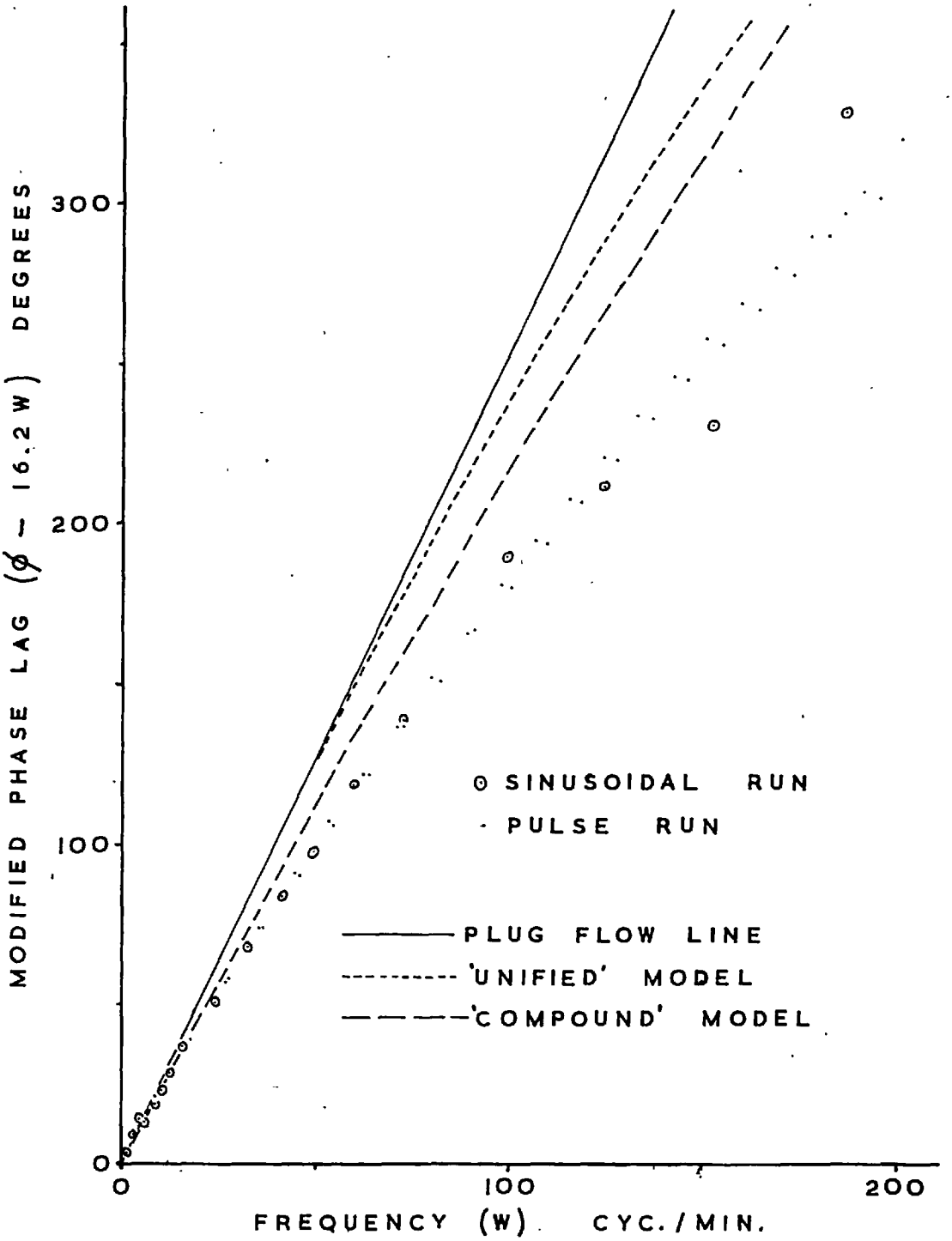


FIG. b 2 700 GAL./HR.

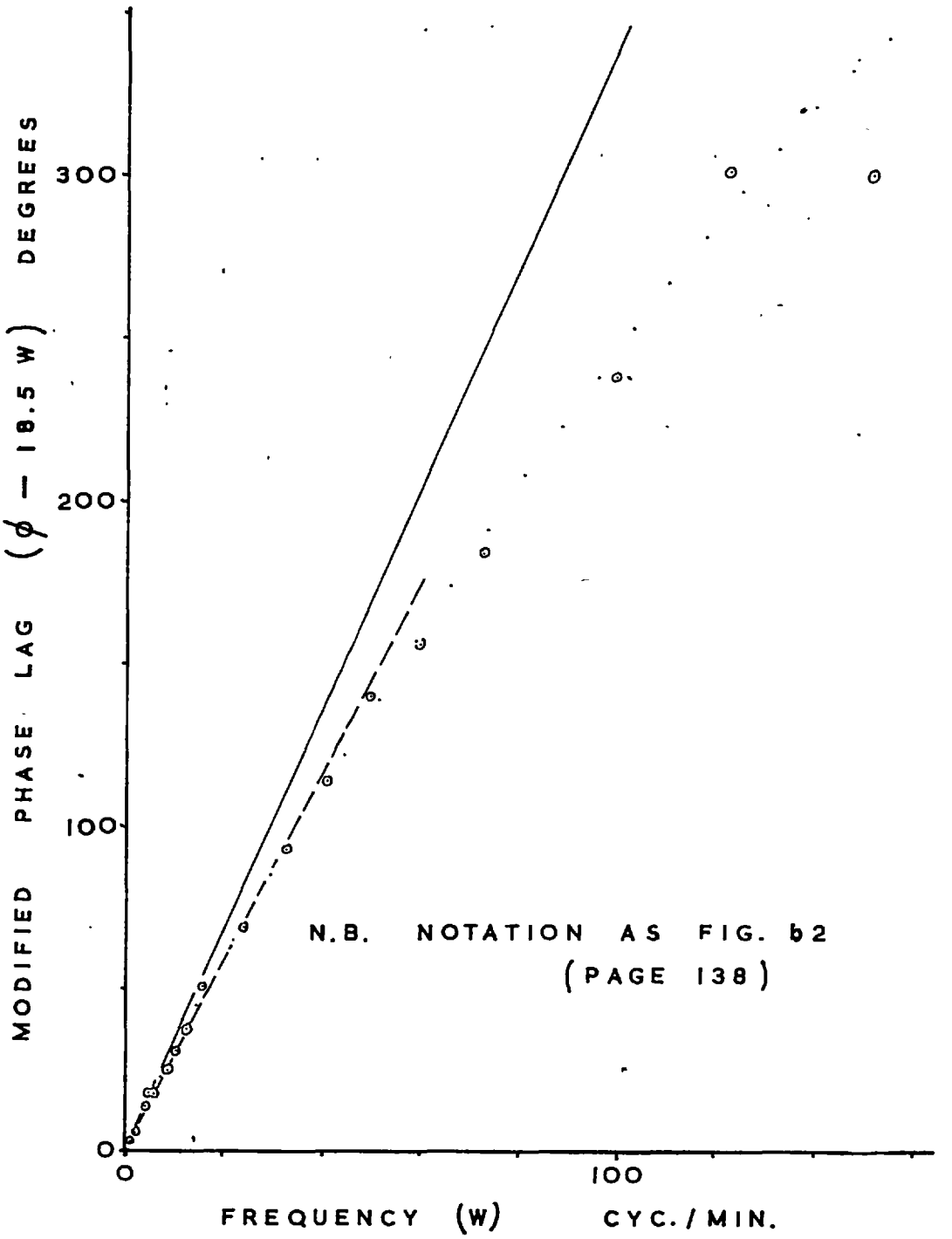


FIG. b 3 600 GAL./HR.

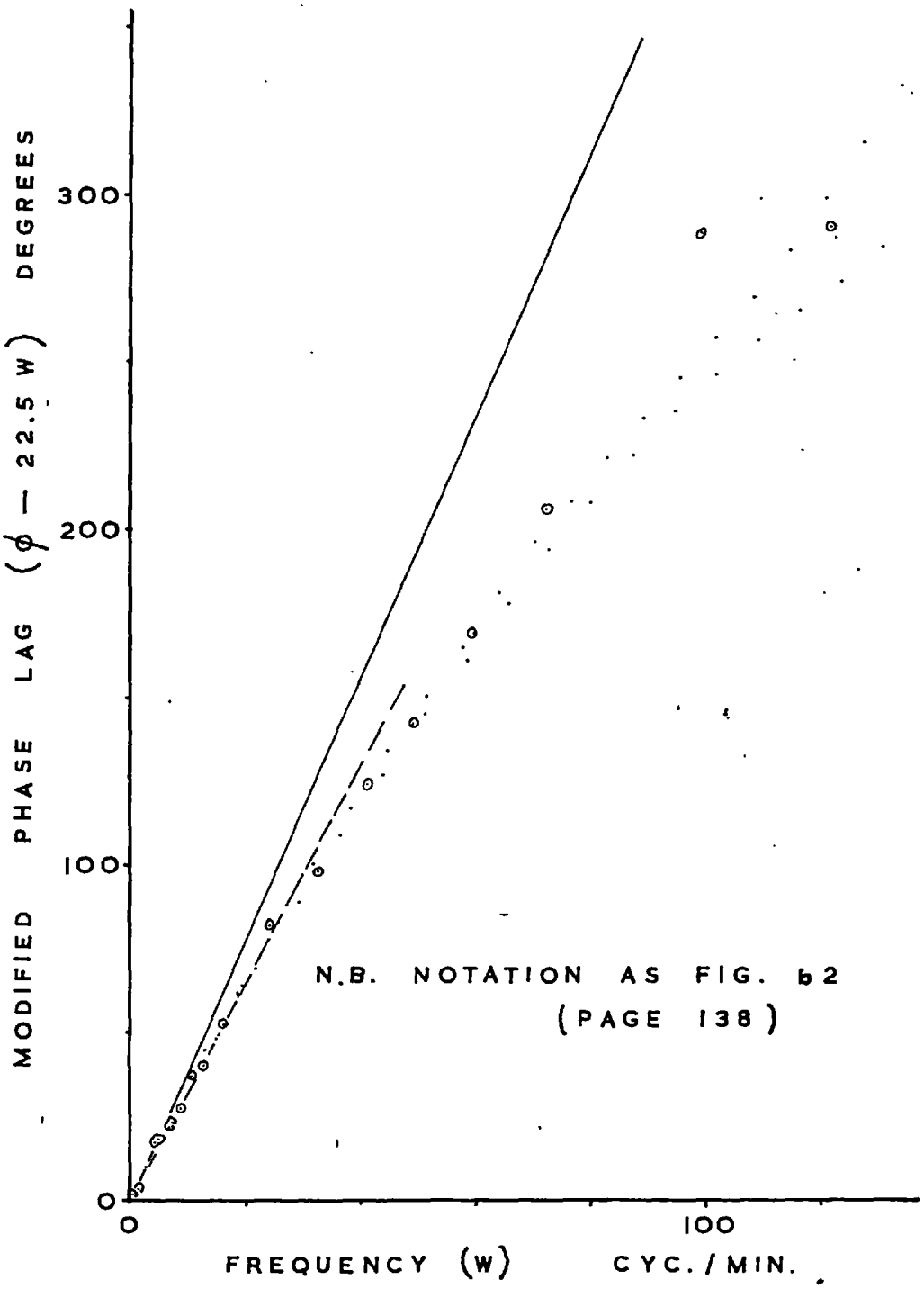


FIG. b 4 500 GAL./HR.

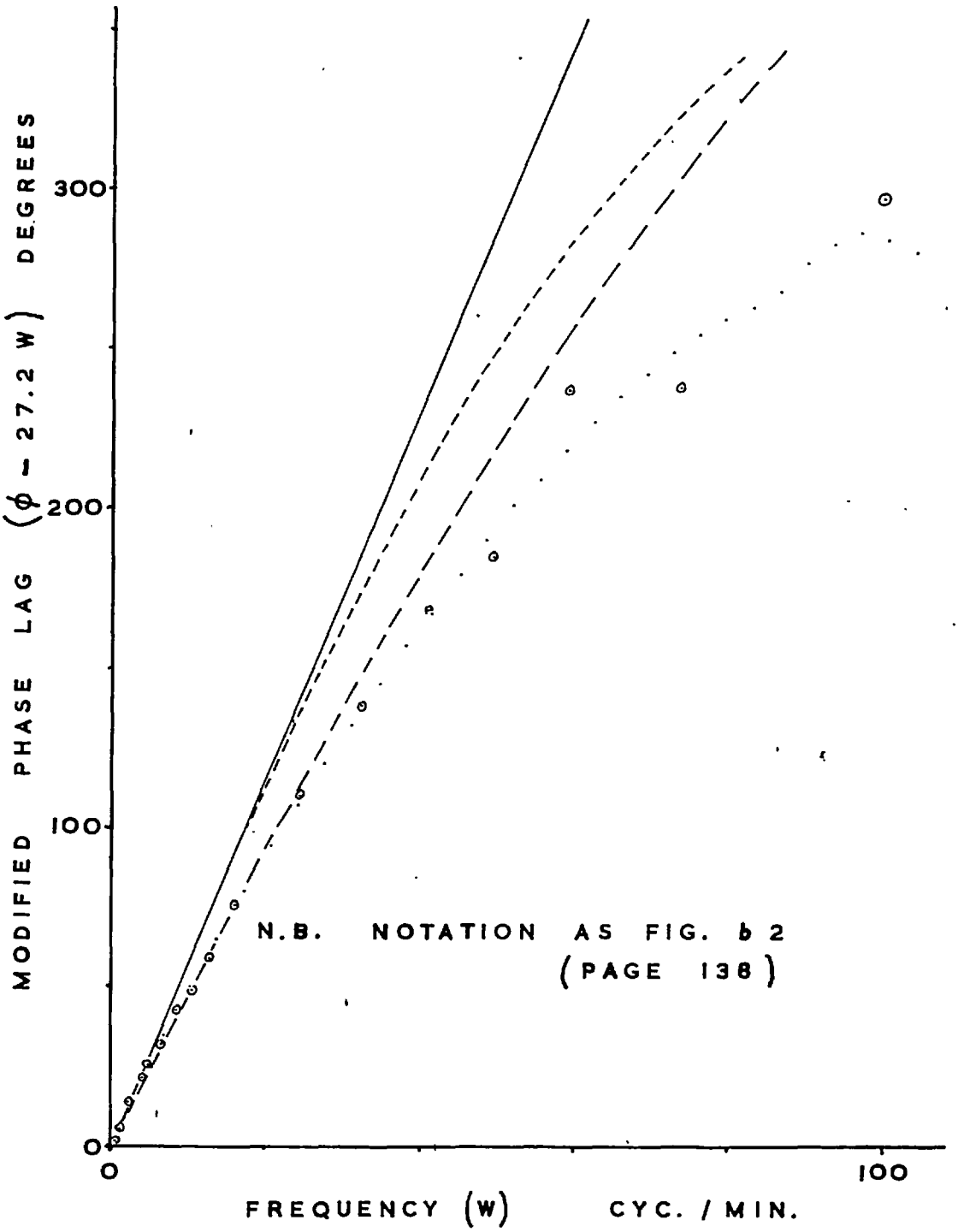


FIG. b 5 400 GAL. / HR.

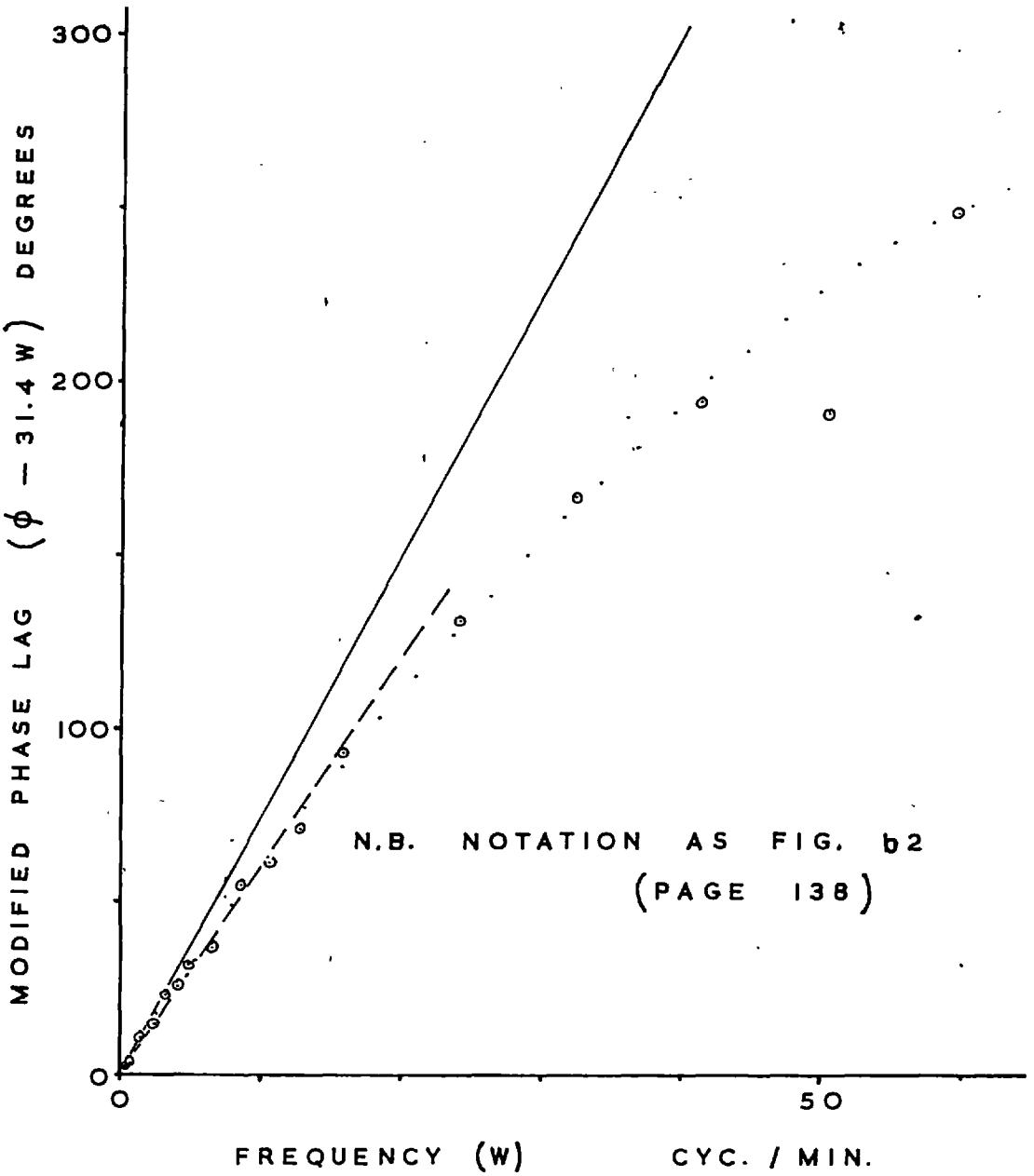


FIG. b 6 340 GAL. / HR.

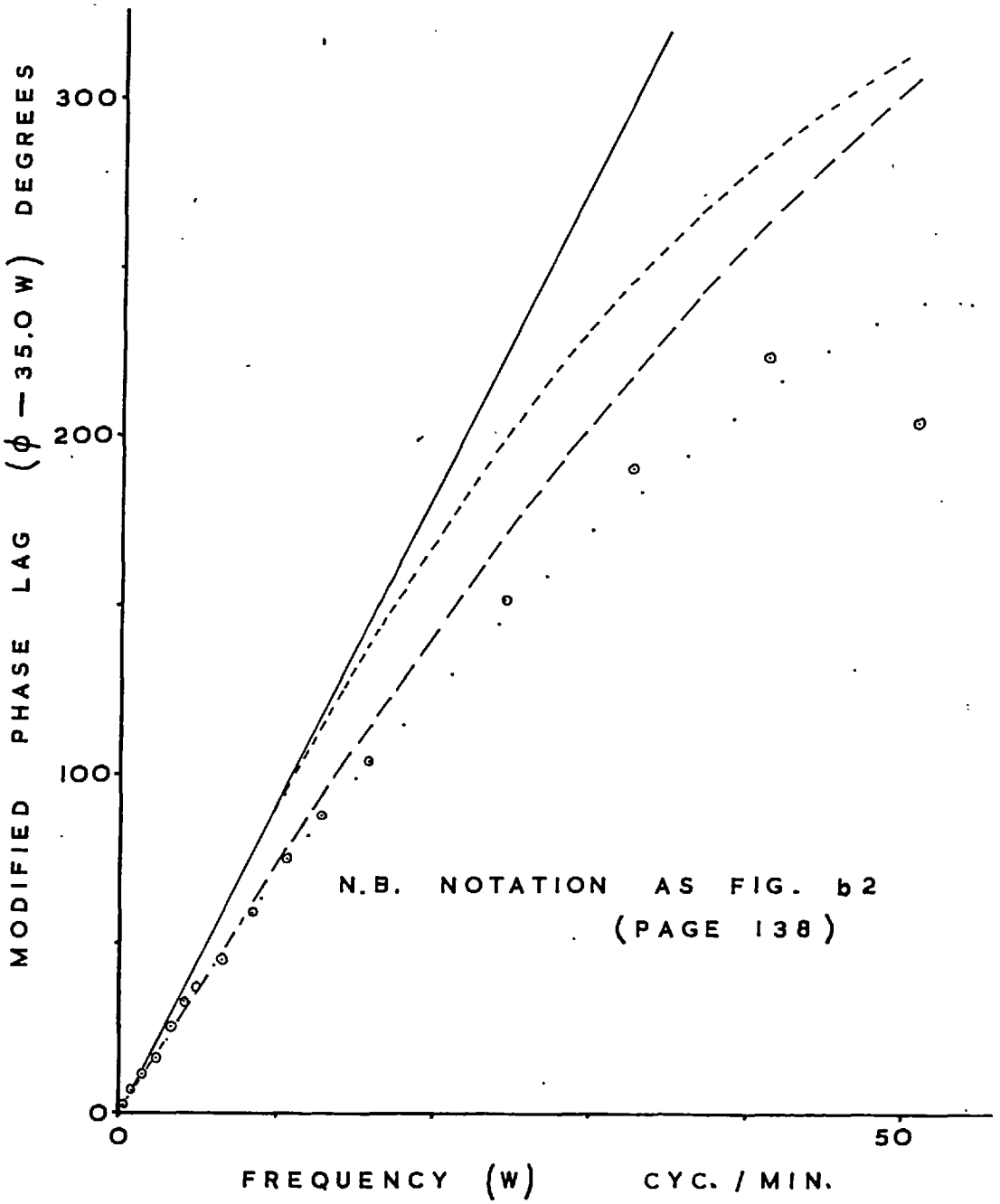


FIG. b 7 300 GAL. / HR.

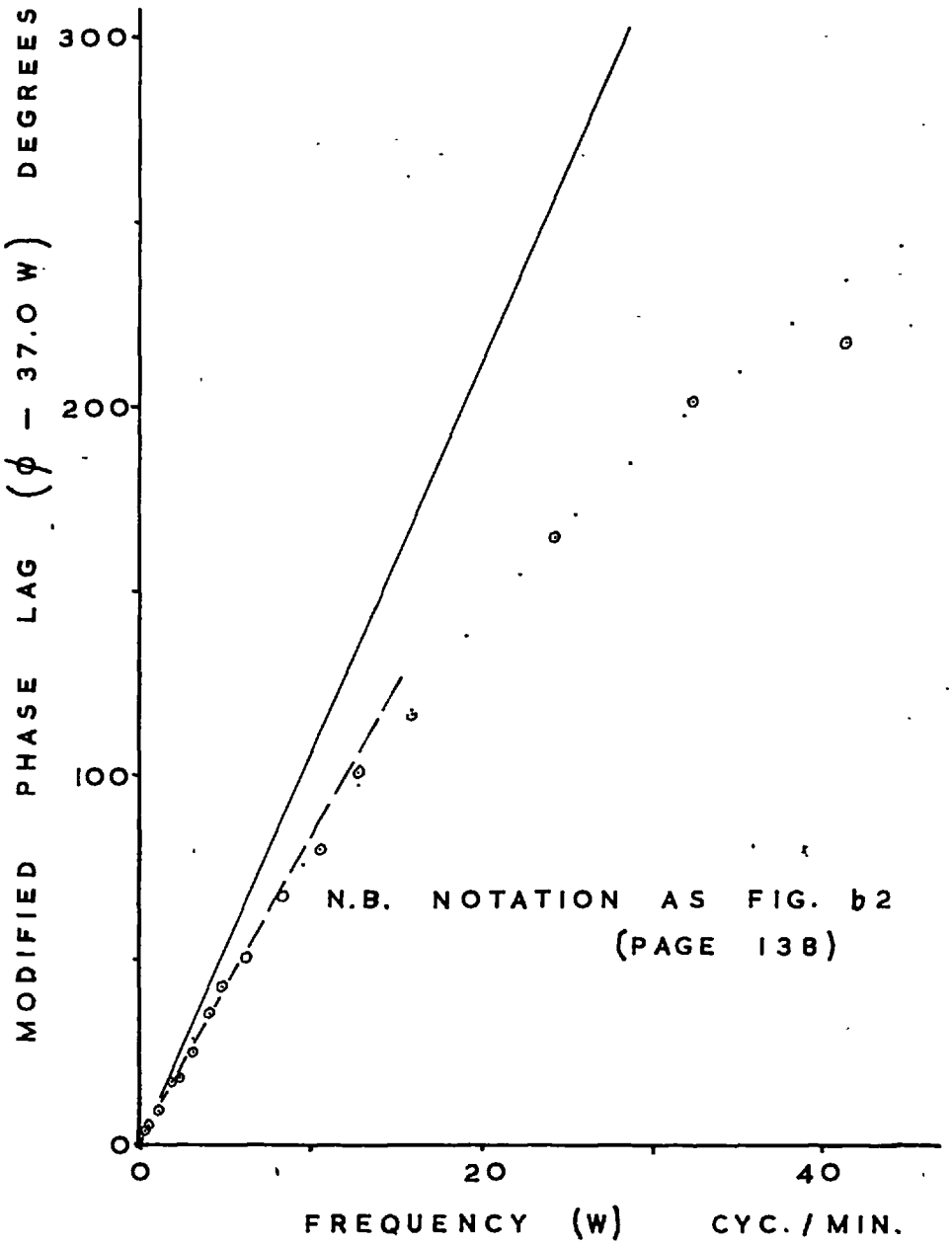


FIG. b 8 280 GAL./HR.

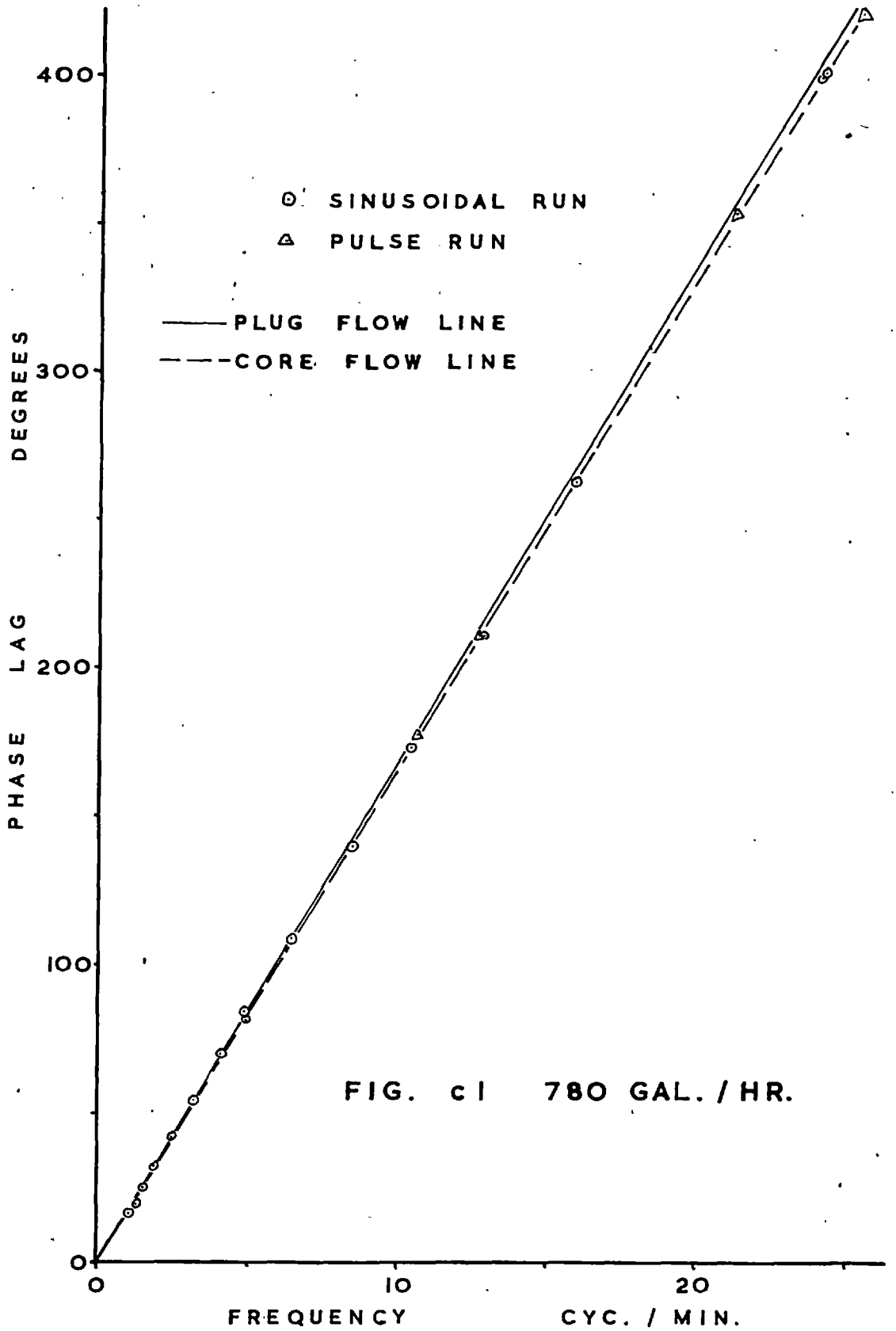


FIG. c1 780 GAL. / HR.

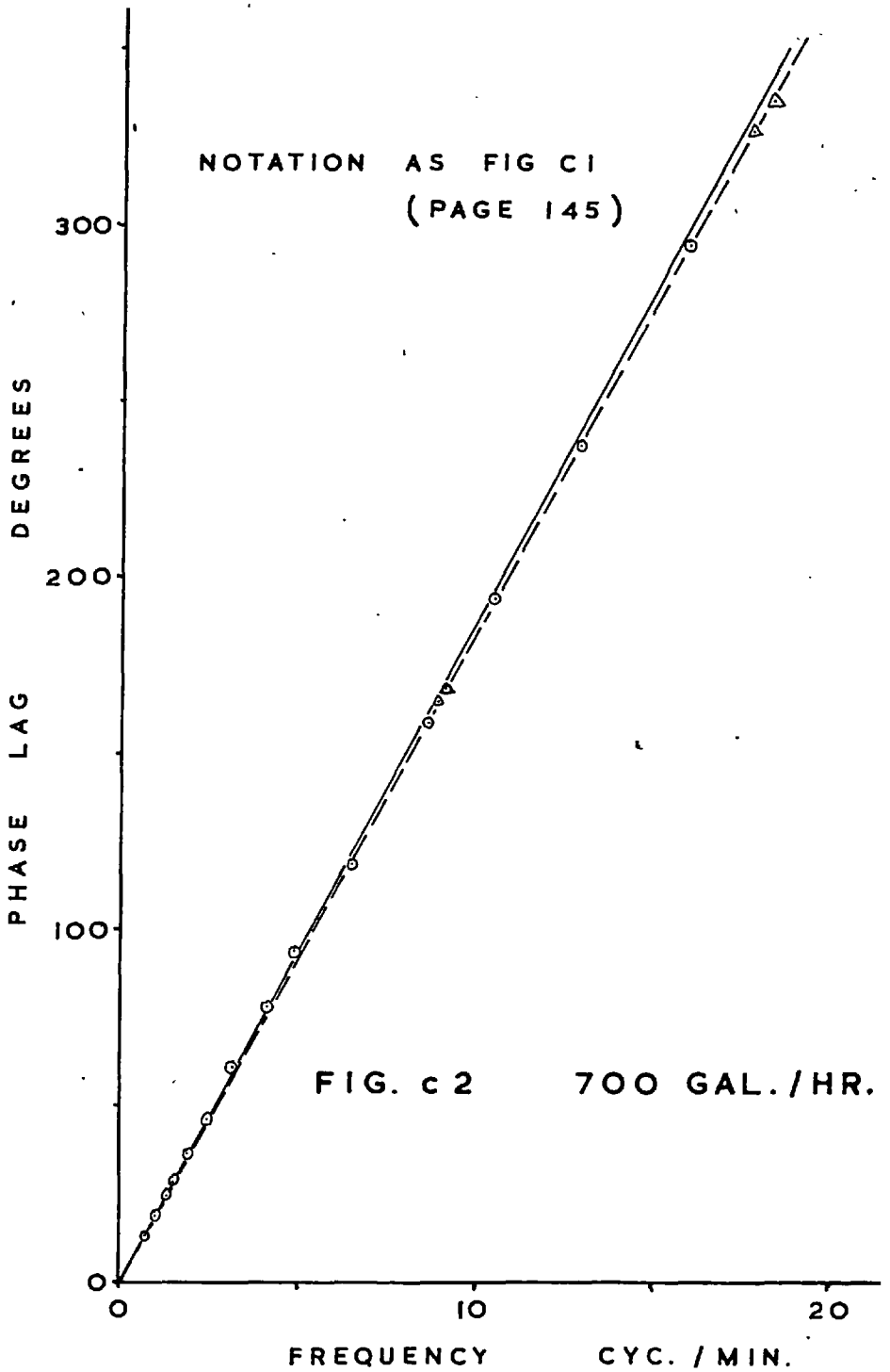


FIG. c 2 700 GAL./HR.

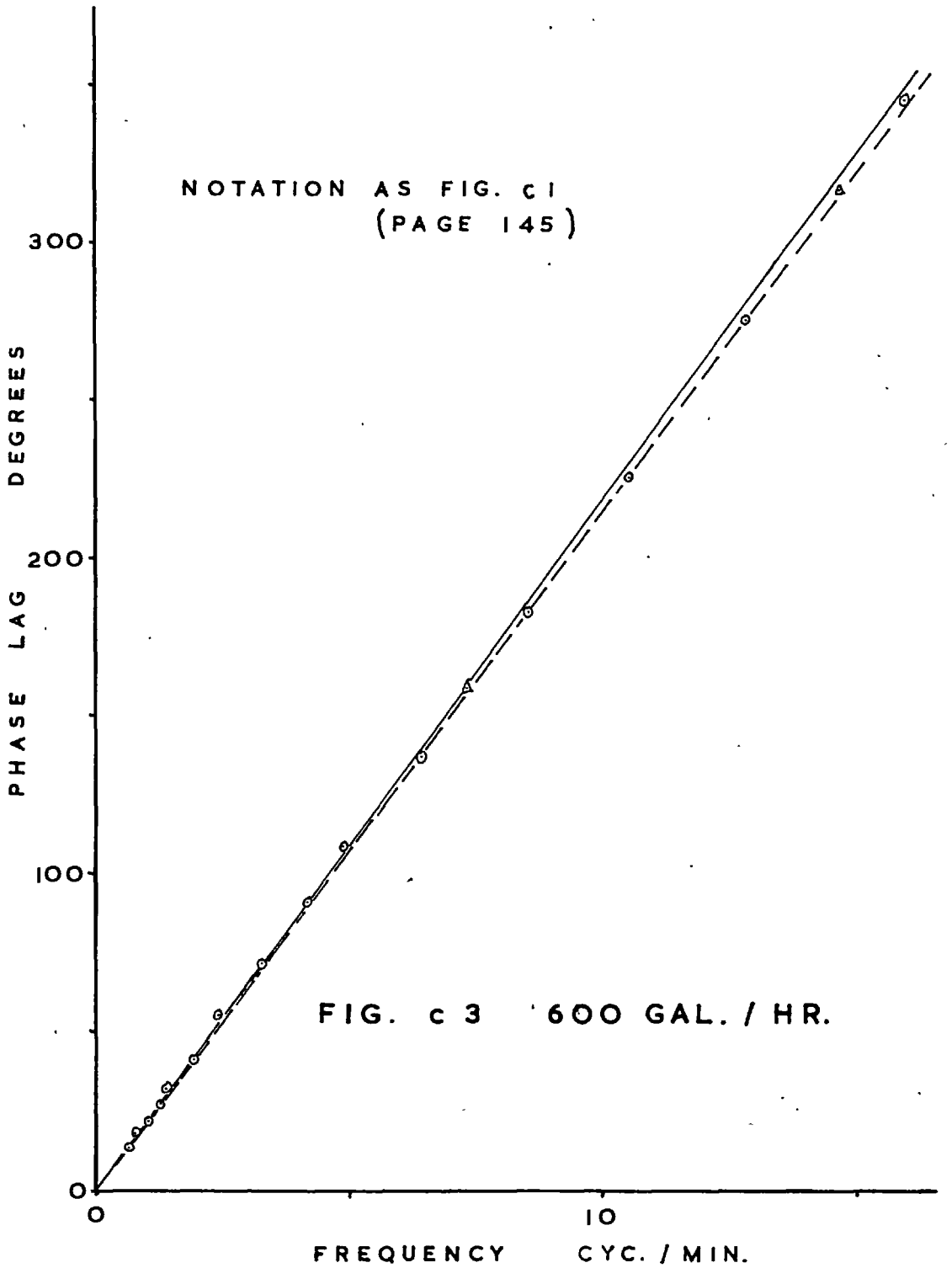


FIG. c 3 600 GAL. / HR.

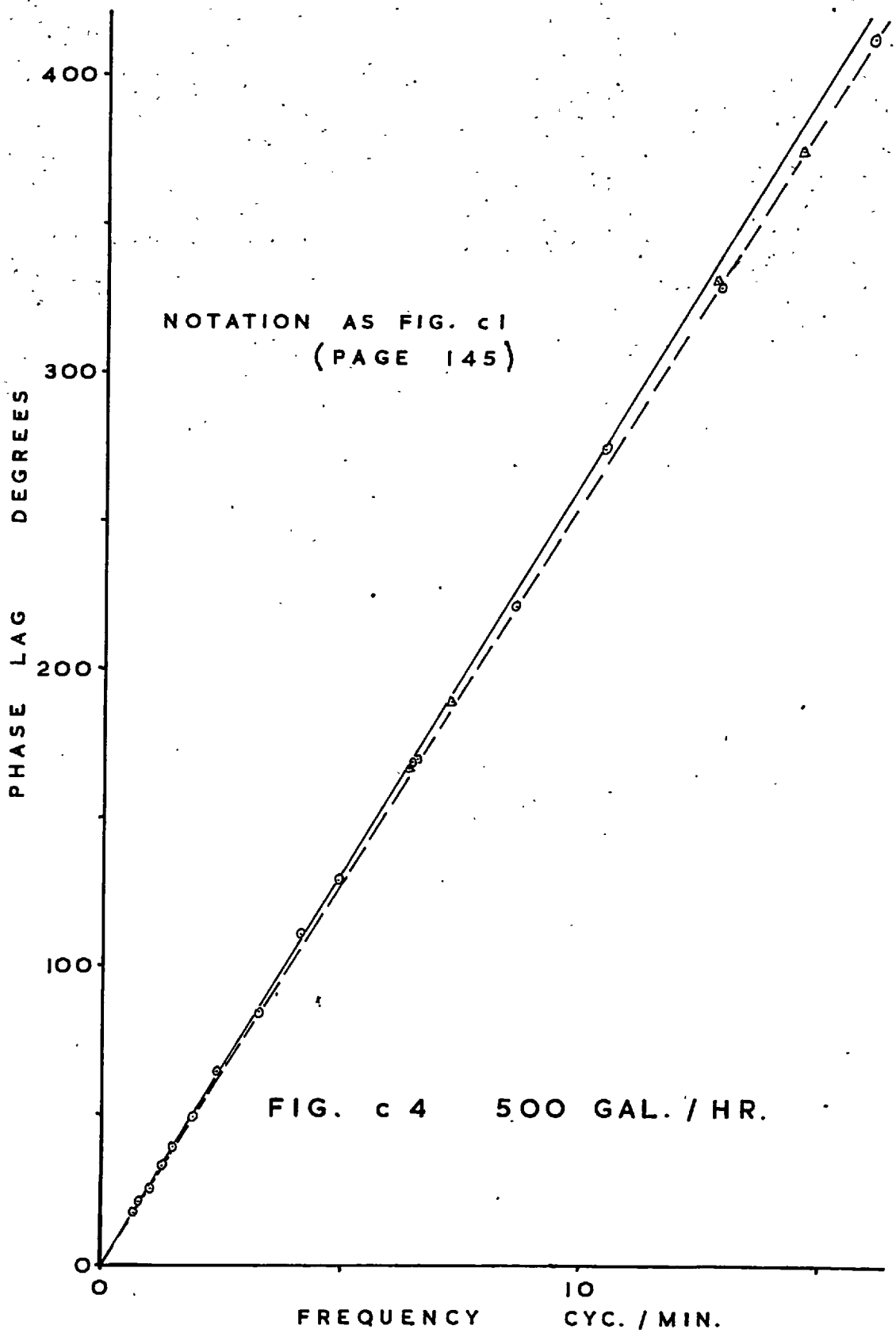


FIG. c 4 500 GAL. / HR.

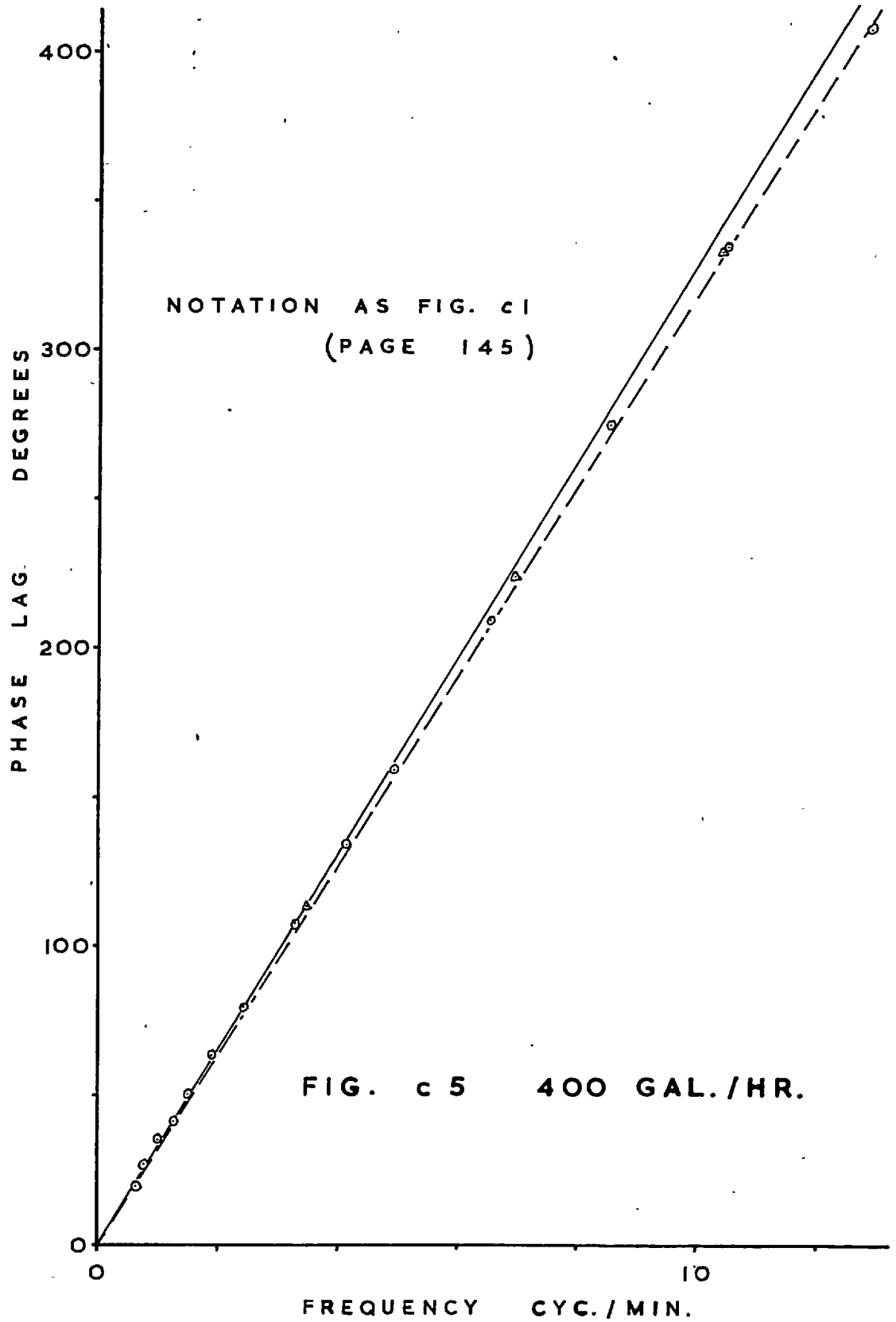


FIG. c 5 400 GAL./HR.

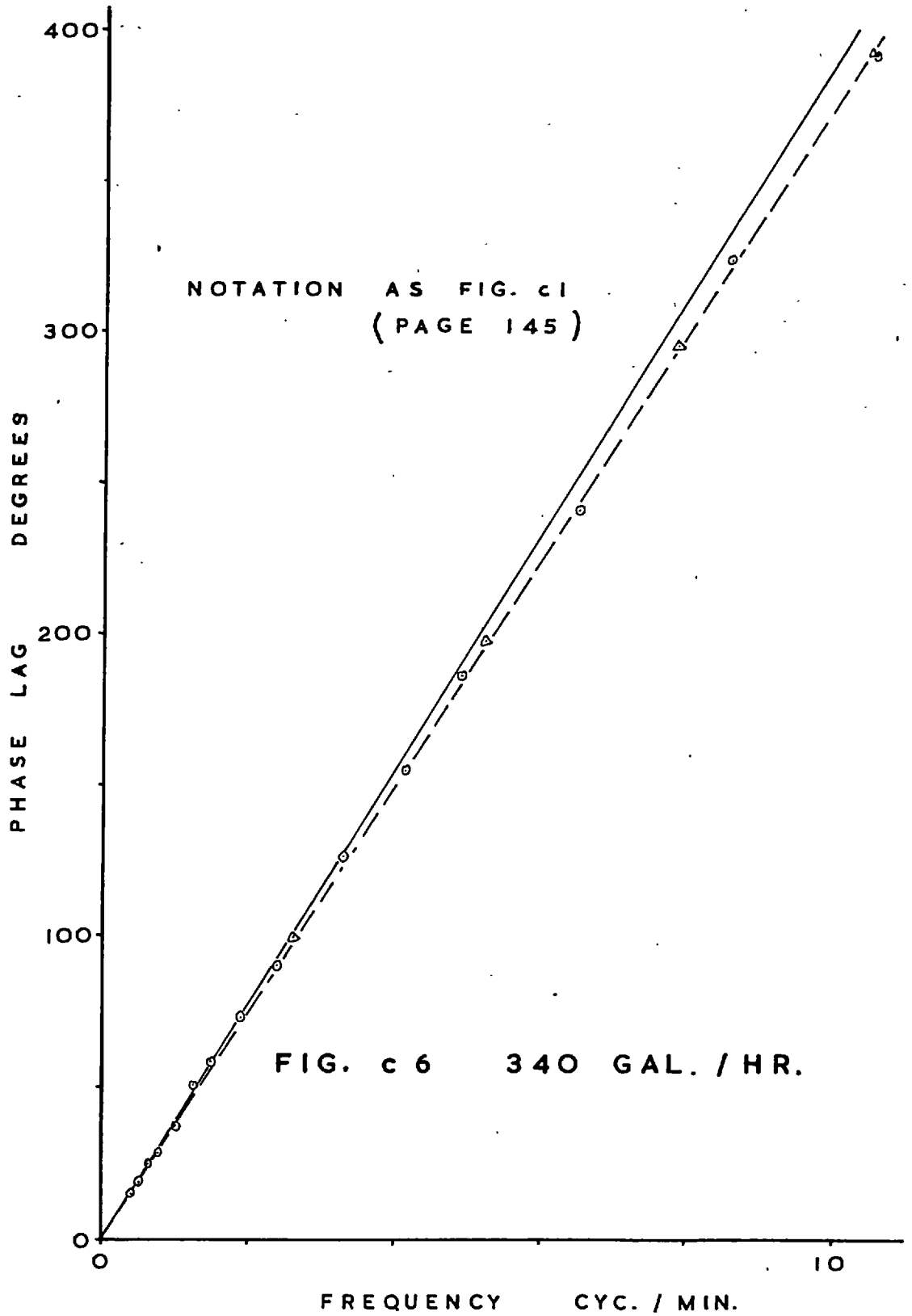


FIG. c 6 340 GAL. / HR.

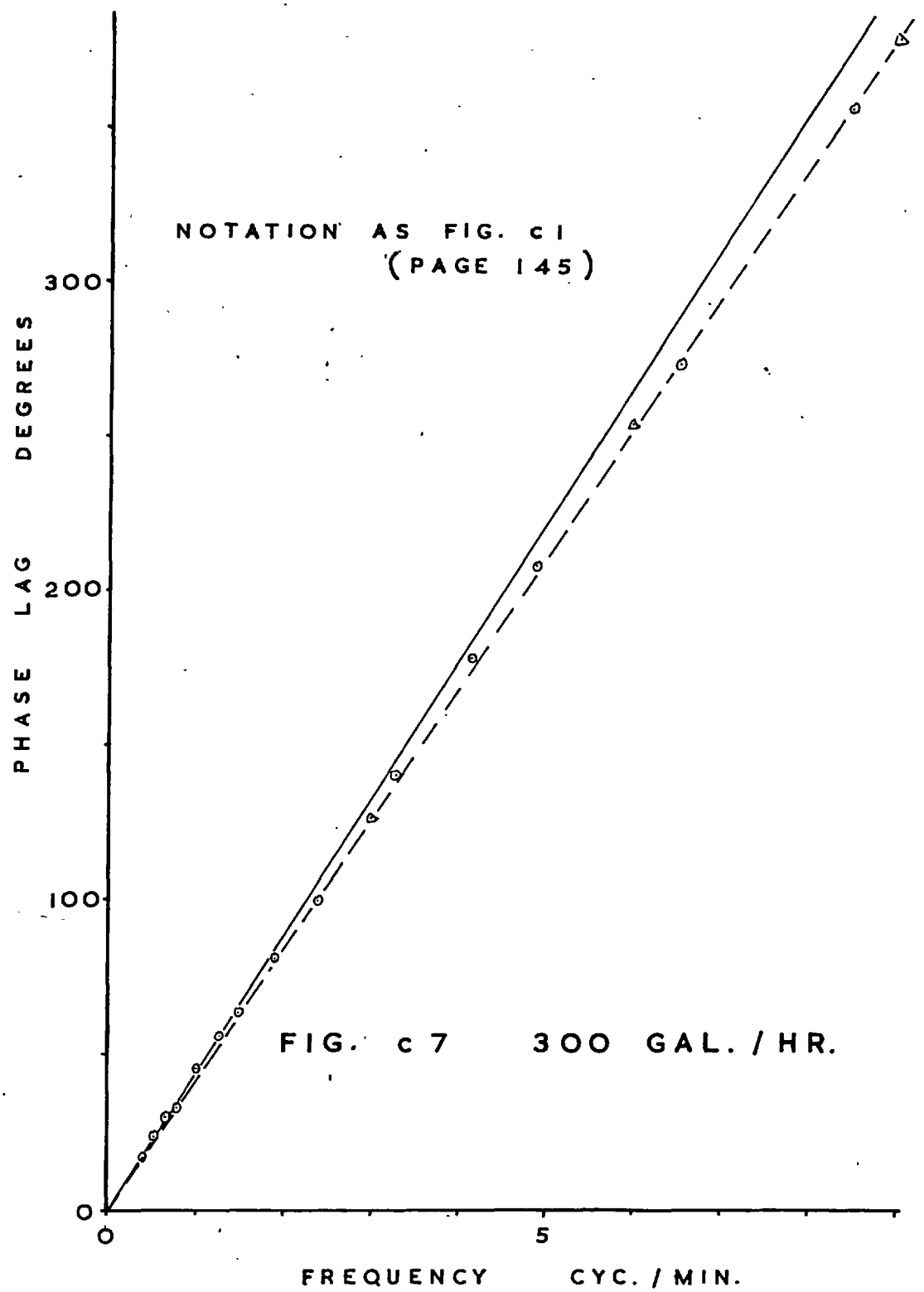


FIG. c 7 300 GAL. / HR.

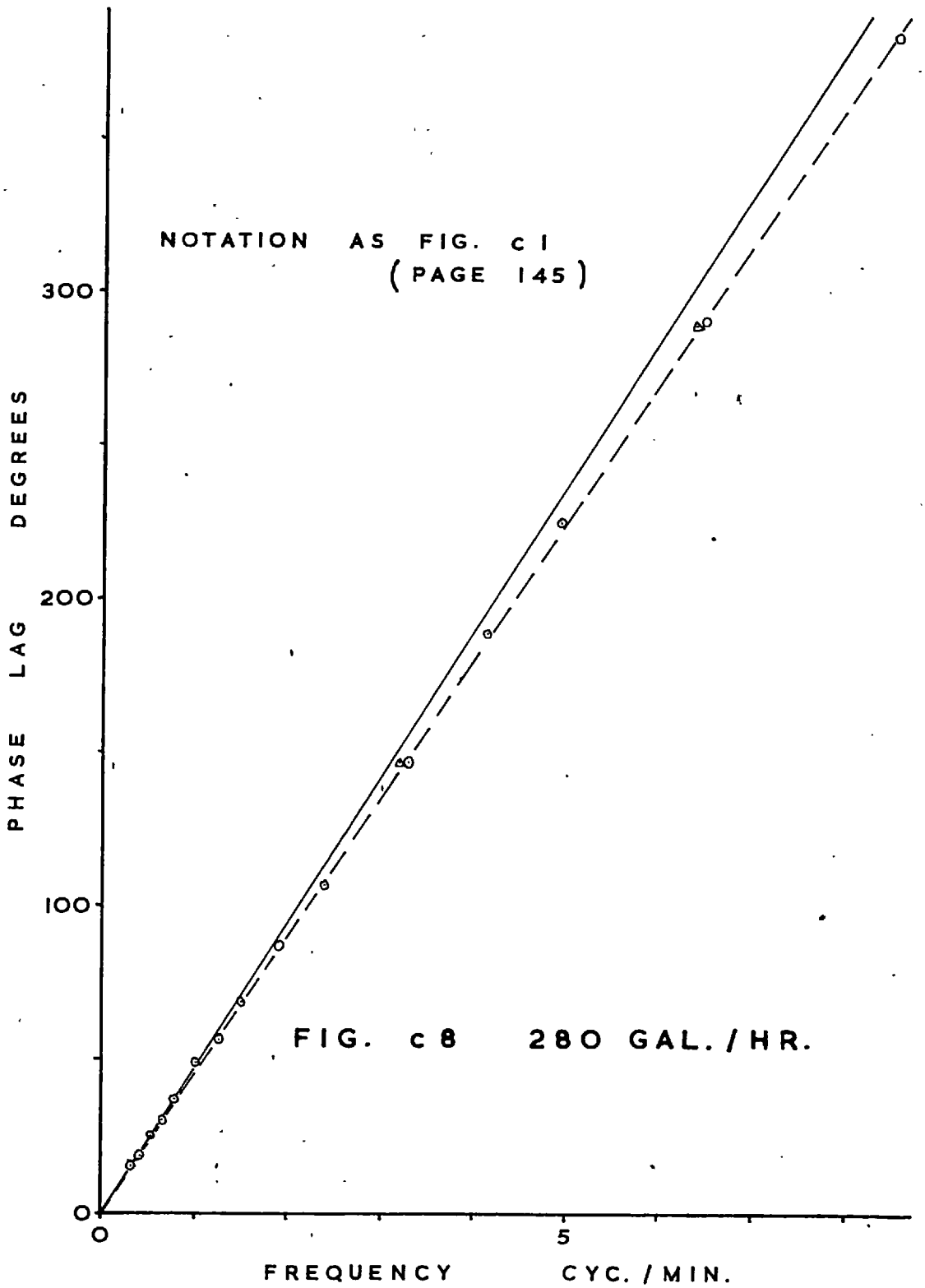


FIG. c 8 280 GAL. / HR.

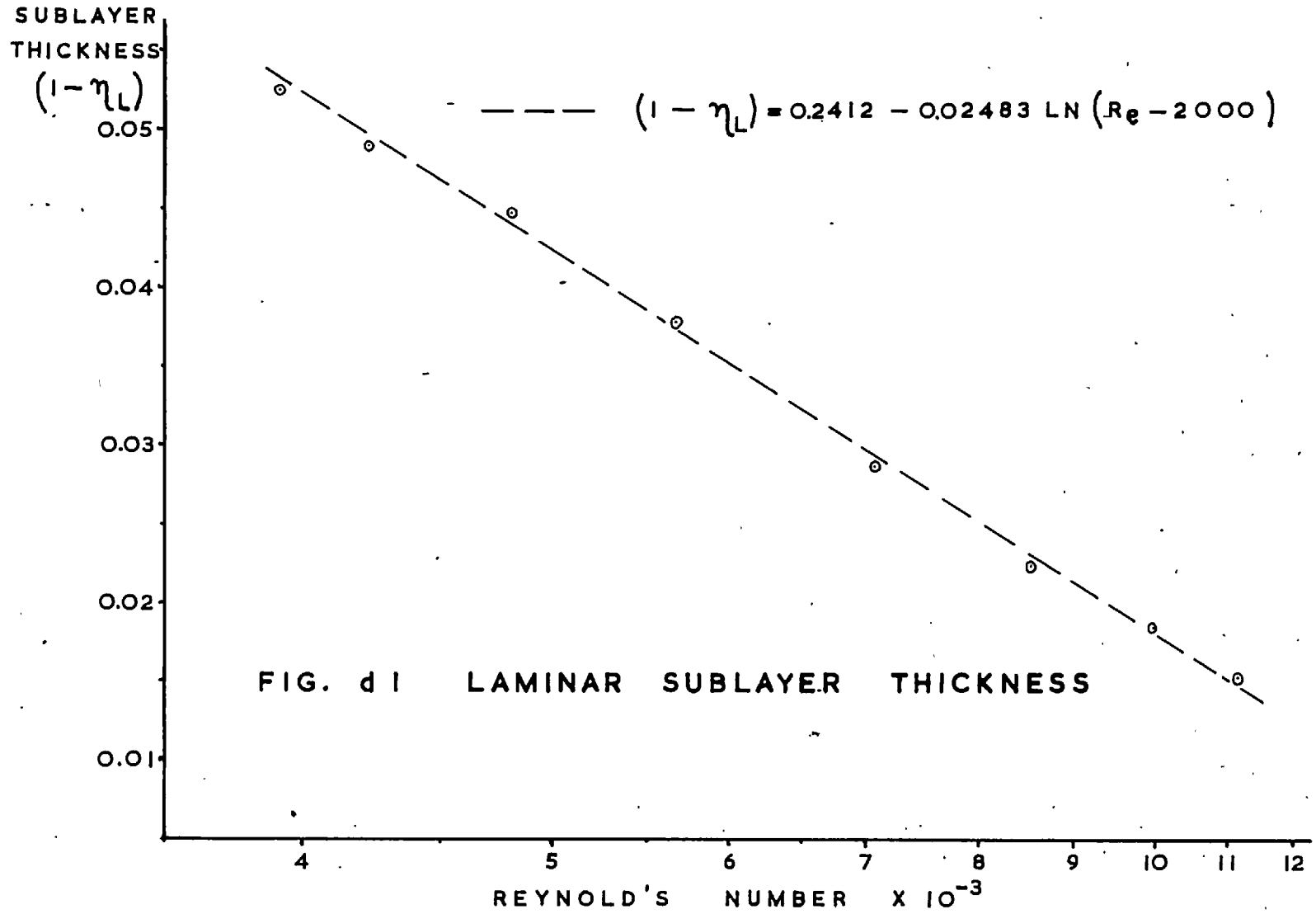


FIG. d 1 LAMINAR SUBLAYER THICKNESS

APPENDIX II

1.1 'L - U' MATRIX INVERSION

This is a fast method (suitable for digital computers) by which any matrix may be premultiplied by the inverse of another matrix. In this particular case the matrix, T, is a tridiagonal matrix.

$$\begin{bmatrix} b_1 & c_1 & & & \\ a_2 & b_2 & c_2 & & \\ & \vdots & & & \\ & & a_n & b_n & c_n \\ & & & \vdots & \\ & & & a_N & b_N \end{bmatrix}$$

The 'L-U' method does not involve actual inversion of the matrix, but merely evolves a set of instructions by which the matrix may be inverted. The 'operating' matrix contains an instruction in place of each element of the original tridiagonal matrix. Hence, a considerable saving is achieved over full inversion where the inverted matrix has a full set of elements.

Since it is assumed that diagonal elements have values of the same order of magnitude as non-diagonal elements, no row or column exchanges are necessary. The operating matrix is written:-

$$\begin{bmatrix} b_1' & c_1' & & & \\ a_2 & b_2' & c_2' & & \\ & \vdots & & & \\ & & a_n & b_n' & c_n' \\ & & & \vdots & \\ & & & a_N & b_N' \end{bmatrix}$$

where,

$$b_1' = \frac{1}{b_1}$$

$$c_n' = b_n' \, c_n$$

$$n \neq 1 , \qquad b_n' = (b_n - c_{n-1}' \, a_n)^{-1}$$

The vector matrix:-

$$\begin{bmatrix} f_1 \\ f_2 \\ \vdots \\ f_n \\ \vdots \\ f_N \end{bmatrix}$$

is premultiplied by the inverse of matrix, T, in two stages.
The first stage is:-

$$\begin{bmatrix} f_1' \\ f_2' \\ \vdots \\ f_n' \\ \vdots \\ f_N' \end{bmatrix}$$

where

$$f_1' = b_1' \, f_1$$

$$n \neq 1 , \qquad f_n' = b_n' (f_n - a_n f_{n-1}')$$

In the final stage, the vector:-

$$\begin{bmatrix} f_1'' \\ f_2'' \\ \vdots \\ f_n'' \\ \\ f_N' \end{bmatrix}$$

where

$$n \neq N \ , \qquad f_n'' = f_n' - c_{n-1}' f_{n+1}''$$

1.2 SECONDARY SOLUTIONS OF EQUATION (CII; 5;3)

These solutions are generated by the same method as that of the primary solutions (see Chapter II section 5.2), with an additional stage in which the primary solution is eliminated. The primary solution is eliminated by using the fact that it is approximately orthogonal to the secondary solution.

$$\int_0^1 f_{rs}\, f_{rs'}\, w\, d\eta = 1, \qquad s = s'$$

$$= 0, \qquad s \neq s'$$

The weighting function, w, in the case of equation (CII; 5;3) is the flow velocity profile. Orthogonality in terms of the vector solutions of this equation is expressed:-

$$F_{rs}^T\, W\, F_{rs'} = 1, \qquad s = s'$$

$$= 0, \qquad s \neq s'$$

where the elements of diagonal weighting matrix, W, represent the velocity profile.

During solution of equation (CII; 5;3), the generated vector, F_r, may be represented by a series of orthogonal vectors.

$$F_r = e_1 F_{r1} + e_2 F_{r2} + e_3 F_{r3} + \ldots.$$

The primary vector, F_{r1}, is already known. When the terms of the series are premultiplied by the combination, $F_{r1}{}^{T}W$, the coefficient, e_1, is isolated.

$$e_1 = F_{r1}^{T} W F_r$$

Hence, the component of the primary vector is eliminated from the original vector.

$$F_r' = F_r - e_1 F_{r1}$$

The components of the vectors less important than the secondary vector will decay as solution progresses. The secondary solution of equation (CII; 5;3) is thus isolated.

2. TRACER CONCENTRATION FROM RECORDER CHART READING

Values of tracer concentration are calculated from the readings on the recorder chart in three stages. First the conductivity in the conductivity cell is found. Then the contribution of the tracer to the conductivity is found. Finally the tracer concentration is calculated from this contribution.

CELL CONDUCTIVITY

The voltage output from the wheatstone bridge circuits is found from the recorder chart readings and the known characteristics of the phase sensitive detector circuits, and the preamplifier and amplifiers, (see figure f 7).

$$v'' = m\, v''' = m\, z$$

$$v' = f(v'')$$

The cell conductivity, q, is then calculated assuming there to be finite resistance in the detector arm of the wheatstone bridge circuits.

$$q = \frac{K\left(1 + A\frac{v'}{V}\right)}{R_R\left(P - B\frac{v'}{V}\right)}$$

where

$$A = \left(1 + \frac{R_R}{R_D}\right)(1+P)^2 + P\frac{R_P}{R_D}$$

$$B = (1+P)^2 + P\frac{R_P}{R_D}$$

and cell constant, K, is expressed in reciprocal centimetres.

N.B. the ratio, P, is that of the resistance in the lower arm of the potentiometer, Rp, to that in the upper arm (as in diamgram f 7).

Contribution to Conductivity by Tracer

The conductivity contributed by the sodium chloride tracer, q', is found by subtracting the known residual conductivity, q_w, (corrected to the temperature of the run) from the actual conductivity, and correcting the resulting conductivity to 18°C.

$$q' = \frac{1}{\beta}(q - \alpha q_w)$$

where

$$\alpha = e^{0.0217(\theta - 18)}$$

$$\beta = e^{0.0227(\theta - 18)}$$

and θ is the temperature of the run (degrees centigrade).

Tracer Concentration

The tracer concentration, C_A, is found by solution of the 'Kohlrausch' relationship by means of the 'Newton-Raphson' technique.

$$q' = 10^{-6}(\Lambda_\infty - \delta\sqrt{C_A})C_A$$

where, for sodium chloride at 18°C

C < 10 millimoles per litre, $\Lambda_\infty = 108.50$

$\delta = 2.167$

3. PLATINISATION OF ELECTRODES

The platinum electrodes forming the upstream and downstream conductivity cells were platinised using a variation of the conventional method. Since plastic and epony resin were involved in their construction, a solution of detergent ('tepol') and hot water rather than aqua regia was used for cleaning the electrode surfaces. A special cell was made so that the outer and inner electrodes of each conductivity cell could be platinised simultaneously.

Platinisation involved four stages.

1 Ten minutes degreasing of electrodes in hot tepol solution

2 Washing with distilled water

3 Electrolysis in platinising solution[+]: current of 30 mA five minutes in each direction.

4 Thorough washing and electrolysis in 5% sulphuric acid: two volts short-circuited across cell, three minutes each way.

[+]Platinising solution:-

Lead acetate 20% by weight

Chlorplatanic acid 2.5% by weight in distilled water.

4. INVERSE VERSUS DIRECT CROSS-SECTIONAL MEAN CONCENTRATION

The cross-sectional mean value of tracer concentration derived from a conductivity measurement is an inverse rather than a direct mean. The case of a sinusoidal tracer signal in a parallel walled flow system in turbulent flow is considered. Since any tracer signal may be resolved into sinusoidal components, the results of this analysis will apply to all tracer signals. The largest possible differences between the response measured through direct mean and that measured through inverse mean are calculated. These differences are shown to be insignificant, even under the worst possible conditions.

The concentration in any cross-section, C_A, may be expressed as the sum of its cross-sectional mean, $\bar{C}_A$, and a variable element, C.

$$C_A = \bar{C}_A + C$$

concentration for this purpose is the sum of that of the tracer and that equivalent to the residual conductivity of the water. The inverse cross-sectional mean is defined:-

$$\tilde{C}_A = \left[\frac{1}{2} \int_{-1}^{1} C_A^{-1} \, d\eta \right]^{-1}$$

$$= \left[\frac{1}{2} \int_{-1}^{1} (\bar{C}_A + C)^{-1} \, d\eta \right]^{-1}$$

The term to be integrated may be expressed as a binominal series.

$$\tilde{C}_A = \bar{C}_A \left[\frac{1}{2} \int_{-1}^{1} \left(1 - \frac{c}{\bar{C}_A} + \frac{c^2}{\bar{C}_A^2} - \ldots \right) d\eta \right]^{-1}$$

$$= \bar{C}_A \left[1 + \frac{1}{2\bar{C}_A^2} \int_{-1}^{1} c^2 \, d\eta + \ldots \right]^{-1}$$

Since variations in concentration are much smaller than the mean, all further terms of the series are neglected. The resulting expression is again subjected to a binomial expansion.

$$\tilde{C}_A = \bar{C}_A - \frac{1}{2\bar{C}_A} \int_{-1}^{1} c^2 \, d\eta + \ldots$$

With the convergence condition (CII; 3;19) satisfied, concentration, C_A, at any point in the parallel walled flow system is expressed:-

$$C_A = \bar{\bar{C}}_A + \mathcal{R} \left\{ X_{110} \, e^{i\omega t} f_{11}(\eta) \right\}$$

For convenience, the amplitude, X_{110}, is assumed to be real and positive.

$$C_A = \bar{\bar{C}}_A + X_{110} \, \mathcal{R} \left\{ e^{i\omega t} f_{11}(\eta) \right\}$$

$$\bar{C}_A = \bar{\bar{C}}_A + X_{110} \, \mathcal{R} \left\{ e^{i\omega t} \right\}$$

$$c = X_{110}\, R\left\{ e^{i\omega t}\left[f_{11}(\eta) - 1 \right] \right\}$$

$$\tilde{C}_A = \bar{C}_A - \frac{X_{110}^2}{2\bar{C}_A} \int_{-1}^{1} \left[R\left\{ e^{i\omega t}\left[f_{11}(\eta) - 1 \right] \right\} \right]^2 d\eta$$

DIFFERENCE IN AMPLITUDE MEASUREMENT

The amplitude of a sinusoidal tracer signal, A, is half the difference between the mean concentration at its maximum and at its minimum.

$$A = \frac{1}{2}\left[\bar{C}_A\,(t=0) - \bar{C}_A\,(t=\frac{\pi}{\omega}) \right] = X_{110}$$

The amplitude measured through the inverse mean, A', is written:-

$$A' = \frac{1}{2}\left[\tilde{C}_A\,(t=0) - \tilde{C}_A\,(t=\frac{\pi}{\omega}) \right]$$

$$= X_{110} - \frac{X_{110}^3}{2(\bar{C}_A^2 - X_{110}^2)} \int_{-1}^{1} \left[R\left\{ f_{11}(\eta) - 1 \right\} \right]^2 d\eta$$

An expression for the proportional difference is this derived:

$$\frac{A' - A}{X_{110}} = \frac{X_{110}^2}{2(\bar{\bar{C}}_A^2 - X_{110}^2)} \int_{-1}^{1} [R\{f_{11}(\eta) - 1\}]^2 \, d\eta$$

The largest differences will be at low flow rates (where concentration profiles are most curved), and at high tracer signal frequencies. At a flow rate of 280 gallons per hour and a signal frequency of 48 cycles per minute;-

$$\frac{1}{2} \int_{-1}^{1} [R\{f_{11}(\eta) - 1\}]^2 \, d\eta = 0.109$$

Since

$$\left| \frac{X_{110}}{\bar{\bar{C}}_A} \right| < 0.2$$

$$\left| \frac{A' - A}{X_{110}} \right| < 0.004$$

Hence, the maximum possible difference between the measured and the actual amplitude, arising from the use of conductivity measurement, is 0.4 per cent.

DIFFERENCE IN PHASE ANGLE MEASUREMENT

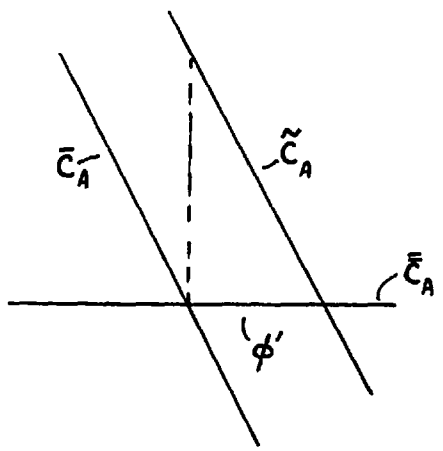
Phase angle ϕ, is measured from the point at which cross-sectional mean tracer concentration is equal to its time-mean value.

$$\bar{C}_A = \bar{\bar{C}}_A \quad , \qquad t = \frac{\pi}{2\omega} \text{ or } \frac{3\pi}{2\omega}$$

At this point, the inverse cross-sectional mean will be different from the direct time mean value.

$$\tilde{C}_A \left(t = \frac{\pi}{2\omega}\right) - \bar{\bar{C}}_A = - \frac{X_{110}^2}{2\bar{\bar{C}}_A} \int_{-1}^{1} \left[I\{f_{11}(\eta)\} \right]^2 d\eta$$

By considering the triangle formed between the curves of direct and inverse cross-sectional mean concentration against time, this amplitude difference is translated into an angular difference, ϕ' .



$$\phi' = \frac{\tilde{C}_A \left(t = \frac{\pi}{2\omega}\right) - \bar{\bar{C}}_A}{\frac{d\bar{C}_A}{d\omega t}} = - \frac{\tilde{C}_A \left(t = \frac{\pi}{2\omega}\right) - \bar{\bar{C}}_A}{X_{110}}$$

$$= \frac{X_{110}}{2\bar{\bar{C}}_A} \int_{-1}^{1} \left[I\{f_{11}(\eta)\} \right]^2 d\eta$$

For a flow rate of 280 gallons per hour and a tracer signal

frequency of 48 cycles per minute:-

$$\frac{1}{2}\int_{-1}^{1}\left[\,I\left\{f_{11}(\eta)\right\}\right]^2 d\eta \;=\; 0.107$$

Hence, $\phi' = 0.0214$ rad.

$= 1.2^{\circ}$

which is negligible.

5.1 LEAST SQUARES FORMULAE FOR SINUSOIDAL TRACER SIGNALS

Frequency and Phase

A reference line is drawn on the recording of the sinusoidal signal, as shown in diagram g_1 (Appendix IV). This line is parallel to the peaks and troughs and approximately centrally between them. The positions of the intercepts between the trace and this line, labelled X_1 to X_{2N} (over N cycles), are measured. These positions are represented mathematically as:-

$$X_n = x_o + n\bar{x} + (-1)^n x' + \xi'(n)$$

where x_o is the reference point, $\bar{x}$ the half wave-length, x' the error length arising from the reference line not being truly central, and $\xi'(n)$ is the random element.

Least squares formulae for the unknowns, $\bar{x}$, x_o and x', are derived in the conventional manner.

$$\bar{x} = \frac{\hat{\bar{\sigma}}^2_{xn}}{\hat{\bar{\sigma}}^2_{n}}$$

$$x_o = \bar{X} - (N + \tfrac{1}{2})\bar{x}$$

$$x' = \hat{X} - \frac{\bar{x}}{2}$$

where:-

$$\bar{X} = \frac{1}{2N} \sum_{n=1}^{2N} X_n$$

$$\hat{X} = \frac{1}{2N} \sum_{n=1}^{2N} (-1)^n X_n$$

$$\hat{\sigma}_x^2 = \sum_{n=1}^{2N} X_n^2 - 2N \bar{X}^2 - 2N \hat{X}^2$$

$$\hat{\sigma}_{xn}^2 = \sum_{n=1}^{2N} n X_n - N(2N+1) \bar{X} - N \hat{X}$$

$$\hat{\sigma}_n^2 = \frac{2}{3} N (N+1)(N-1)$$

The tracer signal frequency, W, is derived from the channel one recorder trace.

$$W = \frac{S}{2\bar{x}}$$

where frequency is in cycles per minute, chart speed, s, in centimetres per minute and half wave-length, $\bar{x}$ in centimetres. Phase lag, ϕ, (in degrees) is calculated from the traces of both channels (the half wave-length from channel one is used in channel two).

$$\phi = 180 \frac{{}_2x_o - {}_1x_o - z}{\bar{x}}$$

The correction, z, allows for displacement between the recorder pens.

The accuracy of the least squares correlation is expressed as the standard deviation, ϵ .

$$\epsilon = \frac{\sqrt{\hat{\sigma}_x^2 \, \hat{\sigma}_n^2 - \hat{\sigma}_{xn}^4}}{\hat{\sigma}_x^2 \sqrt{2N}}$$

The standard deviation is in units of length along the time axis of the recorder chart. Where standard deviation is much greater than that expected from the quality of the tracer signals, measurements are checked for mistakes.

AMPLITUDE

Concentration measurements at successive peaks and troughs, C_1 to C_{2N}, are represented;

$$C_n = C_o + (-1)^n C_a + n C' + \zeta''(n)$$

where C_o is the central concentration value, C_a the amplitude of the concentration signals, C' an allowance for a steady drift in concentration, and ζ' a random element.

$$C' = \frac{\hat{\sigma}_{cn}^2}{\hat{\sigma}_n^2}$$

where C' represents the rate of drift of tracer concentration.

$$C_o = \bar{C} - (N + \tfrac{1}{2})\,C'$$

$$C_d = \hat{C} - \frac{C'}{2}$$

where:

$$\bar{C} = \frac{1}{2N} \sum_{n=1}^{2N} C_n$$

$$\hat{C} = \frac{1}{2N} \sum_{n=1}^{2N} (-1)^n C_n$$

$$\hat{\bar{\sigma}}_c^2 = \sum_{n=1}^{2N} C_n^2 - 2N\bar{C}^2 - 2N\hat{C}^2$$

$$\hat{\bar{\sigma}}_{cn}^2 = \sum_{n=1}^{2N} n\,C_n - N(2N+1)\bar{C} - N\hat{C}$$

The standard deviation of the correlation expressed as concentration is written:-

$$\epsilon = \frac{\sqrt{\hat{\bar{\sigma}}_c^2\,\hat{\bar{\sigma}}_n^2 - \hat{\bar{\sigma}}_{cn}^4}}{\hat{\bar{\sigma}}_c^2\sqrt{2N}}$$

5.2. FOURIER ANALYSIS OF PULSE SIGNALS

For the purpose of Fourier analysis, a pulse signal is divided into strips for the main part, and a tail in which the signal decays approximately exponentially (see figure g_2 in Appendix IV). The size of each strip is chosen such that the shape of the tracer signal which it covers approximates to being parabolic. The integration procedure is the same as that of Simpson's rule. The Fourier integral for the strip covering the time period from t to t + 2h is written:-

$$\int_t^{t+2h} c\, e^{-i r \omega t}\, dt = e^{-i r \omega t} [B_0 C_n + B_1 C_{n+1} + B_2 C_{n+2}]$$

where the tracer concentration values, C_n, C_{n+1} and C_{n+2}, are the initial, centre and final concentrations for the strip. The coefficients B_0 B_1 and B_2 are defined:-

$$B_0 = -\frac{i}{r\omega} + \frac{3}{2hr^2\omega^2} + \frac{i}{h^2r^3\omega^3} + e^{-2ir\omega h}\left(\frac{1}{2hr^2\omega^2} - \frac{i}{h^2r^3\omega^3}\right)$$

$$B_1 = -\frac{2}{hr^2\omega^2} - \frac{2i}{h^2r^3\omega^3} - e^{-2ir\omega h}\left(\frac{2}{hr^2\omega^2} - \frac{2i}{h^2r^3\omega^3}\right)$$

$$B_2 = \frac{1}{2hr^2\omega^2} + \frac{i}{h^2r^3\omega^3} + e^{-2ir\omega h}\left(\frac{i}{r\omega} + \frac{3}{2hr^2\omega^2} - \frac{i}{h^2r^3\omega^3}\right)$$

These formulae are derived for parabolic interpolation.

The tail of each pulse signal is assumed to be of exponential form.

$$C = C_M e^{-\frac{t - t_M}{t'}}$$

where concentration, C_M, is that at time, t_M, at which the tail begins, and t' represents the time elapse during which the signal concentration decays to 1/e of its value at time t_M. The Fourier integral is expressed:-

$$\int_{t_M}^{T'} C_M \; e^{-\frac{t - t_M}{t'}} \; e^{-i r \omega t} \, dt = \ldots .$$

$$\frac{C_M}{\left(\frac{1}{t'} + i r \omega\right)} \left[e^{-i r \omega t_M} - e^{-\frac{T' - t_M}{t'} - i r \pi} \right]$$

APPENDIX III

TABLE 1. DIMENSIONS OF ANNULAR FLOW SYSTEM

Internal diameter of outer tube	(2 3/8 in)	6.03 cm.
External diameter of inner tube	(2 in)	5.08 cm.
Width of annular gap		0.476 ± 0.030 cm
Cross-sectional area of flow (calculated from volume)		8.18 cm^2
Length between conductivity measuring cells		333.4 cm
Length of annular flow section above upstream cell		56 cm
Length of annular flow section below downstream cell		71 cm

TABLE 2. SOLUTION OF EQUATION (CII; 5;3) WITH RESPECT TO INCREMENT SIZE

N.B. This sample of convergence data covers most cases.

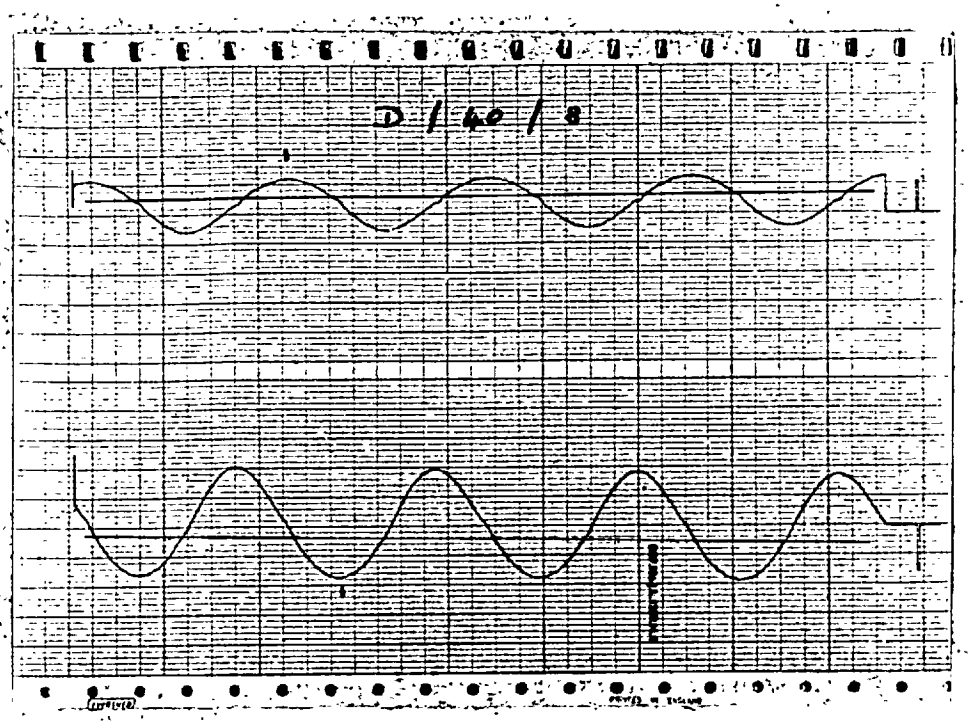
Flow Rate Gal/Hr.	Frequency Cyc /min	% error in phase shift increments				% error in amplitude ratio increments			
		20	40	60	100	20	40	60	100
300	12	-0.18	-0.11	-0.07	-0.04	+0.90	+0.50	+0.30	+0.16
400	64	-0.30	-0.10	-0.05	-0.02	+3.4	+1.7	+1.1	+0.6
780	14	-0.11	-0.03	-0.02	-0.01	+0.11	+0.04	+0.03	+0.01
600	104	-0.26	-0.12	-0.08	-0.05	+5.4	+2.4	+1.2	+0.6
340	5	-0.15	-0.05	-0.03	-0.01	+0.33	+0.16	+0.0)	+0.05
700	224	-0.35	-0.14	-0.08	-0.05	+4.0	+1.6	+0.9	+0.4

TABLE 3. DECAY OF SECONDARY SOLUTIONS OF EQUATION (CII; 5;3)

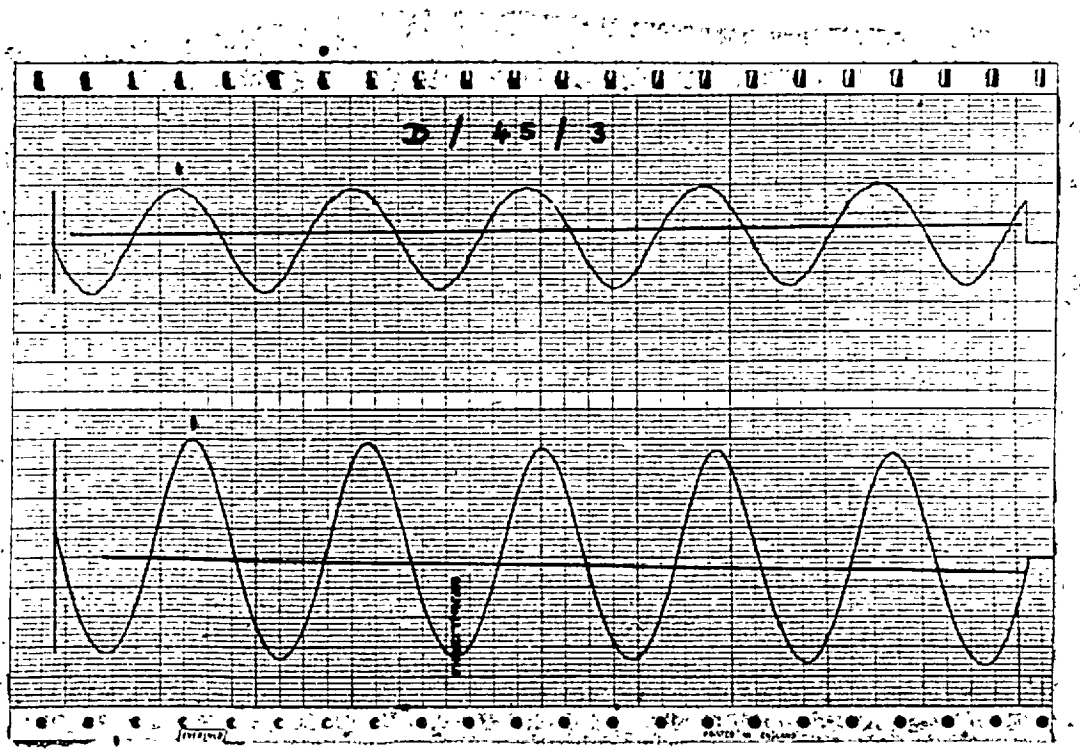
Flow Rate Gal/Hr.	Frequency Cycle/Min	Transfer Factor cm^{-1}	Decay in initial length (56 cm) of annular flow system
340	80	-0.211	1/140,000
700	224	-0.274	1/4,200,000
300	6	-0.162	1/5,800
400	8	-0.207	1/110,000
780	28	-0.249	1/1,000,000
500	44	-0.235	1/380,000

4. MEASURED FLOW RATES

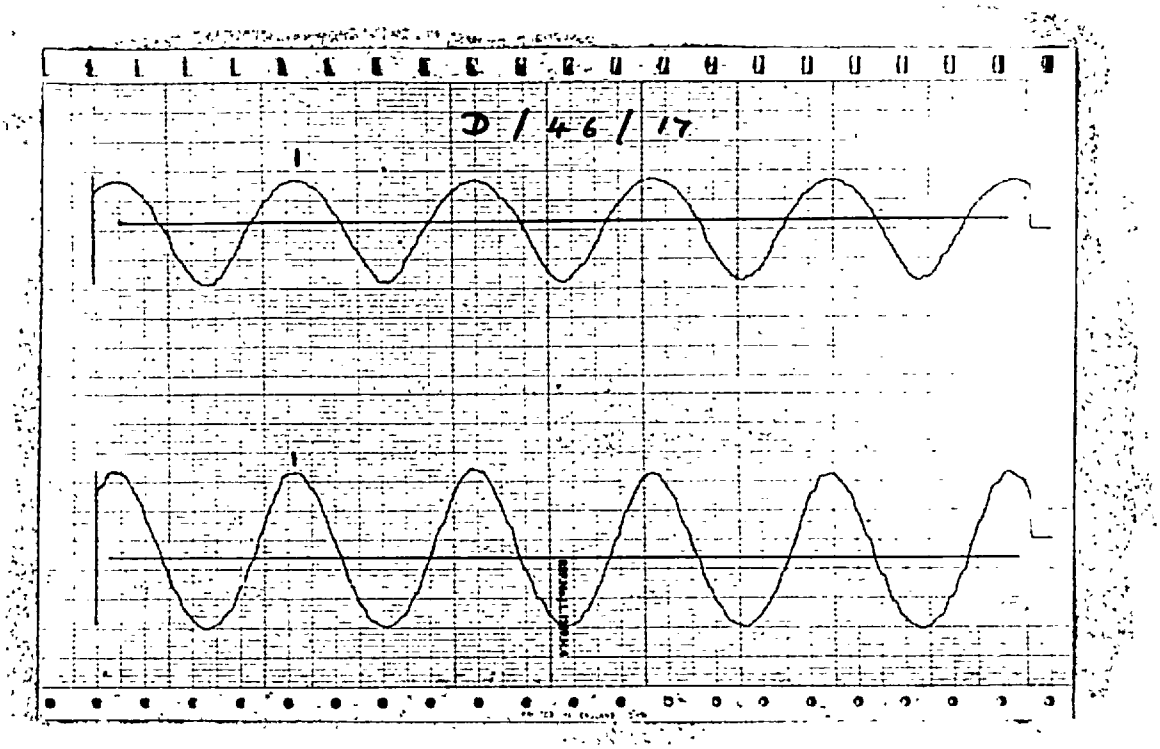
Flow Meter Reading Cal/Hr.	Actual Flow Rate gal/Hr.	Flow Velocity cm/sec.	Reynolds Number $4\bar{U}b$
280	272	42.0	3,940
300	293	45.2	4,240
340	333	51.4	4,820
400	393	60.7	5,680
500	491	75.7	7,090
600	591	91.3	8,550
700	691	106.8	9,990
780	771	119.0	11,150



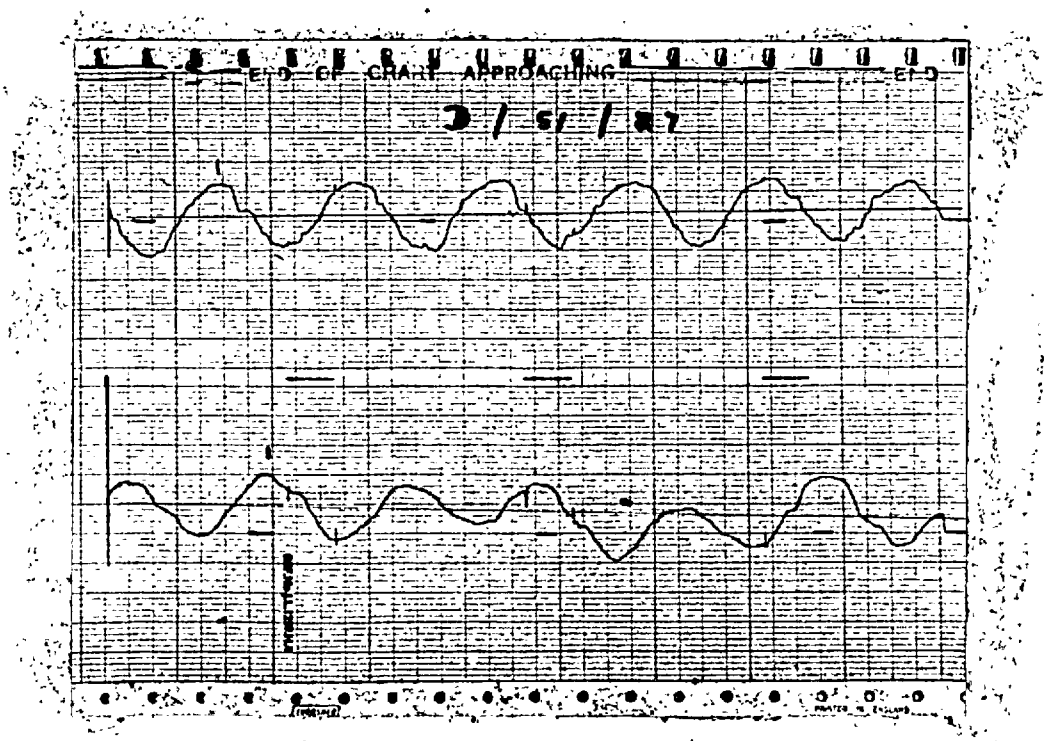
9. 280 GAL/HR. 1.90 CYC./MIN.



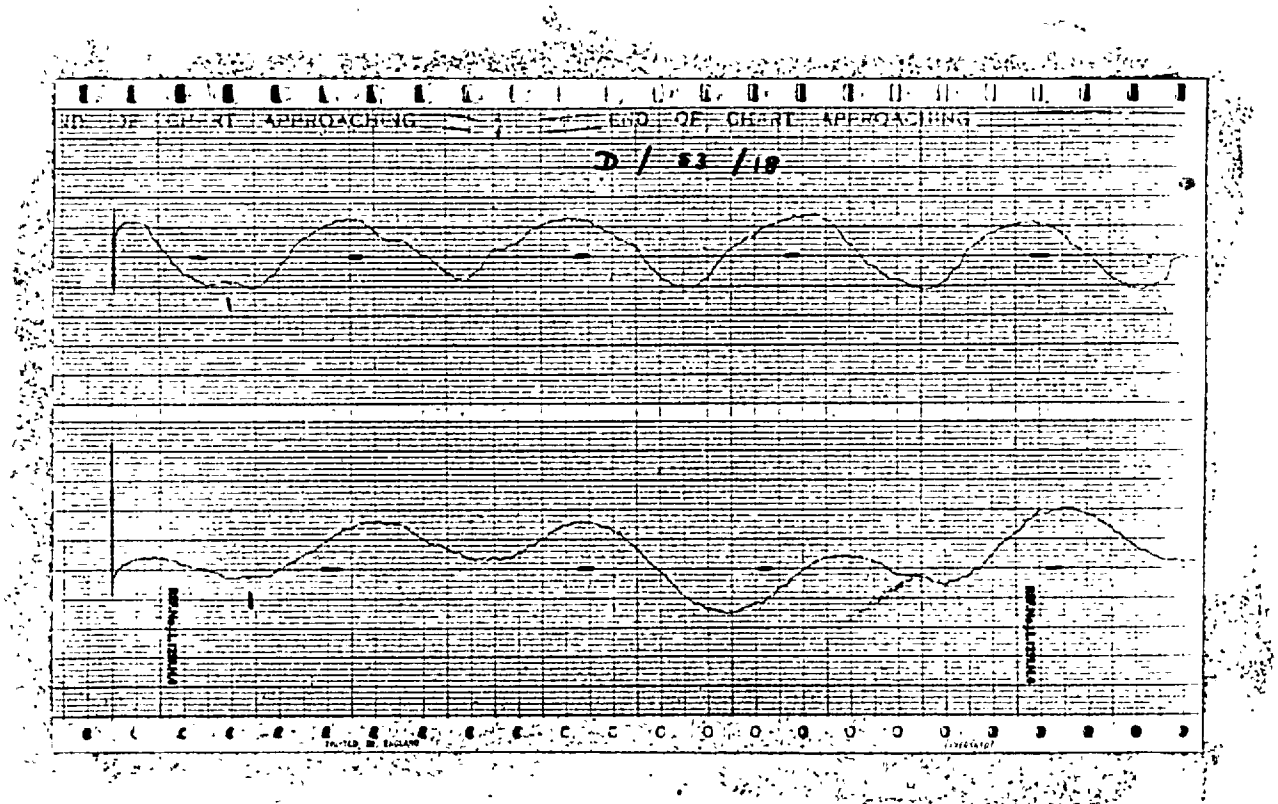
10. 400 GAL/HR. 6.51 CYC./MIN.



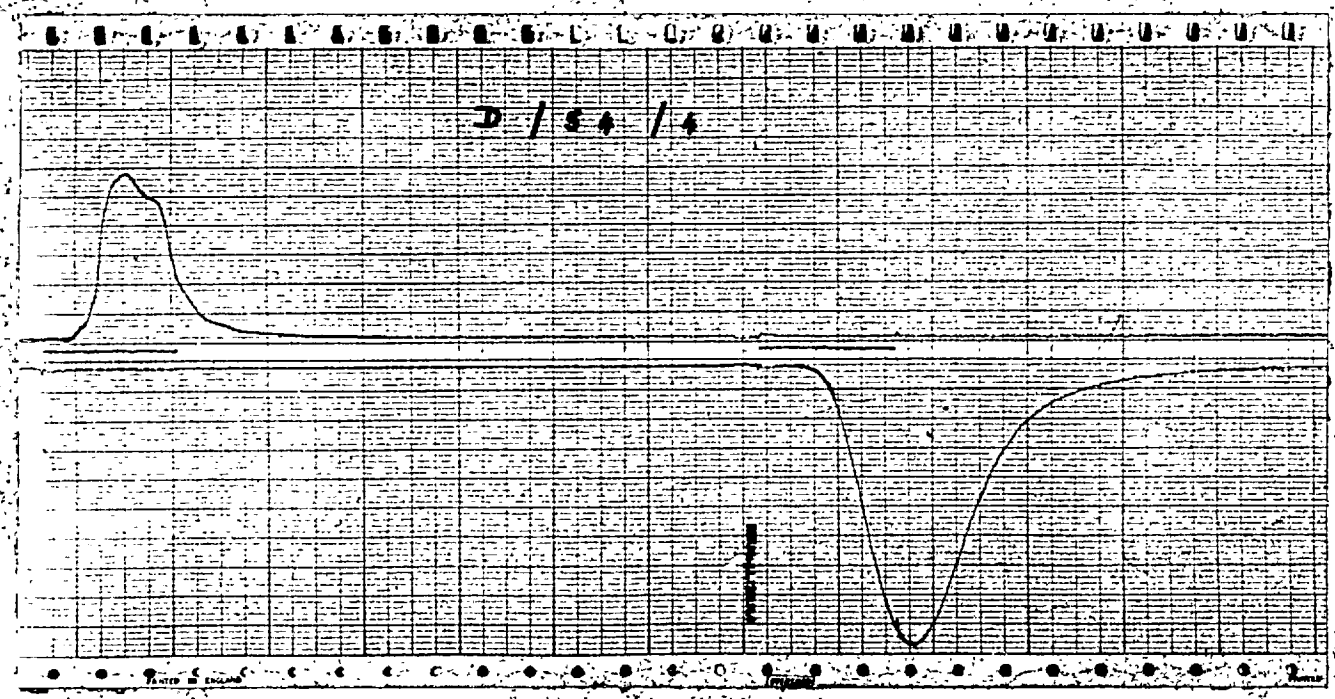
11. 300 GAL/HR. 12.8 CYC./MIN.



12. 280 GAL/HR. 41.5 CYC./MIN.

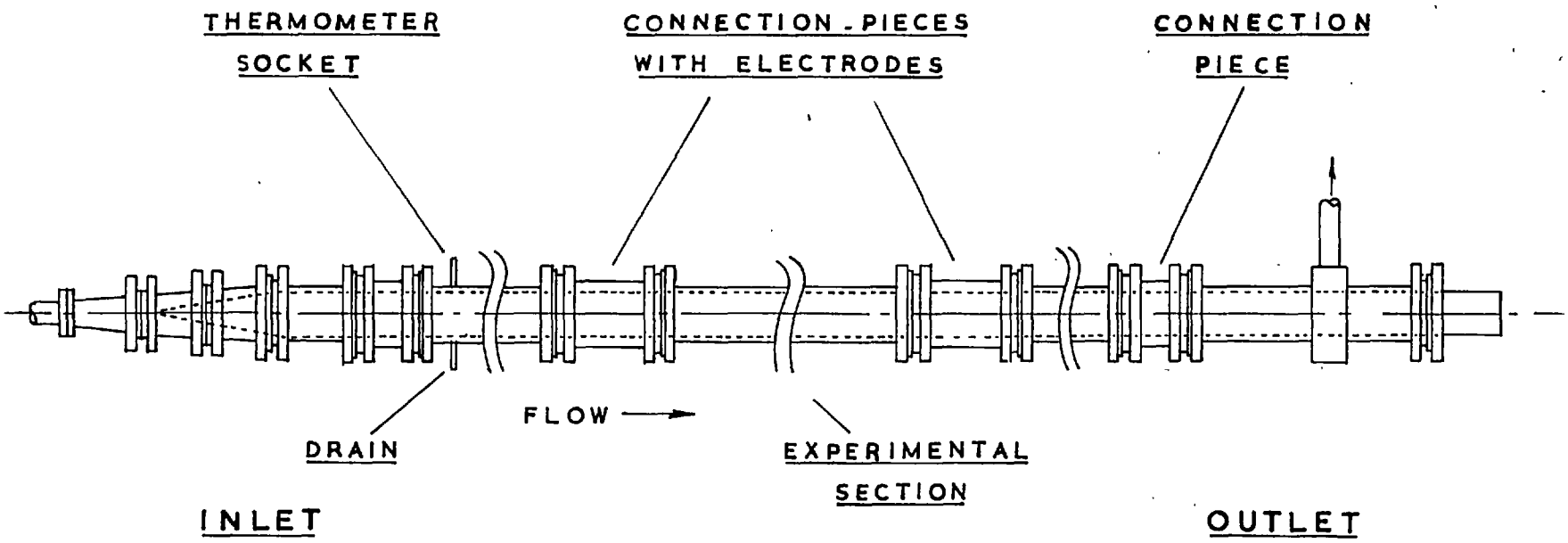


13. 600 GAL/HR. 152 CYC./MIN.



14. 780 GAL/HR. PULSE PEAK LAPSE 2.7 SEC.

A P P E N D I X IV



N.B. INNER TUBE SHOWN AS BROKEN LINE

FIG. f1 ASSEMBLED ANNULAR FLOW SYSTEM

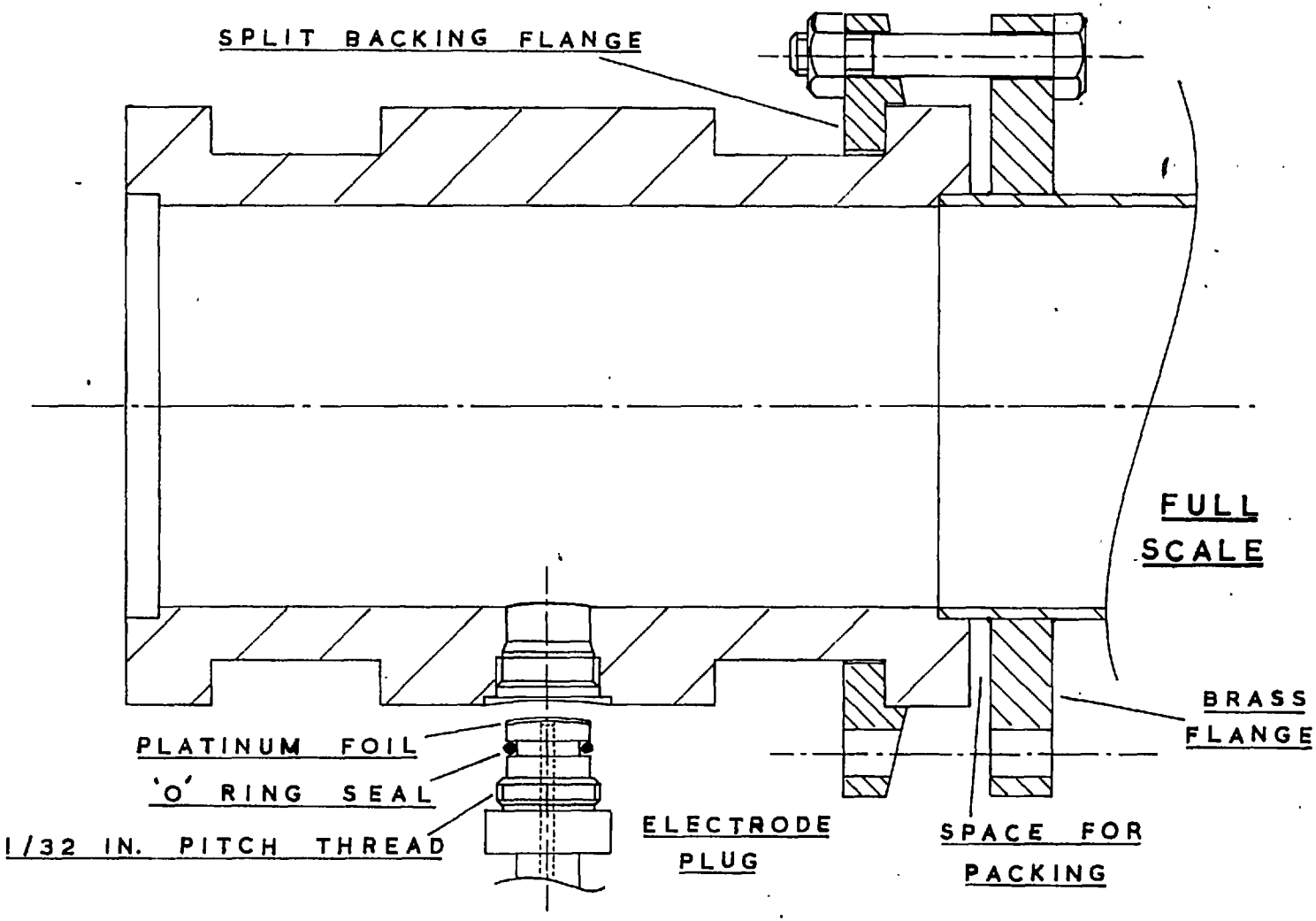


FIG. 12 OUTER CONNECTION PIECE WITH ELECTRODE

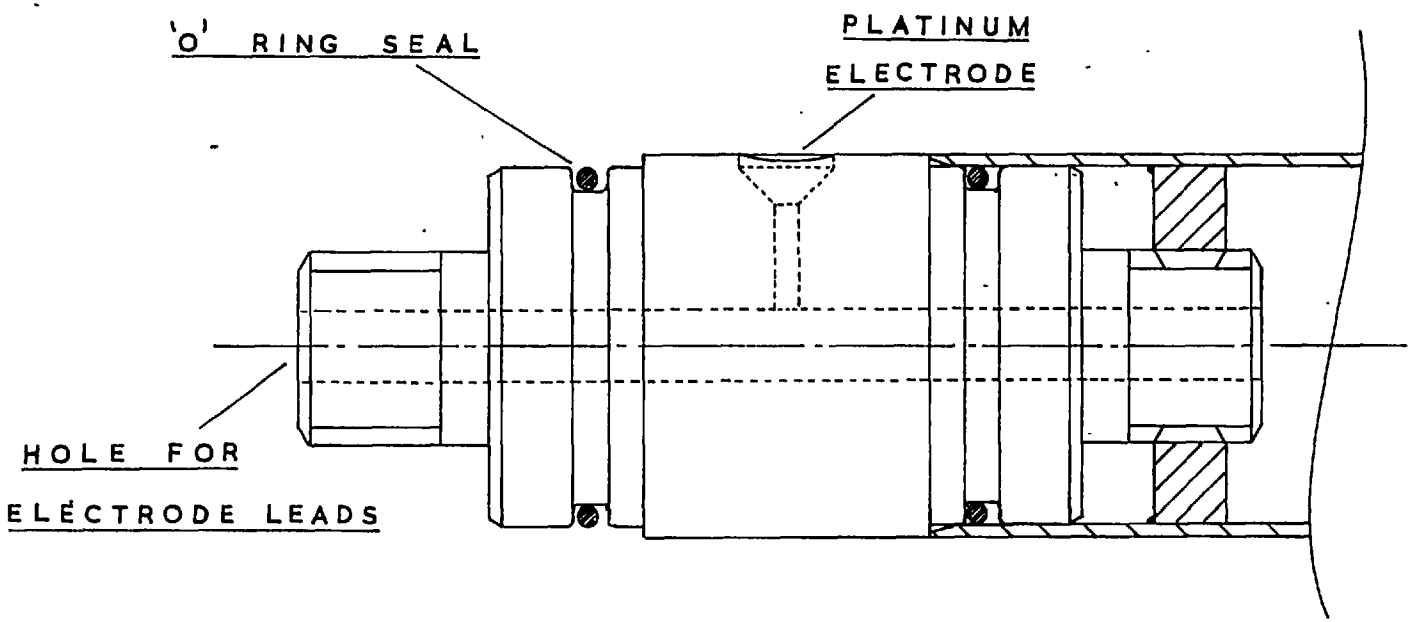


FIG. f 3 INNER CONNECTION PIECE WITH ELECTRODE

FULL SCALE

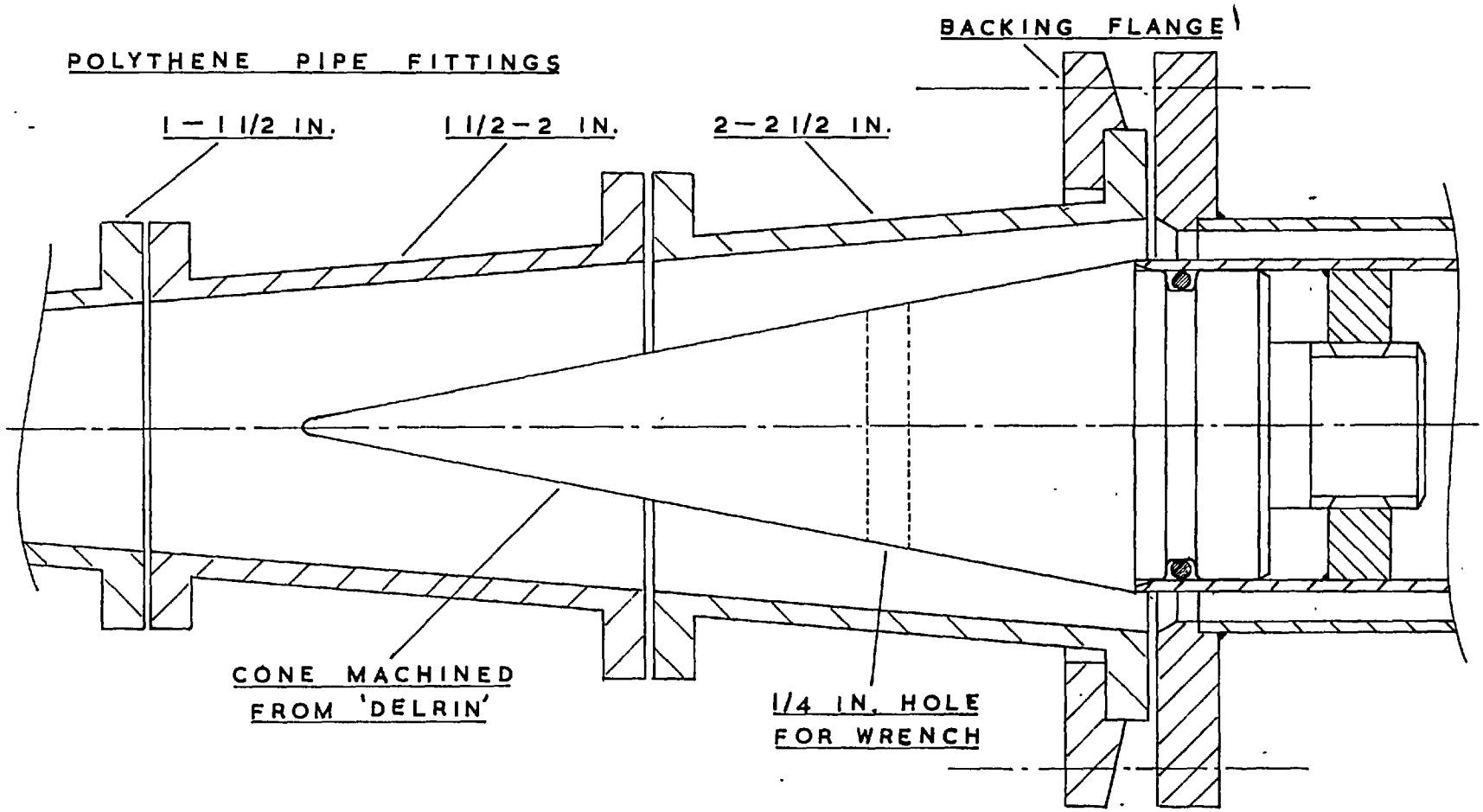


FIG. f 4 FLOW SYSTEM INLET

FULL SCALE

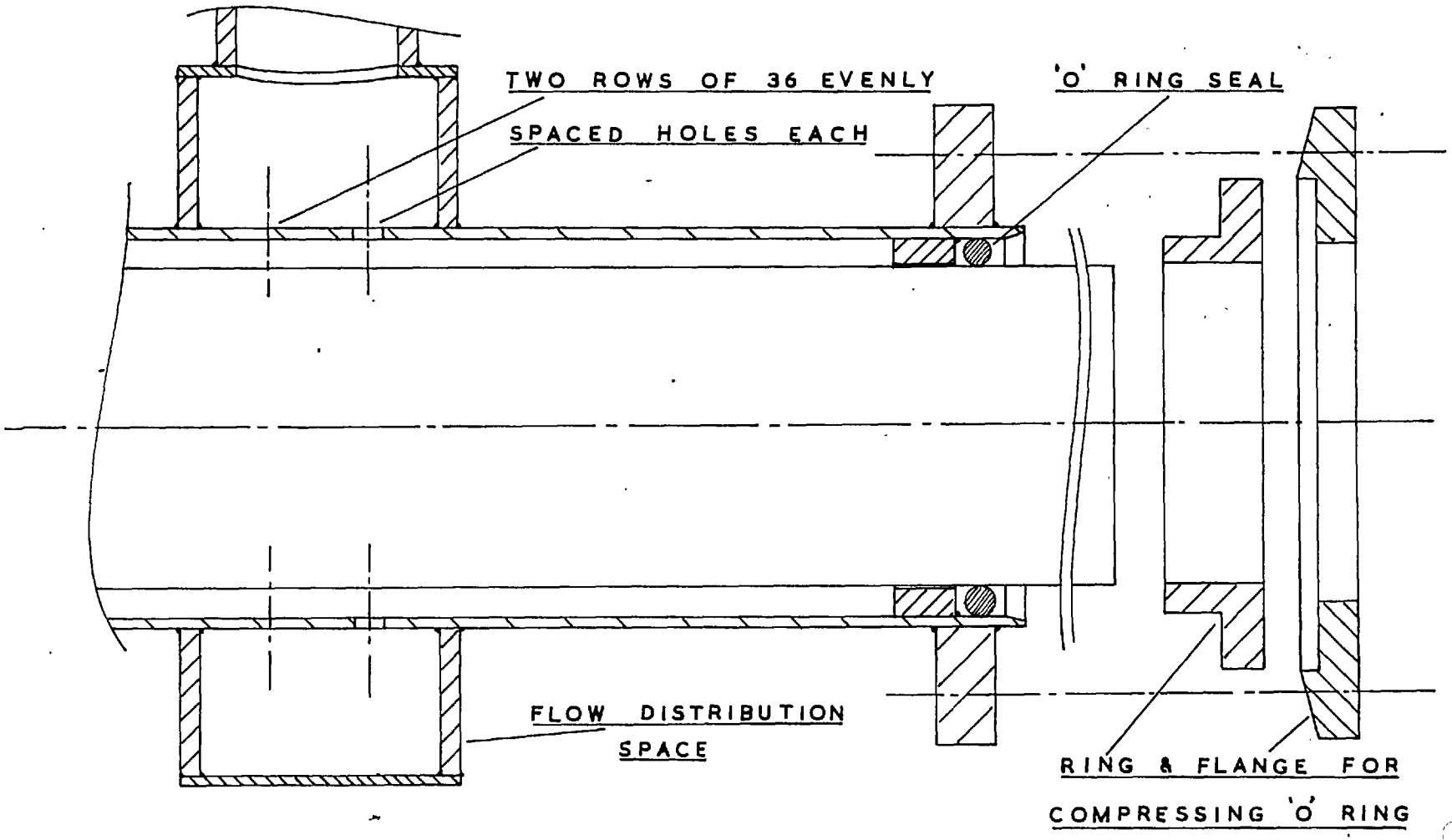
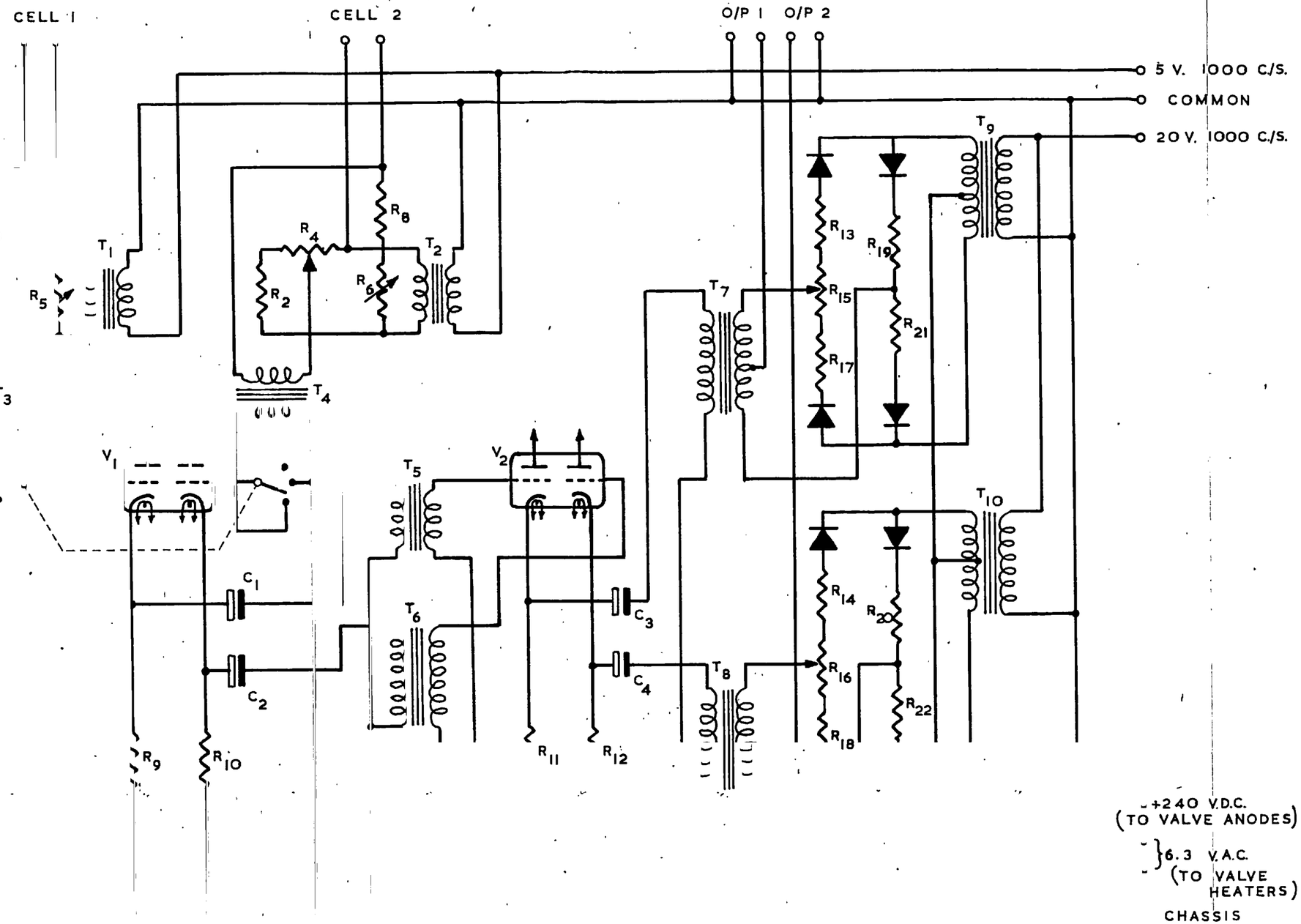


FIG. f 5 FLOW SYSTEM OUTLET

FULL SCALE



COMPONENT	VALUE
FIXED RESISTORS;—	
R_1 R_2	6,800 OHMS
R_8	200 "
R_9 R_{10} R_{11} R_{12}	2,000 "
R_{13} R_{14} R_{17} R_{18}	1,900 "
R_{19} R_{20} R_{21} R_{22}	2,200 "
POTENTIOMETERS;—	
R_3 R_4	2,500 OHMS
R_{15} R_{16}	500 "
VARIABLE RESISTORS;—	
R_5 (SELECTION SWITCH)	2,240 OHMS 696 " 266 "
R_6 (POTENT.)	2,500 "
TRANSFORMERS;—	RATIO PRI:SEC
T_1 T_2	1:1
T_3 T_4 T_5 T_6	1:10
T_7 T_8 T_9 T_{10}	1:1 (C.T.)
CAPACITORS;—	
C_1 C_2 C_3 C_4	16 MFD. 20 V.D.C.
THERMIONIC VALVES;—	
V_1 V_2	ECC 82
RECTIFIERS;—	SILICON TYPE

+240 V.D.C. (TO VALVE ANODES)

6.3 V.A.C. (TO VALVE HEATERS)

CHASSIS

FIG. 16 BRIDGE/DETECTOR CIRCUIT

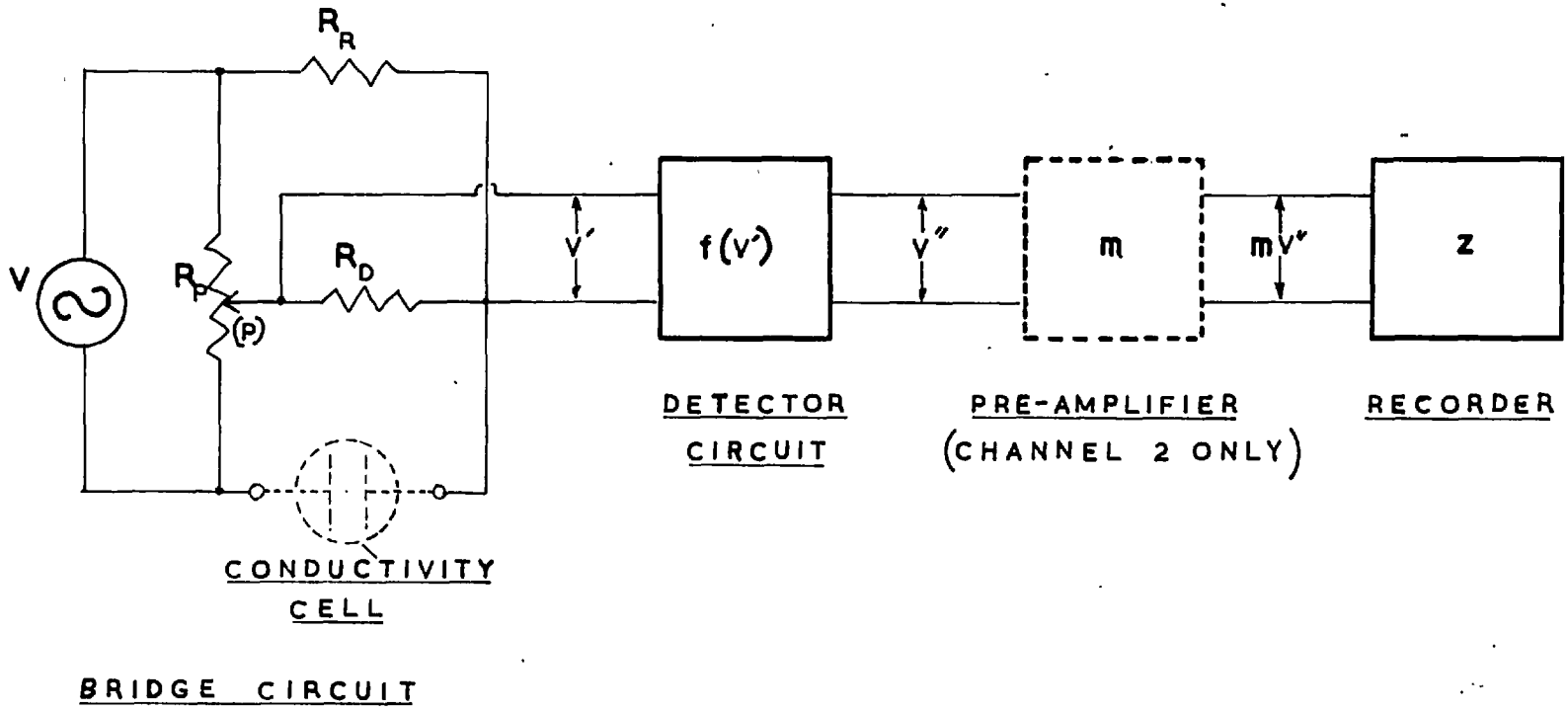


FIG. f 7 MATHEMATICAL MODEL OF CONDUCTIVITY MEASURING SYSTEM

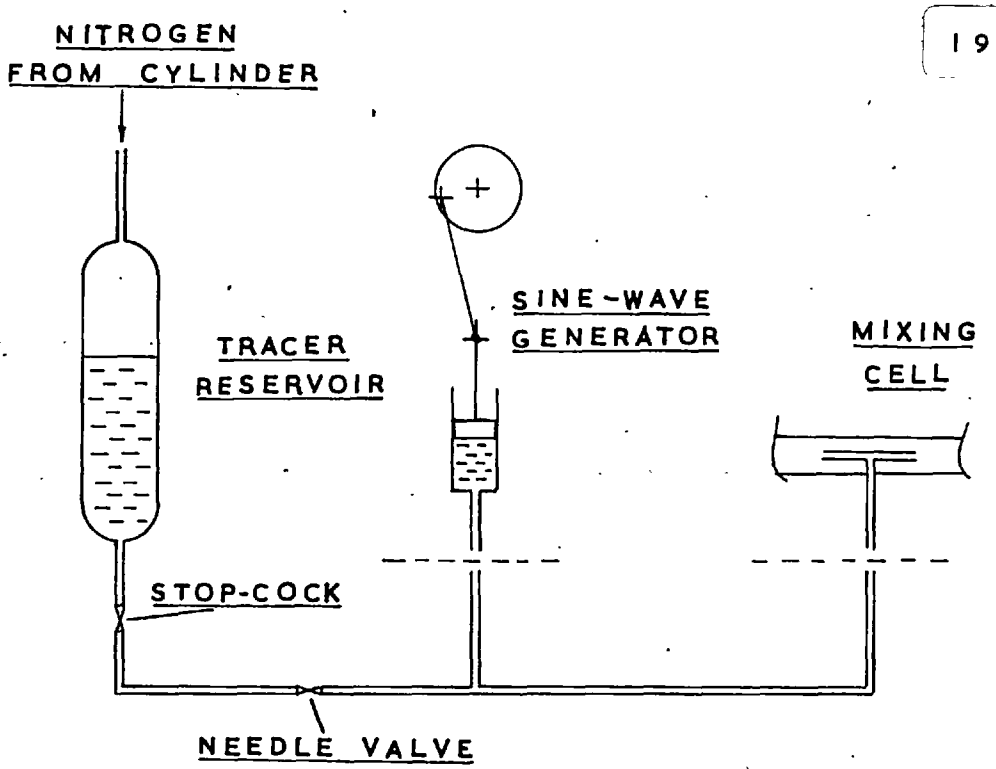


FIG. f 8 TRACER INJECTION SYSTEM

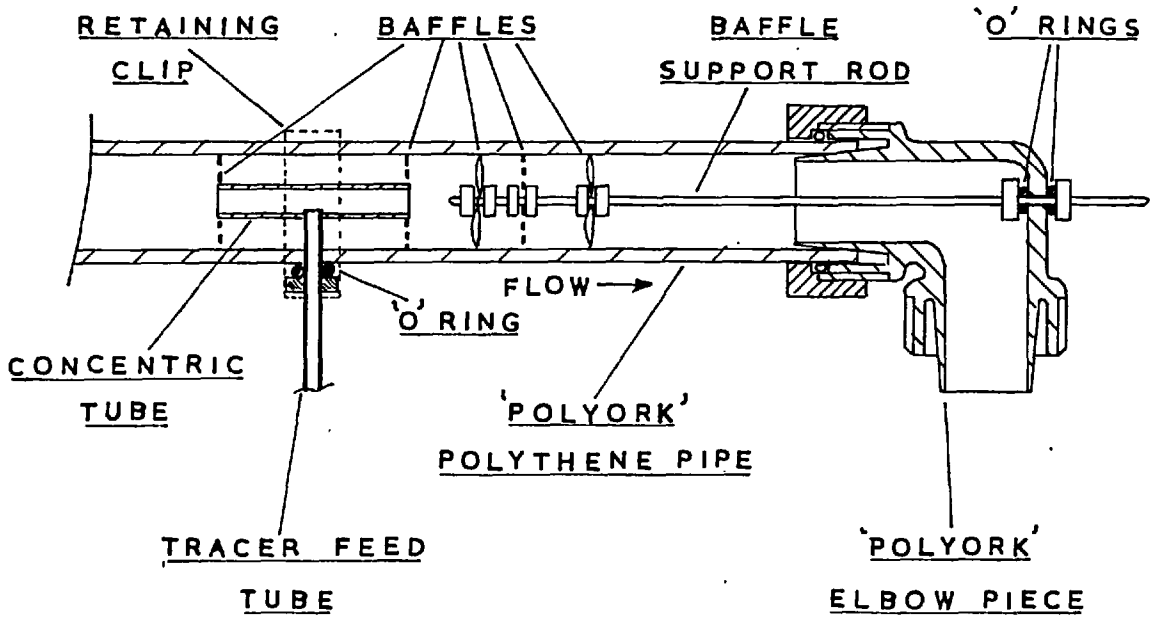


FIG. f 9 TWO STAGE MIXING CELL

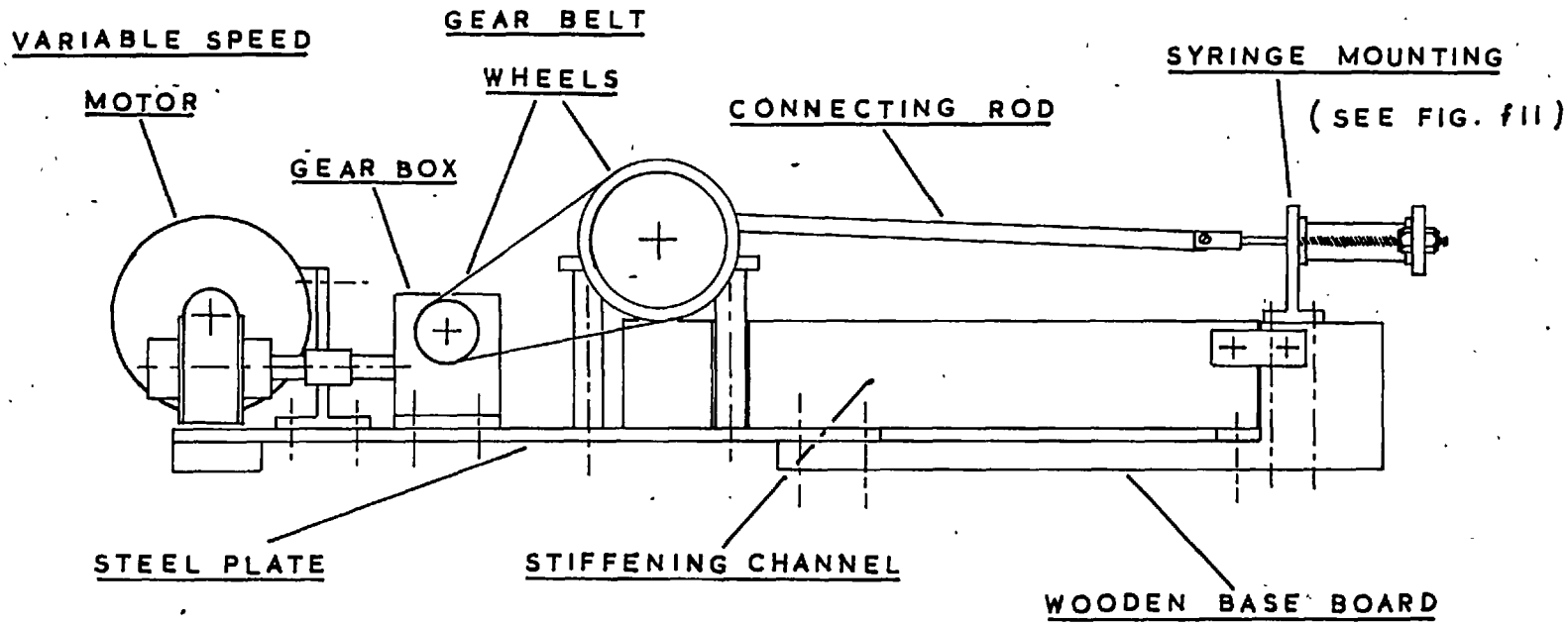


Fig. f10 Sine Wave Generator
(low frequency arrangement)

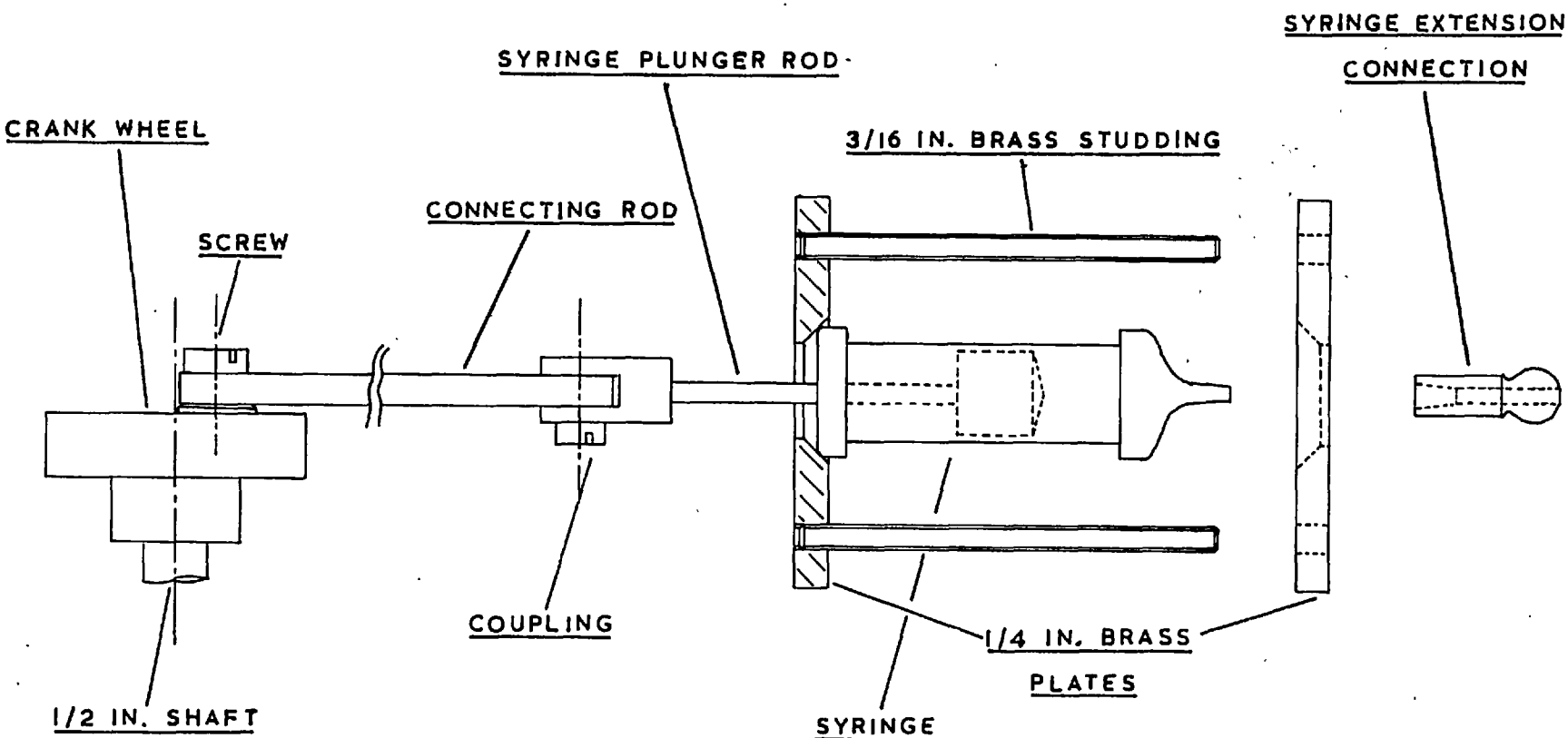


Fig. f 11. Detail of Syringe Mounting
(top view)

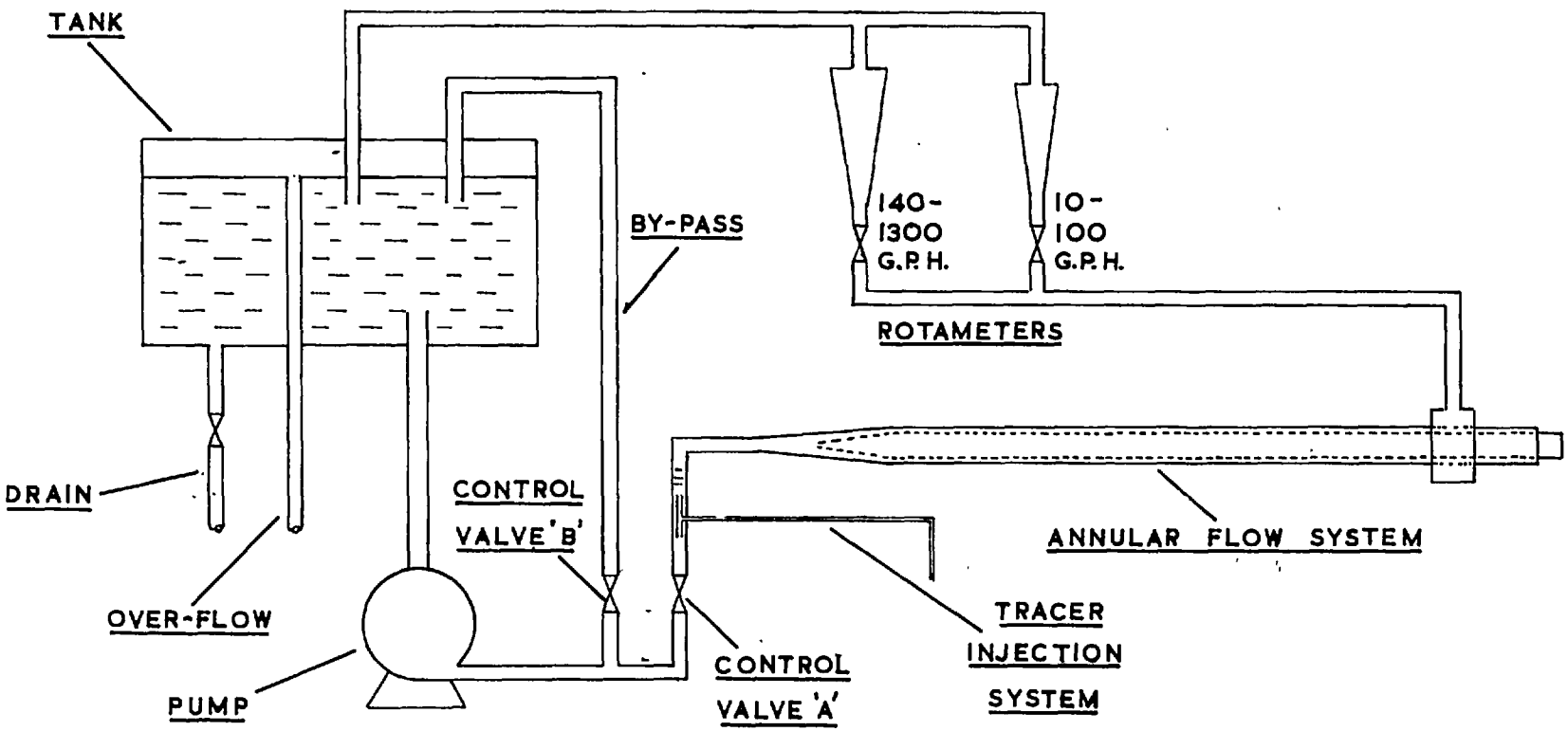


Fig. f12 General Flow System

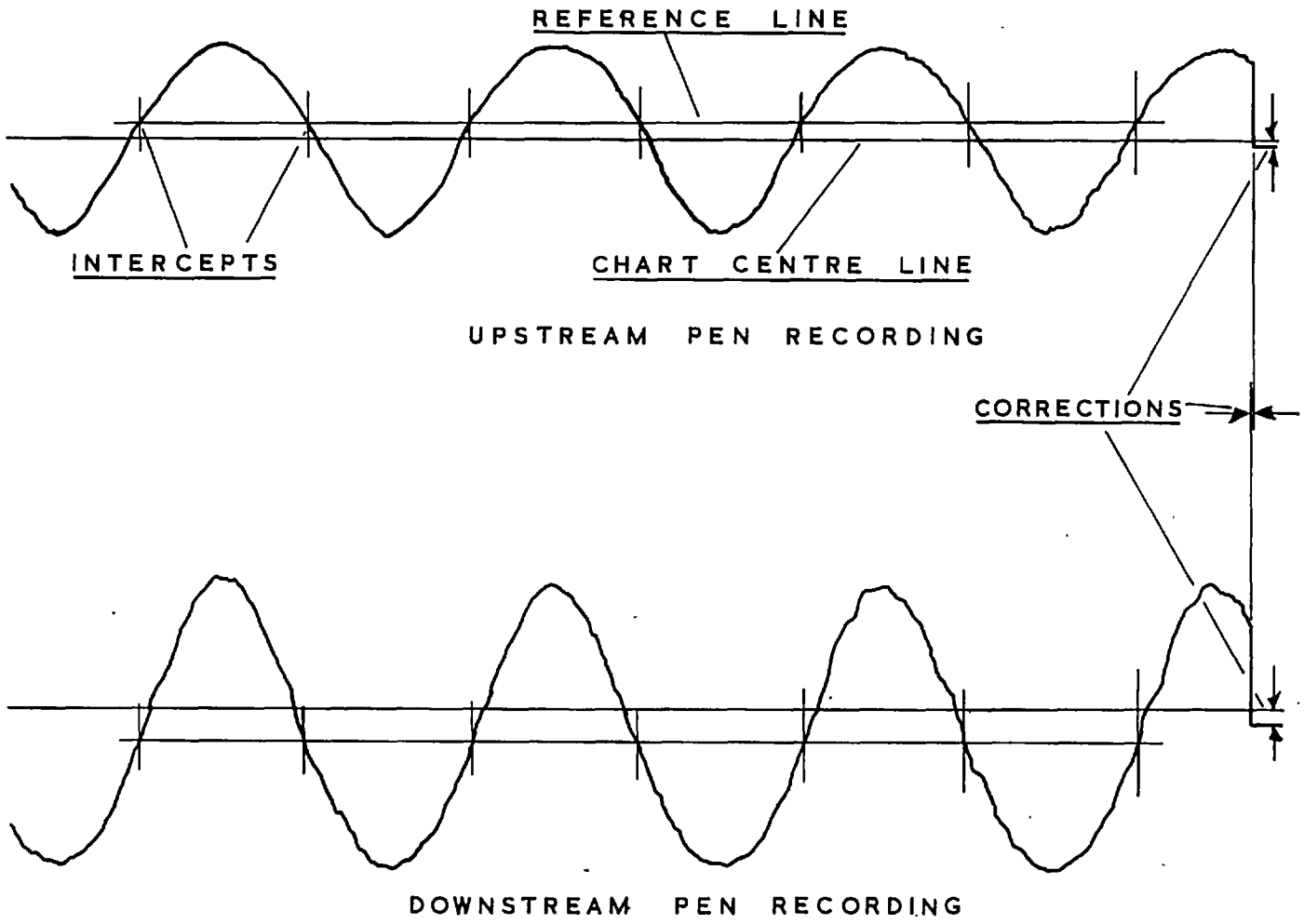


FIG. g l Analysis of Sinusoidal Tracer Signal Recordings

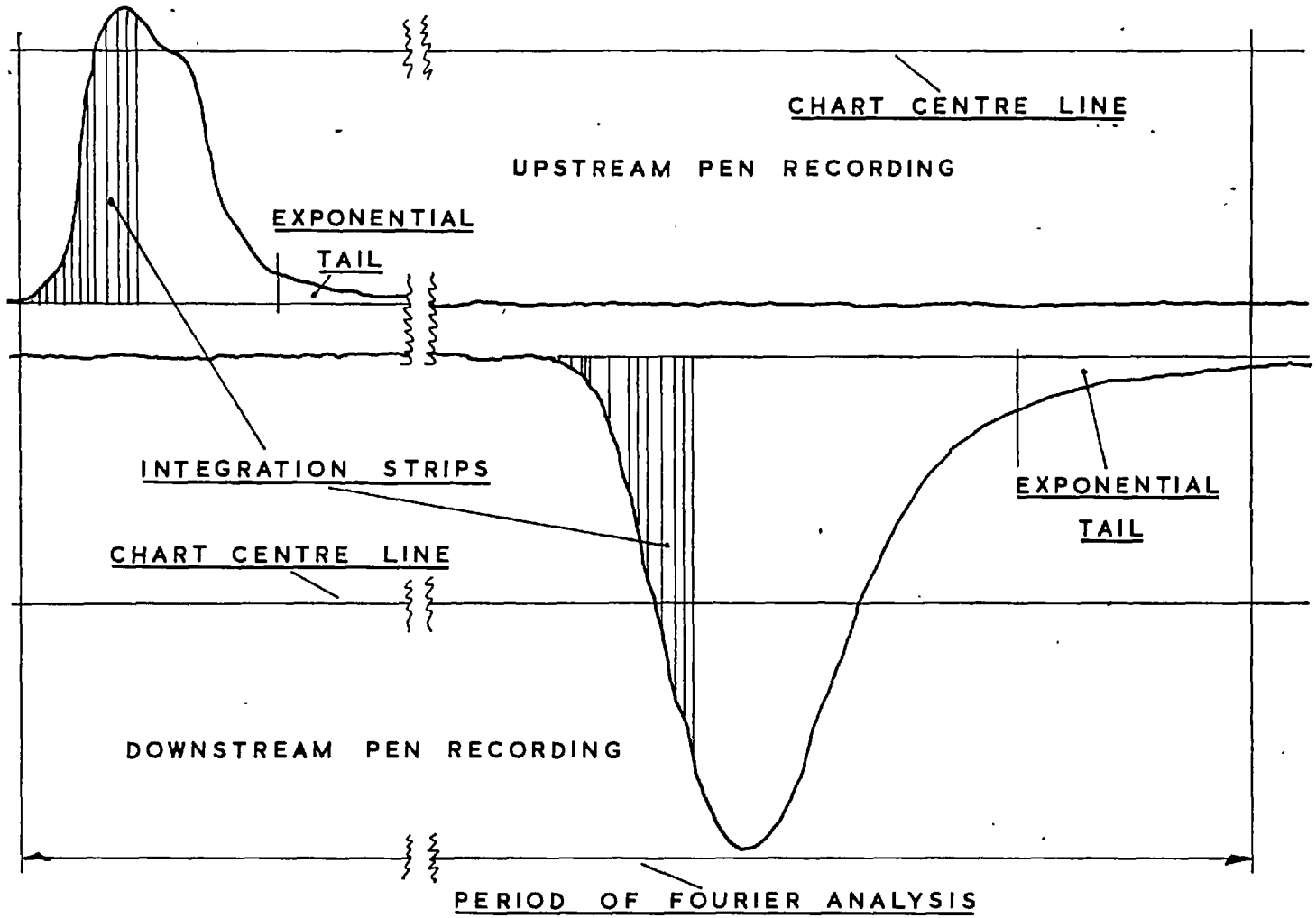


FIG. g 2 Analysis of Pulse Tracer Signal Recordings

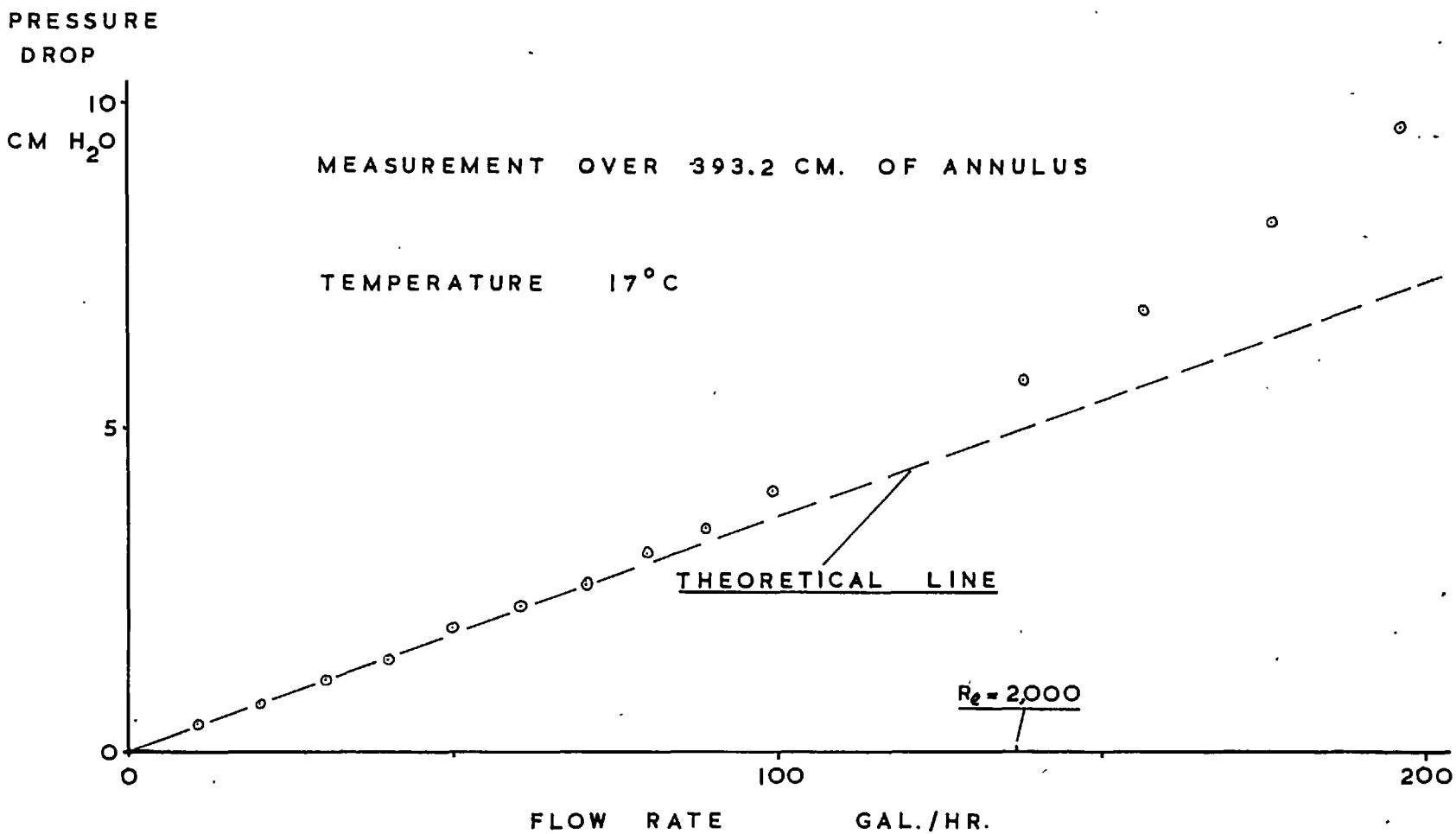


FIG. m1 Pressure Drop at low Flow Rate

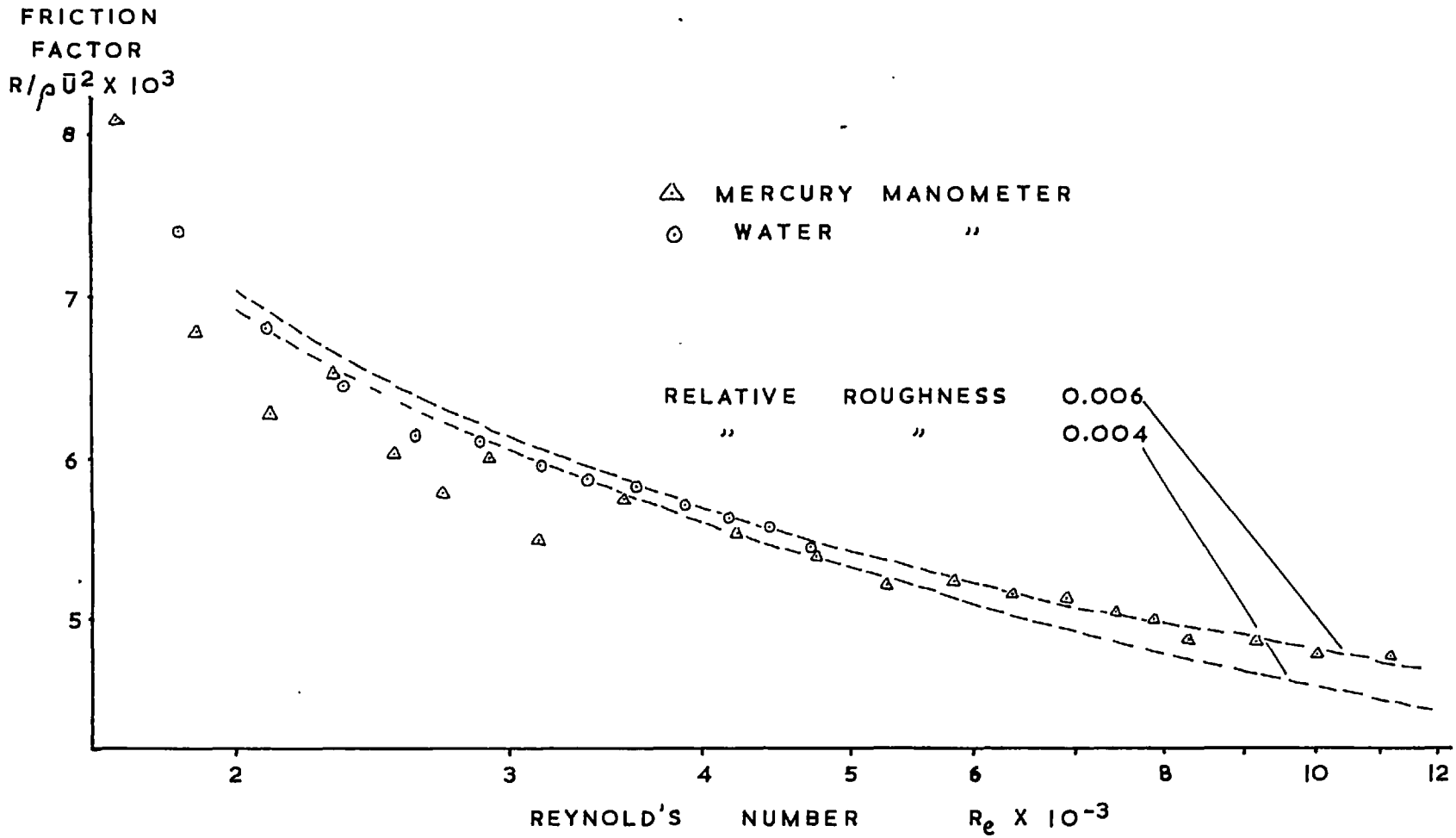


FIG. m 2 Friction Factors in Annulus

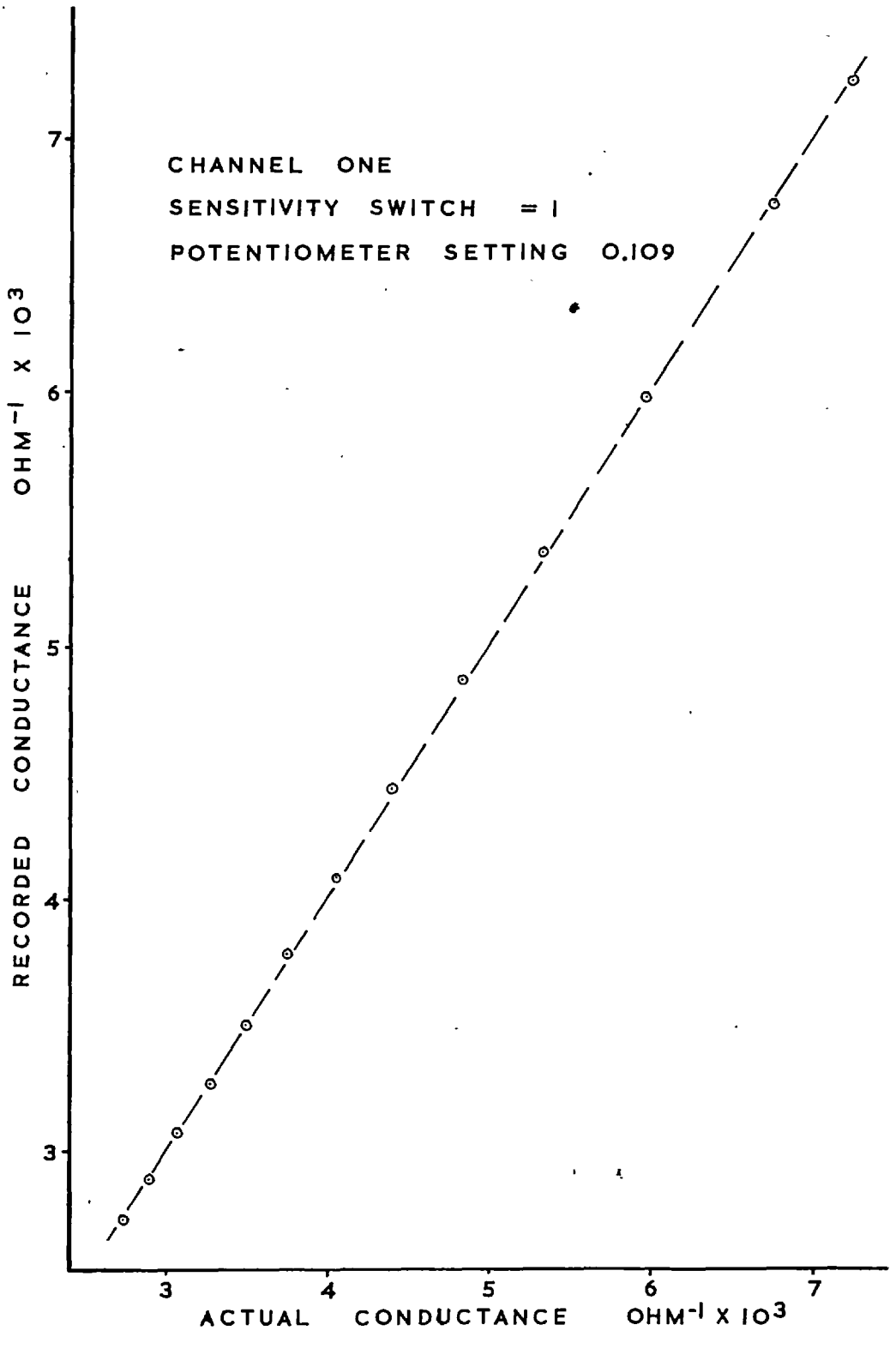


FIG. m 3 Conductivity Measuring System Test

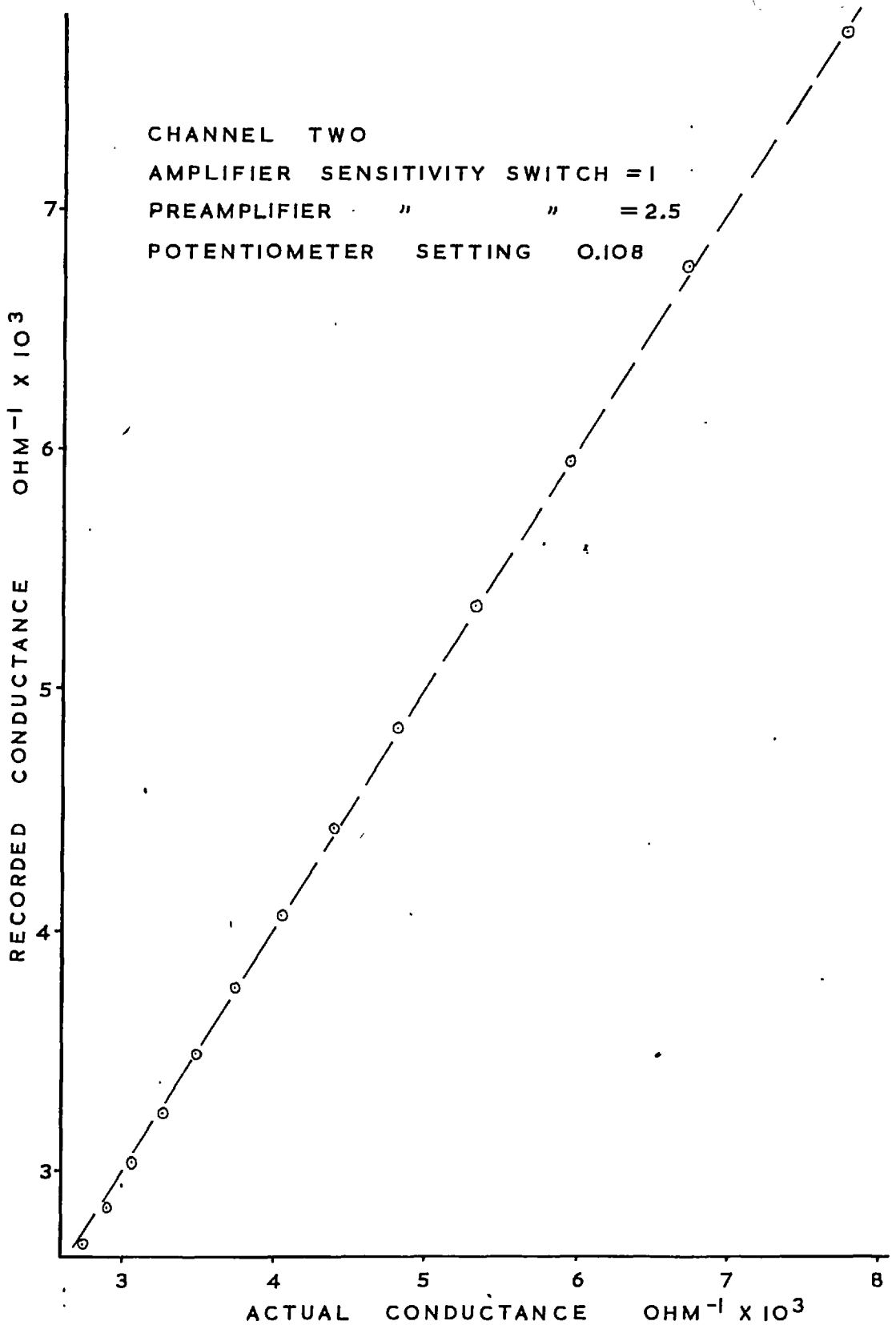


FIG. m 4 Conductivity Measuring System Test

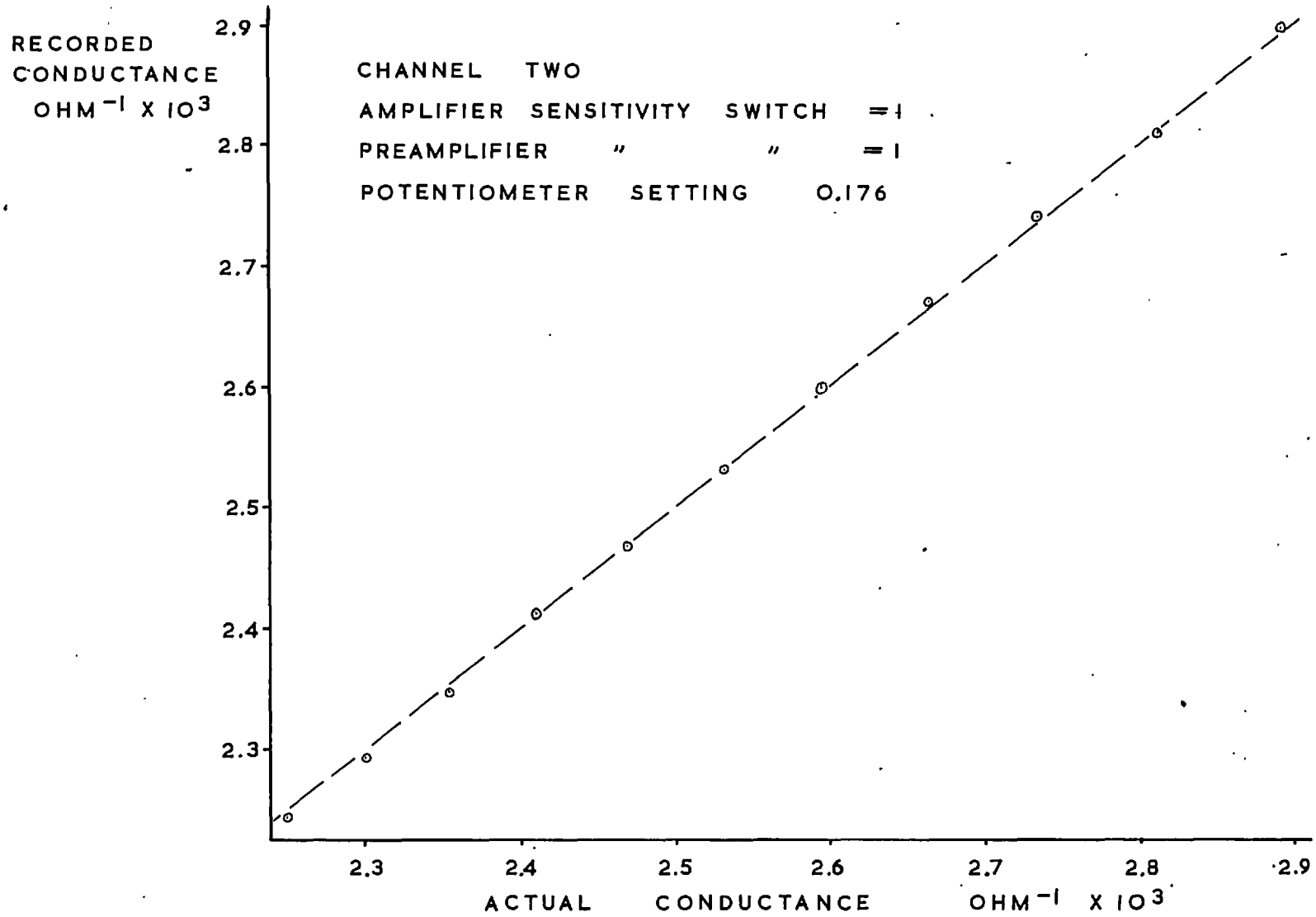


FIG. m 5 Conductivity Measuring System Test

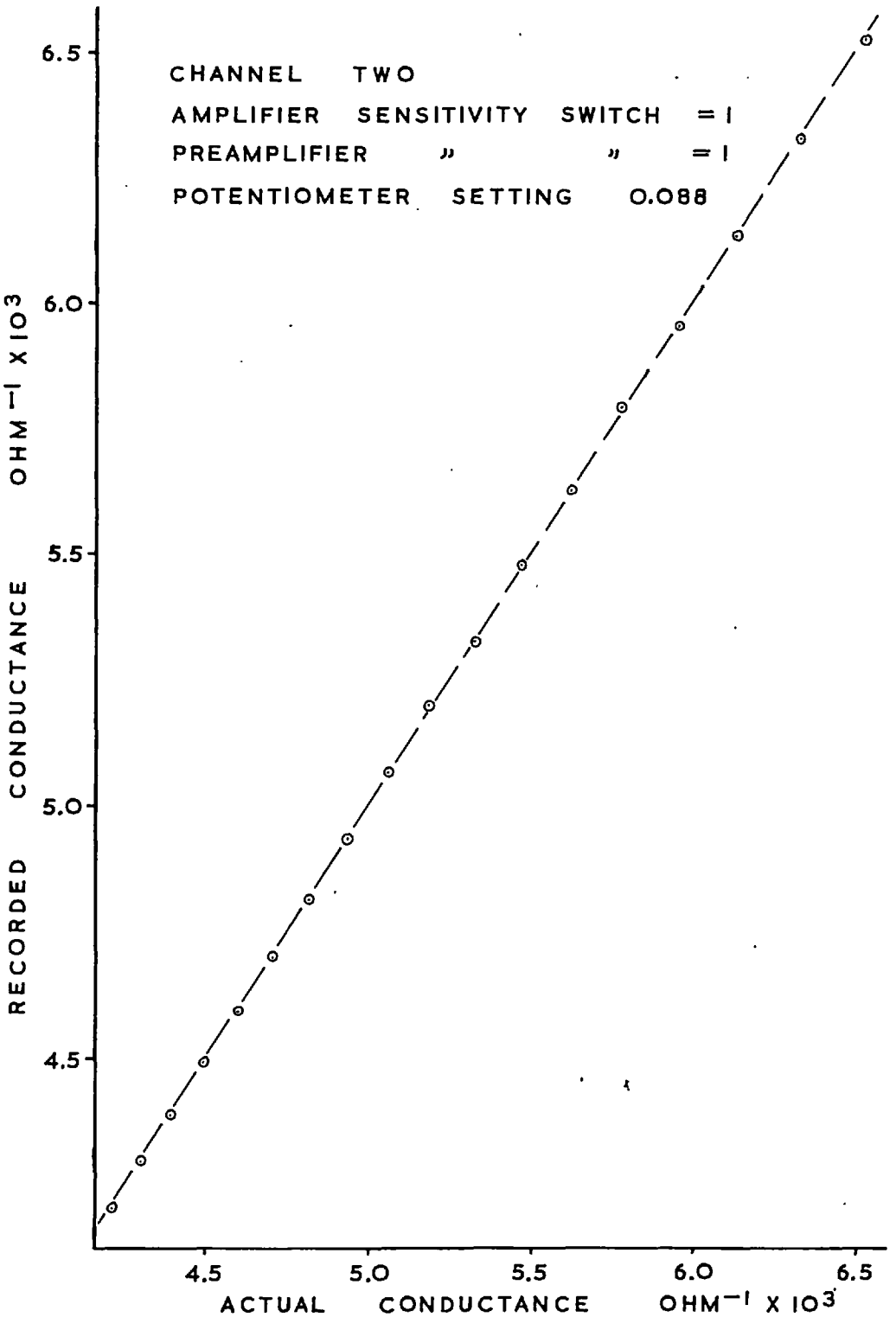


FIG. m 6 Conductivity Measuring System Test

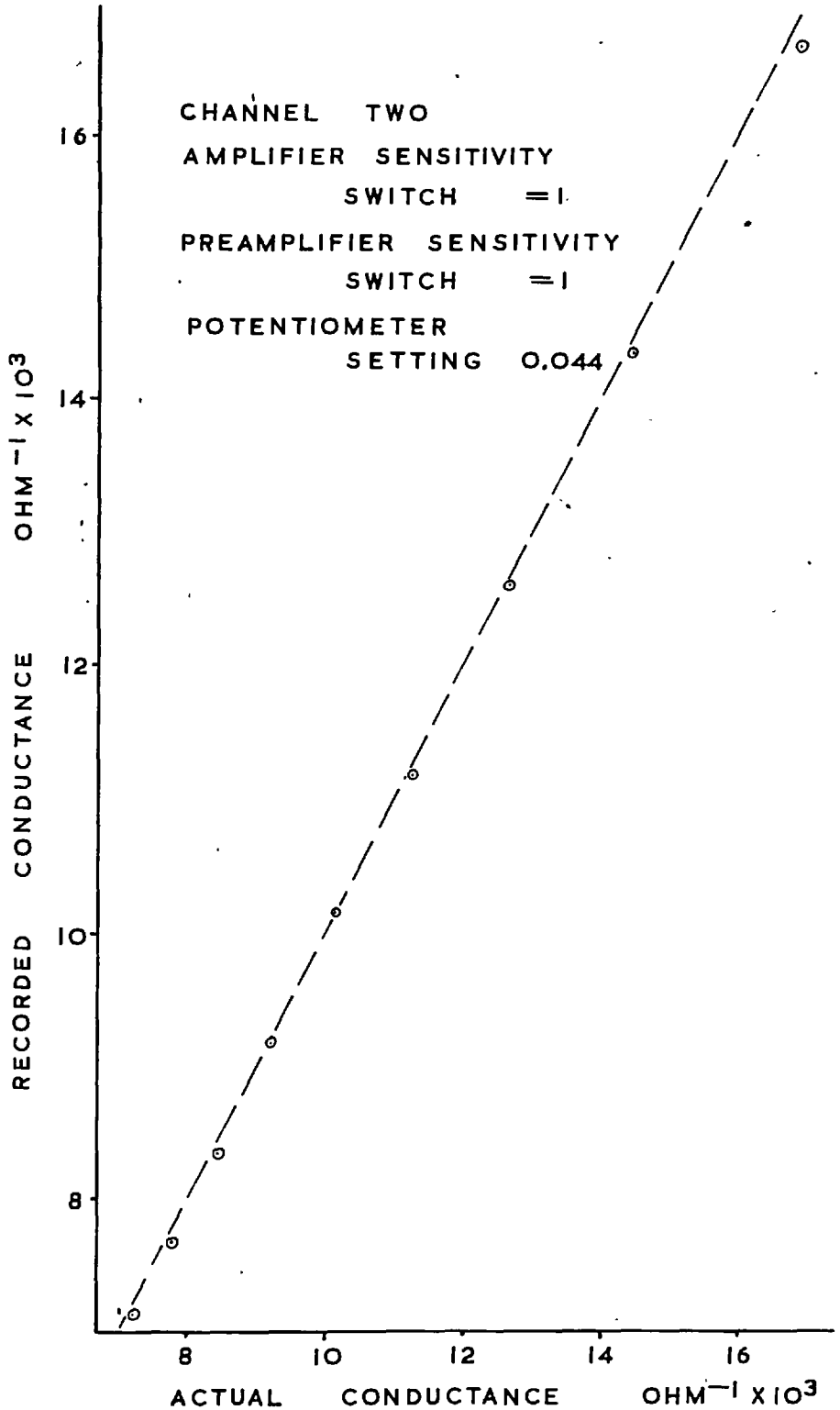


FIG. m 7 Conductivity Measuring System Test